JPC 444

Report Number
F-68-1

An Experimental Investigation of the Aerodynamic Force Characteristics of a Jet Issuing Transverse to a Wedge

FINAL REPORT

by

William L. Allan

NASA Grant NsG 592

January 1968

JET PROPULSION CENTER
PURDUE UNIVERSITY

SCHOOL OF MECHANICAL ENGINEERING
LAFAYETTE, INDIANA

JPC 444

Report Number

F-68-1

PURDUE UNIVERSITY

and

PURDUE RESEARCH FOUNDATION

Lafayette, Indiana

AN EXPERIMENTAL INVESTIGATION OF THE AERODYNAMIC FORCE CHARACTERISTICS OF A JET ISSUING TRANSVERSE TO A WEDGE

by

William L. Allan

Final Report

NASA Grant NsG 592

Jet Propulsion Center

January, 1968

ACKNOWLEDGEMENTS

The author wishes to express his gratitude to his major professor, Dr. B. A. Reese, for his suggestions, recommendations and assistance during the course of the research program.

The assistance of R. D. Guhse during the research program is gratefully acknowledged. The author also wishes to thank Mr. C. Merkle of the Jet Propulsion Center Machine Shop and Mr. C. F. Schanke of the Central Machine Shope for their advice and assistance in the fabrication of the experimental apparatus. The help of Mrs. Suzanne H. Waszilycsak, Mrs. Velda Mayhugh, Mrs. Karen Ketzler, and Mrs. Frances Haniford in the preparation of the manuscript is gratefully acknowledged.

The assistance of the Department of the Army and in particular Mr. John L. McDaniel of the U. S. Army Missile Command for their assistance in providing the opportunity to pursue graduate studies.

Finally, the author wishes to acknowledge the support of the National Aeronautics and Space Administration during the experimental phase of this investigation.

TABEE OF CONTENTS

LIST OF FIGURES

Figure | Page

ABSTRACT

Allan, William Lorimer, Ph.D., Purdue University, January 1968. An Experimental Investigation of the Aerodynamic Force Characteristics of a Jet Issuing Transverse to a Wedge. Major Professor: Bruce A. Reese.

The aerodynamic interaction of a sonic jet issuing from a 15° wedge with a transverse supersonic stream produces a side force due to flow interaction in addition to the jet thrust. The magnitude of this interaction force equals or even exceeds the value of the jet thrust. There is a substantial lack of agreement in the literature as to the effect of the flow parameters on the jet interaction; the prediction of the flow interaction for any given set of circumstances is in terms of empirical "scaling" laws. Over the range of experimental conditions employed in the published research there is substantial agreement as to a physical model. This model is based on the inviscid or inertial effects of the interaction of a jet issuing from a flat plate.

The experimental conditions for this study were as follows:

Primary stagnation pressure: 100 psig

Primary stagnation temperature: Ambient

Free stream Mach number: 1.90

Secondary stagnation pressure: 50 to 250 psig

Secondary stagnation temperature: Ambient

Secondary Mach number: 1.00

Secondary gases: Air, argon, ethane, helium, nitrogen

The model was a 15^{o} two-dimensional wedge with a variable width two-dimensional injection slot. The angle-of-attack of the model could be varied between -5 and $+15^{o}$.

Data acquisition was by means of spark shadowgraphs of the flow field and surface pressure taps on the model. The surface pressures were measured by means of mercury manometers.

The results of this study employing flow visualization and the measurement of surface pressure distributions on the wedge do not agree with previously published flat plate results. The results from these experiments show a more abrupt separation ahead of the slot, a shorter separation region and a thicker boundary layer or wake downstream of the "reattachment" point than the previous flat plate experiments. These differences may be all attributed to the higher viscous forces; in previous published experiments at lower values of free stream static pressure, the inviscid or inertial effects were considered dominant.

The results of the experiment may be summarized as follows:

a. As the angle-of-attack is increased from 0^{o} the magnitude of the jet interaction is decreased for fixed free stream conditions and jet stagnation pressure.

b. The effect of angles-of-attack between $+5^{o}$ and $+15^{o}$ and a range of values for the secondary stagnation pressure of 50 to 250 psig is predicted by the following expression:

$$F_t = (F_i + F_j + F_a) = 1.023^n(F_j + F_a)$$

where n is a function of jet stagnation pressure.

c. An increase in weight flow rate of the injectant increases the interaction force. This effect is a maximum at 0^{o} angle-of-attack and is diminished by both positive or negative angles-of-attack, and is enhanced by an increase in secondary stagnation pressure.

d. A moderate change in the molecular weight of the secondary injectant as the air is changed to argon, nitrogen or ethane, does not significantly affect the interaction. A large change in molecular weight, air to helium increased the force, $F_i + F_j$, by approximately 20%.

e. A 50% change in the specific heat ratio, k, did not affect the interaction for conditions of approximately equal molecular weight (ethane and nitrogen) and with an average temperature differential of $120^{o}F$ between the primary and secondary stream static temperature.

I. INTRODUCTION

The mission envelope for many spacecraft and rockets requires active guidance and control both within and beyond the earth's atmosphere. A unique approach for a control system would be to employ a single system to provide the required maneuver capability throughout the flight envelope. It would also be desirable that such a system be independent of main engine operation.

The use of a jet reaction device is attractive because control may be effected over the wide range of operational conditions within and beyond the earth's atmosphere. In vacuum, the control force due to the jet is a function only of the fluid momentum and the pressure at the nozzle exit plane. For operation within the atmosphere the available control force depends on the aerodynamic interaction with the external flow as well as the reaction force of the jet. Under most conditions the actual control force is increased during operation in the denser regions of the atmosphere; as is the control force requirements. However, in many applications a jet reaction control system cannot provide the required force levels without undue volume and weight penalties; typically, this includes control systems for high velocity, short range missiles designed for use in anti-ballistic missile defense systems.

For operation within the earth's atmosphere, a new technique is being widely explored that appears capable of providing very high force levels, along with very large values of specific impulse. This technique is referred to as "External Burning" or "EB", and involves the use of a liquid pyrophoric fuel. This fuel is injected into the free stream adjacent to the flight vehicle and a control force is produced by the combination of the jet thrust and the combustion of the injectant with the oxygen in the free stream. The pyrophoric fuels under current investigation are triethyhaluminum, aluminum borohydride, and pentaborane. Thermochemical calculations for these fuels predict a specific impulse of the order of 6000 seconds. In addition to the advantages inherent in high specific impulse, EB exhibits the high dynamic response normally associated with jet reaction devices.

Unfortunately, EB has some marked disadvantages. The prediction of the rate of the breakup and vaporization, and the mixing of the fluid jet with the air stream is a very difficult task. Many external factors influence this process and in spite of much research, progress has been disappointingly slow. Another problem with EB is the operational use of pyrophoric fuels because of the spontaneous combustion characteristics. Still another obvious limitation is the fact that the flight envelope of a vehicle utilizing an EB system is limited to those portions of the atmosphere where there is sufficient oxygen present to support the pyrophoric reaction in close proximity to the flight vehicle.

There is no discussion in the literature of the possibility of blending jet reaction control and external burning into a single control technique - a technique useful both within and beyond the atmosphere and independent of main engine operation. However, it appears that such a system may be feasible. This research program is concerned with just such a combined jet reaction and EB control concept. It would employ an underoxidized monopropellant in lieu of either a liquid pyrophoric jet, or a hot gas reaction system. The monopropellant would be decomposed in a gas generator, releasing perhaps 20% of its heating value, and the hot gas would then be expanded through a nozzle to provide jet reaction control. Typically such a system could utilize hydrazine with catalytic decomposition, or a combination of hydrazine and N_2O_4. Where the flight regime permits, the control force would be enhanced by the external burning. As the dynamic free stream pressure increases, the control force requirements increase as does the amount of volume expansion that could occur from external burning. Conversely, in vacuum, there is no external burning and the available control force is at a minimum; but the control force requirements are also at a minimum. Regardless of flight regime and attitude, there would always be a usable level of control force available. That is not true of an external burning system that employs a liquid jet. The use of a monopropellant would also remove one of the principle difficulties in obtaining consistent external burning - the prediction of jet breakup and vaporization.

The coincident location well forward on the flight vehicle of the two methods of force generation does not give rise to inconsistency. Much of the literature considers the interaction phenomena of a transverse jet as a jet flap and thus the argument that the jet should be located well aft on the body to minimize the effects of the decrease in the pressure field immediately downstream of the injection point. Conversely, it is apparent that the injection point for external burning should be well forward on the flight vehicle to allow sufficient length for the combustion to occur in close proximity to the body. In the case of the combined system, when in vacuum it acts as a jet reaction control, not as a jet flap; and within the atmosphere the burning prevents the creation of a low pressure field aft of the injection point.

The injection of a fluid into a supersonic stream for the purpose of producing a control force has been studied actively since 1952*. Studies and applications generally fall into three categories: 1) the injection of a fluid into a rocket exhaust nozzle, transverse to the main flow, 2) injection of inert fluids into external supersonic flow, and 3) the injection of fuel into the air flowing external to a supersonic flight vehicle, or external burning. Although there are some differences in the phenomena associated with the first two cases, those differences are not as important as the differences introduced by external combustion. As mentioned above, when an inert fluid is injected into an exhaust stream or an external supersonic flow, a control force is produced which is made up of two components, a jet reaction force and an aerodynamic interaction force. The latter is associated with a local increase in pressure in the region of boundary layer separation and an increase in pressure downstream of a shock wave which is produced by the injection. This is shown in Fig. 1. When the injectant is a liquid that vaporizes, additional force may be introduced which is related to the volume change produced by the evaporation of the liquid.

In external burning, the aerodynamic interaction force is amplified by the heat release and the volume increase associated with the combustion

---

* The review of the literature pertinent to this investigation is presented in Appendix B.

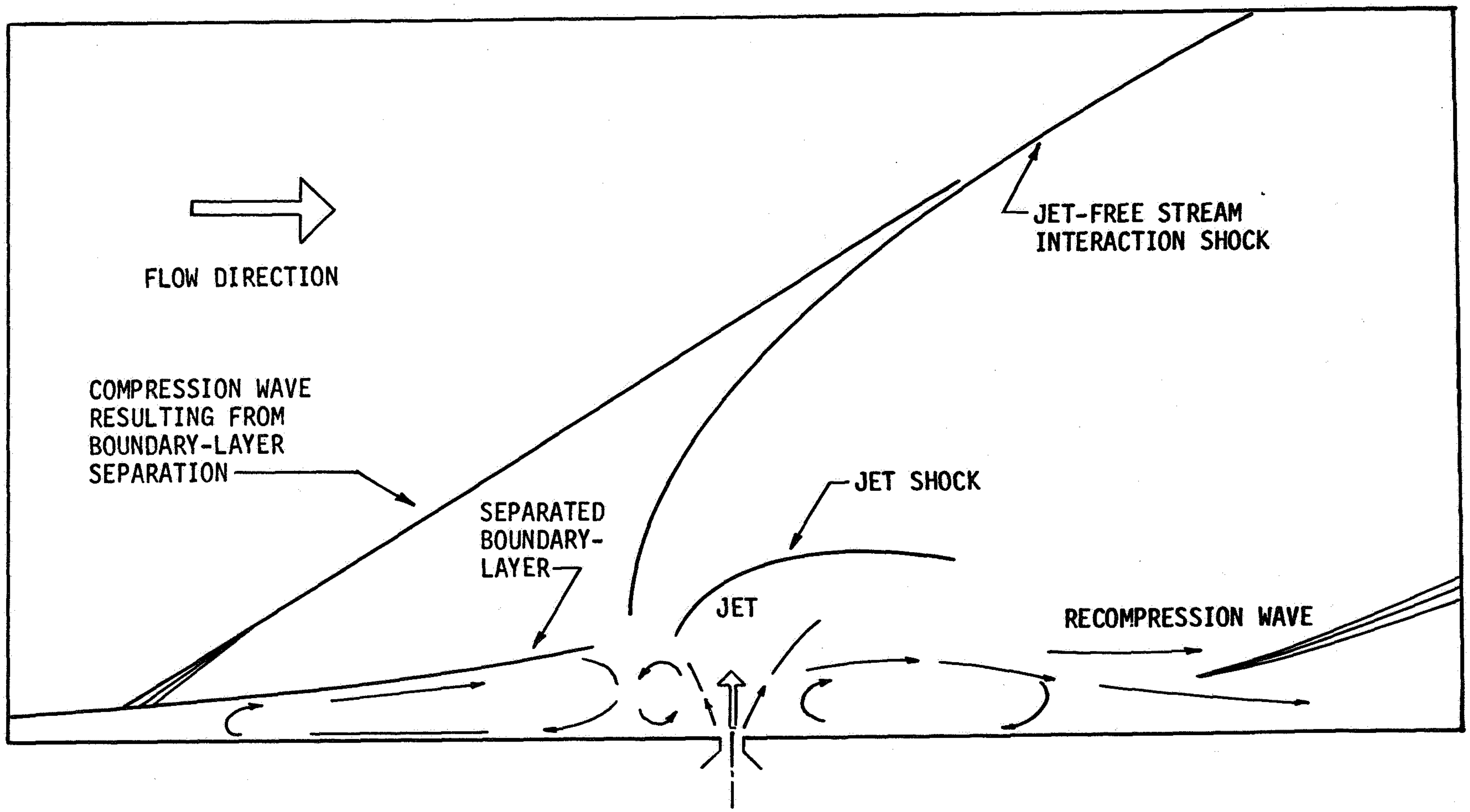

Figure 1. THE TWO-DIMENSIONAL JET FLOW FIELD

process.

Fig. 2 depicts the six interrelated phenomena that contribute to the overall effectiveness of the control system utilizing such a technique:

1. The dynamics of the fluid jet and the net momentum flux.
2. The separation of the boundary layer upstream from the point of injection and the pressure distribution within the separated region as a function of freestream conditions, upstream ablation, etc.
3. The formation of an oblique shock at the point of separation and the pattern of compression and rarefraction waves that form downstream of this shock.
4. The process of jet breakup, evaporation and mixing.
5. The combustion process.
6. The flame-shock interaction.

Items 1-4 are sometimes grouped together and referred to as the "pre-ignition stage" (1), however, the combustion process cannot be clearly separated from its effects on Item 4.

In order to effectively describe the phenomena of external burning in an analytical fashion, it is necessary to use both the primary and secondary flow parameters as model inputs. As detailed in the Review of the Literature (Appendix B), there is a lack of substantial agreement as to the effect of these flow parameters, with respect to either an inert secondary injectant or a combustible secondary injectant. In the case of an inert injectant, several theories appear applicable depending on the range of the experimental data (2-29, 97-101). For EB, there is less agreement than in the case of inert injectants and is further compounded

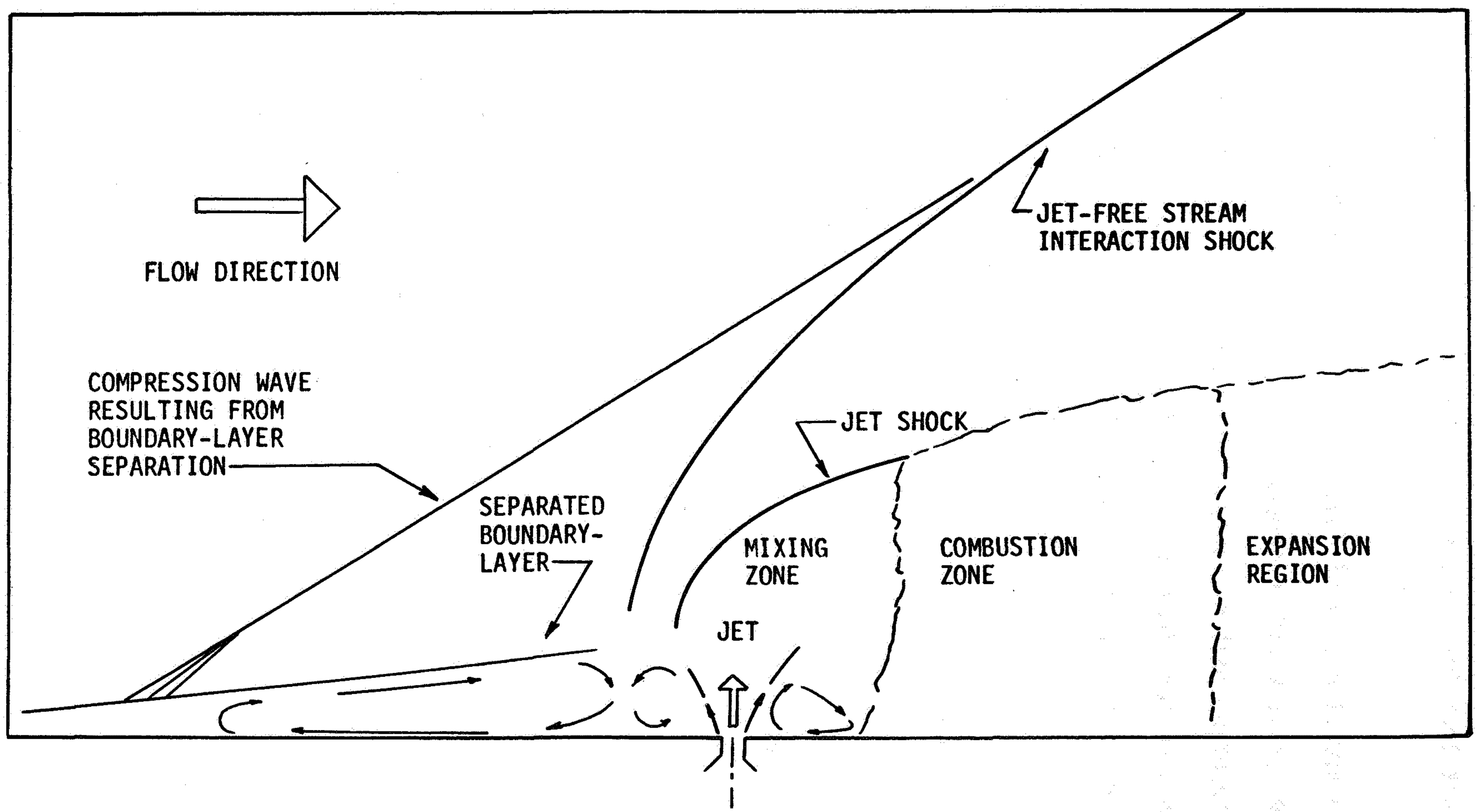

Figure 2. THE TWO-DIMENSIONAL EXTERNAL BURNING FLOW FIELD

by the fact that the theories are closely tied to model geometry (30-96).

The actual choice of input parameters is arbitrary, providing that the chosen primary and secondary sets fully describe the flow field. The primary input parameters chosen for this investigation (2D) were: free stream Mach number, free stream total pressure, free stream total temperature, and angle-of-attack. The secondary input parameters were: size and geometry of injection orifice, secondary total pressure, secondary total temperature, and species of injectant.

The experimental portion of this research investigation is envisioned to comprise two phases: a) an investigation of the flow field produced by the interation of an inert* gas injected through the surface of a wedge and b) a similar investigation with combustible injectants. The purpose of the first phase, which is the subject of this research program, is to more clearly define the effects of the secondary flow parameters prior to combustion.

---

* Ethane was used as one of the injectants. While it is not normally considered as an inert gas, at the temperature involved (421° R) it was effectively non-reactive.

2. METHOD OF INVESTIGATION

2.1 General Discussion

The techniques selected to investigate the effects of the secondary flow parameters was to utilize a two-dimensional supersonic wind tunnel and a wedge model. The details of the apparatus and model are presented in Appendix C and in Figs. 3, 4, and 5. Figure 3 shows the wedge model installed in the tunnel. The flow is from left to right. In the foreground is the spark source. The model is shown at an angle-of-attack of 5^{0}. Behind the model and far tunnel wall is mounted the ground glass screen. Figure 4 is an exploded view of the model. The fore and aft sections of the model are butted together and held in place by the side plates. Figure 5 is a schematic of the flow system. The primary air goes from the supply tanks, through the regulator system, into the plenum chamber, and through the tunnel. The secondary gas is fed from the supply tanks through a remote dome loaded valve, into the secondary plenum and then through the model and the injection slot. Both plenum chambers have stagnation temperature and pressure probes. The aerodynamic interaction of a jet transverse to a supersonic stream is an extremely complicated phenomenon. The reduction to two dimensions retains the fundamental flow structure, eliminates several of the secondary interactions, i.e., wrap-around, and permits straightforward interpretation of the shock structure by means of shadowgraph photography.

The experimental portion of this program utilized a 15^{0} wedge

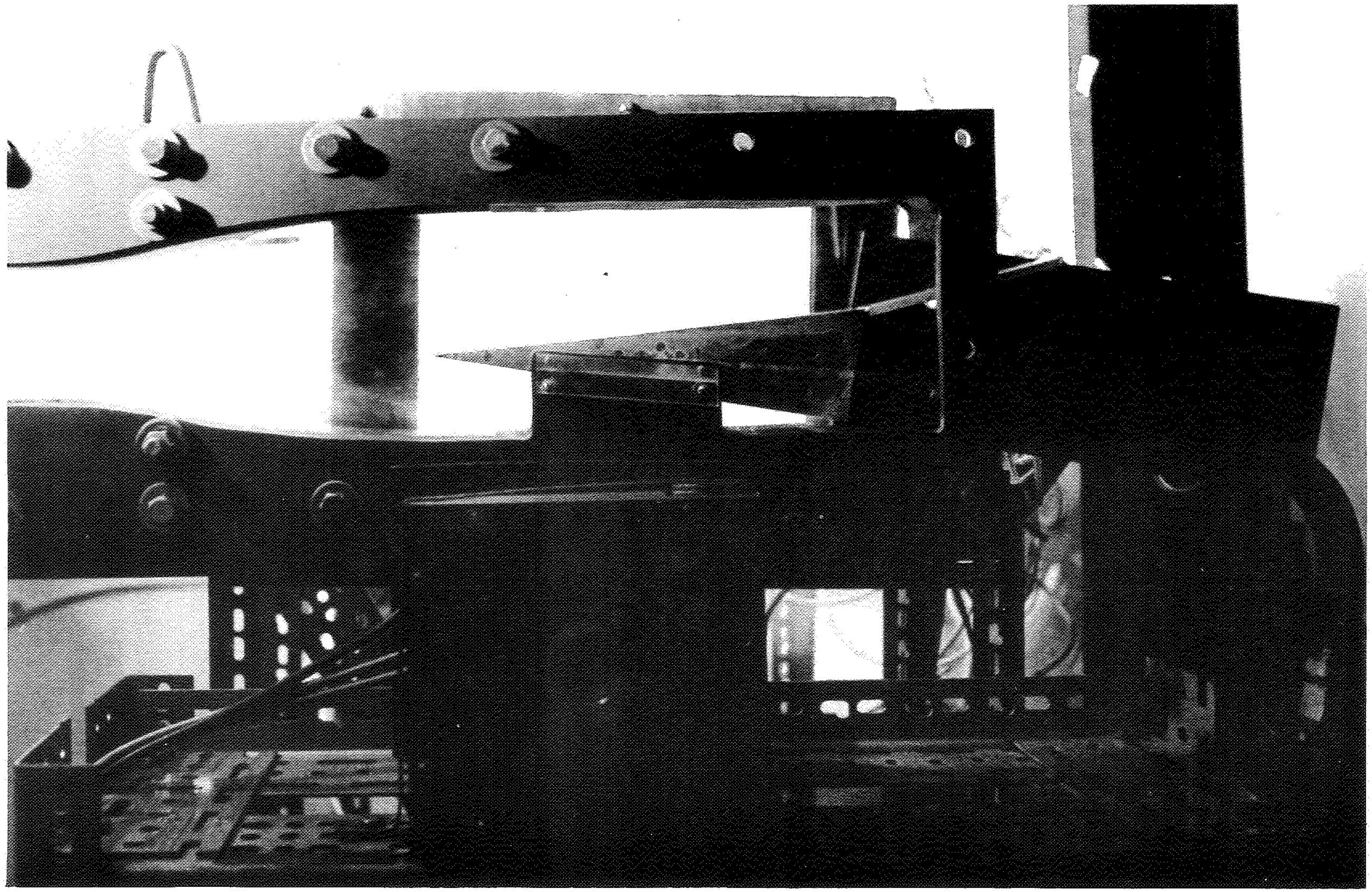

Figure 3. The Wedge Model Installed in the Tunnel

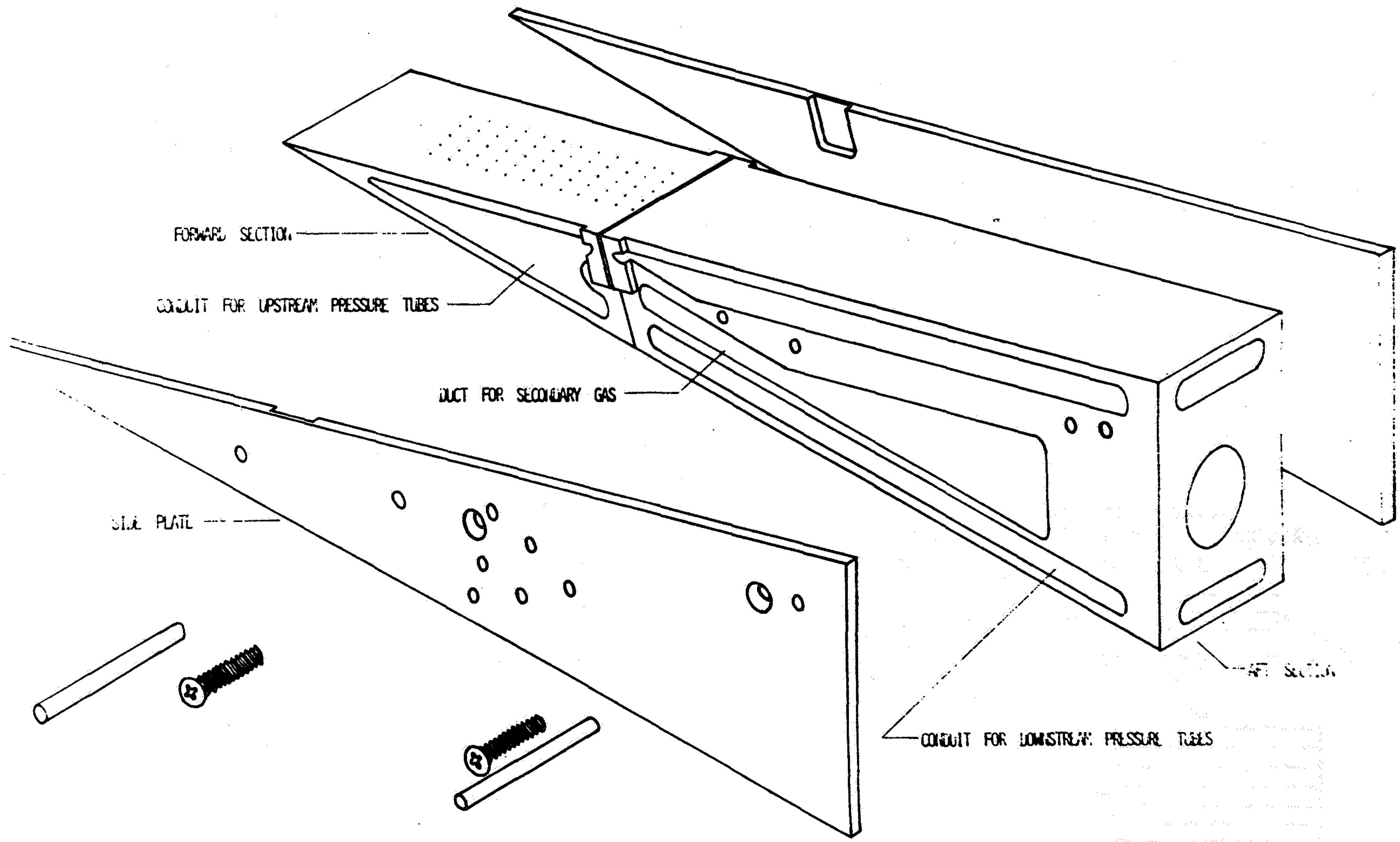

Figure 4. Exploded View of the Wedge Model

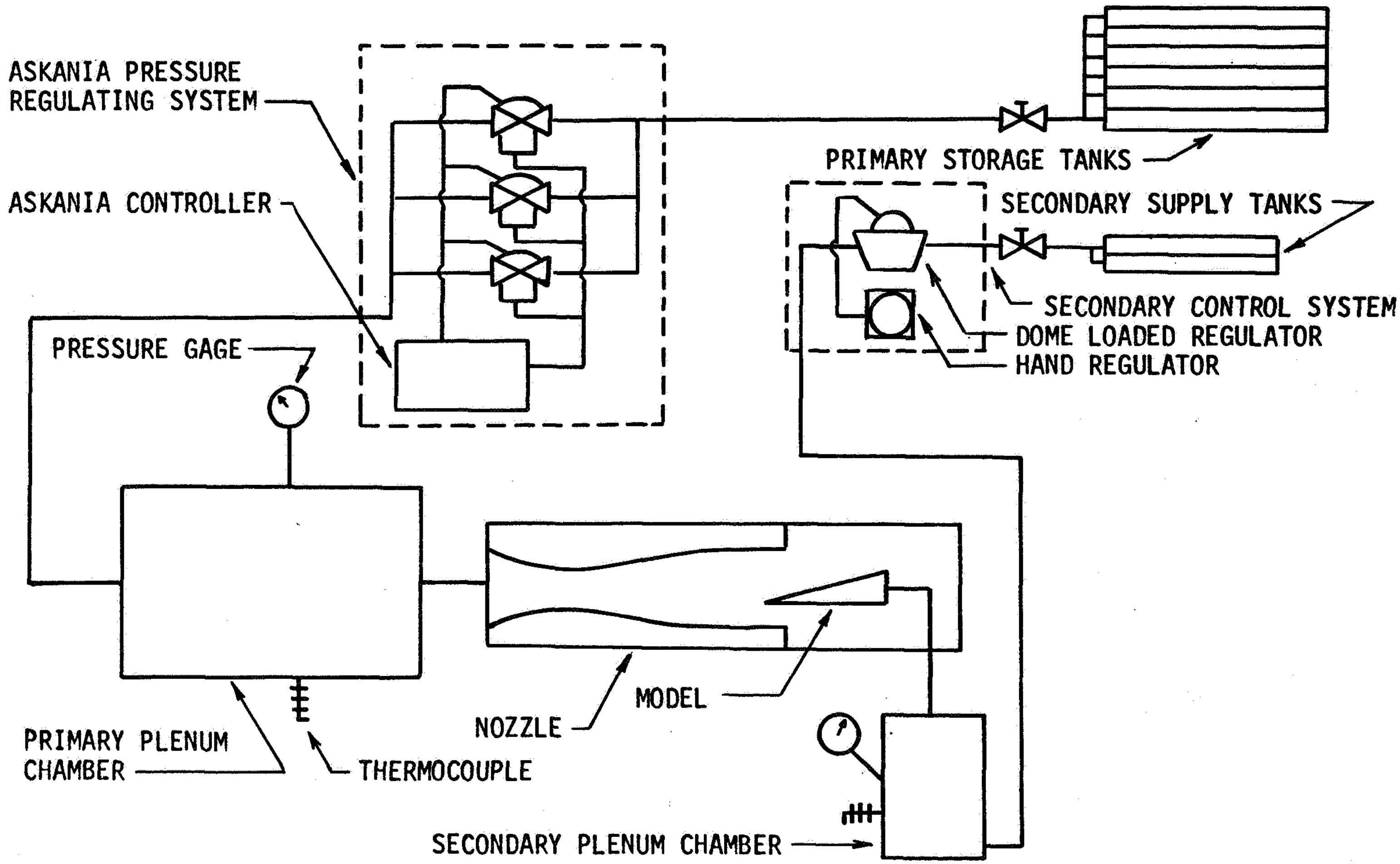

Figure 5. SCHEMATIC DIAGRAM OF THE FLOW SYSTEM

model which was inserted into the exit stream of a two-dimensional supersonic wind tunnel. Air or inert gas was injected perpendicular to the surface of the wedge thru a sonic slot aligned perpendicular to the supersonic flow. Surface pressures on the wedge were obtained from static pressure taps on the wedge surface. These taps were arranged longitudinally on either side of the slot at centerline distances of .050 inches. The resultant shock structure was reproduced concurrently with the pressure map by conventional spark shadowgraph photography.

2.2 Experimental Conditions

The primary and secondary air supply for the experiment was provided from a system of high pressure air tanks. When fully pressurized to 2500 psig, this air supply would provide for five minutes of operation at a mass flow rate of approximately 20 pounds per second. The total temperature of the air supply was subject to diurnal and seasonal variations, and the lapsed time from fill. Over the several experimental runs, the variation of total temperature of the primary and secondary flow was a maximum of 24^{o} F. The secondary supply for the inert gases, nitrogen, ethane, helium and argon, consisted of standard bottles which were maintained at inside ambient temperature.

The total pressure of the primary and secondary flows were maintained within one psig of design conditions by the regulator systems.

The wedge model was mechanically secured with respect to the centerline of supersonic nozzle to an accuracy of one minute of arc.

The static pressure variation of the surface of the wedge was obtained by means of a system of manometers; the readings were recorded to the nearest tenth of an inch of mercury.

2.3 Parameters

2.3.1 Angle of Attack

The angle of attack of the wedge model was varied from -5 degrees to 15 degrees in 5 degree increments.

2.3.2 Molecular Species of Injectant

The principal experiments were run using dry air as an injectant. In order to evaluate the effect of density variations, several runs were using nitrogen, helium, and argon in sequence. The primary and secondary flow total temperature and pressure was held constant and the secondary injectant was changed by means of a three-way valve system. The effect of density variation was obtained by a comparison of the corresponding shadowgraph pictures and the pressure maps of the model surface.

2.3.3 Mass Flow Rate of Injectant

The mass flow rate was increased by increasing the width of the injection slot. In the first series of experiments, the slot width was maintained at 0.012 inches. This series was later reproduced with a slot width of 0.024 inches and the corresponding results were compared with respect to the shadowgraph pictures and the pressure maps.

2.3.4 Total Pressure of Injectant

During each run, the total pressure of the injectant was varied from 50 psig to 250 psig in five equal increments.

2.3.5 Specific Heat of Injectant

A run was made utilizing nitrogen and ethane as the injectants. The molecular weight and specific heat at constant pressure, C_p, for nitrogen are 28.02 and 0.245 (399^{o} R), whereas the values for ethane are 30.07 and 0.367 (421^{o} R). The experiment was conducted at secondary stagnation pressures of 50 and 100 psig.

3. RESULTS

The data from the experimental investigation is presented in two forms:

a. shadowgraph pictures of the flow field; and

b. surface pressure distributions on the wedge model.

The purpose of the photographic data was to provide insight as to the structure of the flow field in terms of shock formation, boundary layer separation, level of turbulence, etc. In addition, when possible, measurements were made from the scaled photographs to check separation distances, height of separated regions, and penetration height of the secondary jet.

The surface pressure measurements were used to obtain points of boundary layer separation, integrated values of the side force due to the jet interaction, and to derive scaling parameters.

3.1 Flow Visualization

Shadowgraphs of the flow field produced by the transverse sonic jet are presented in Figs. 6-20. In these photographs, the flow is from right to left. The vertical etched line represents the exit plane of the nozzle blocks. Significant flow parameters are presented on each photograph. Moving from right to left in the photographs, the oblique shock at the tip of the wedge is followed by a separation shock at the point of boundary layer separation. At the point of boundary layer separation the boundary layer is turbulent, with a length Reynolds number of at least 7 x 10^6. The separation shock merges with a bow shock caused by the secondary jet. Between the separation and bow shocks, there is a region of boundary layer separation on the wedge surface. Downstream of the slot is a second region of boundary layer separation which terminates in or is intersected by a recompression wave. The apparent boundary layer or wake downstream of the recompression wave shows large scale turbs and the boundary layer or wake is approximately ten times thicker than the boundary layer prior to the initial separation upstream of the slot. In the upper right hand corner of the photograph a Mach wave may be observed that originates at the surface of the nozzle block at the exit plane. This wave traverses the flow field intersecting the surface of the wedge downstream of the recompression wave. A second Mach line can be seen which is due to the intersection of the forward oblique shock and the slip line between the flow from the nozzle blocks and atmosphere. In an attempt to avoid the interference effects because of the aforementioned Mach wave, the "cutoff point" for the integration of surface pressure was chosen as 0.70 inches downstream of the slot. This was in all cases, except the 0^0 and -5^0 angle of attack cases, at least five boundary layer thicknesses upstream of the point of interaction.

In most cases, the size and shape of the separate zones, as well as the penetration height of the secondary jet can be determined from the photographs. The zones are outlined in Fig. 6. It is also evident from Fig. 6 that the boundary layer or wake downstream of the recompression wave is highly turbulent.

From a comparison of the various photographs taken under different test conditions, the following general observations may be made:

a. For a given angle-of-attack and slot width, an increase in secondary pressure increases the size of the separated zones and the height of penetration of the secondary jet.

b. For a given slot width and secondary pressure, there is little variation in size and shape of the separated zones as a function of angle-of-attack. However, the overall shock structure is inclined more downstream as the angle-of-attack decreases.

c. At constant angle-of-attack and constant secondary pressure, the different gases all exhibit a very similar boundary layer separation and shock structure.

The unsteadiness of the flow, which is evidenced by the shock structure in several of the photographs is attributed principally to the mechanical vibration of the tunnel. This vibration is a result of the high flow rate of the primary air coupled with the lack of damping associated with the cantilever construction. A comparison of runs made under identical conditions demonstrated that the vibration did not affect the reproducibility of the data systems.

In some of the photographs it was not possible to identify the penetration height of the secondary flow. This is considered to be caused either by turbulence associated with the separated zones and/or a lack of sufficient local contrast ratio on the shadowgraph negative.

For the experiments at angles-of-attack of 0 and -5 degrees, it was determined that the initial position of the model with respect to the nozzle blocks caused choking of the flow on the underside of the model. For these runs, the model was moved downstream so that the leading edge of the model was at the exit plane of the nozzle blocks.

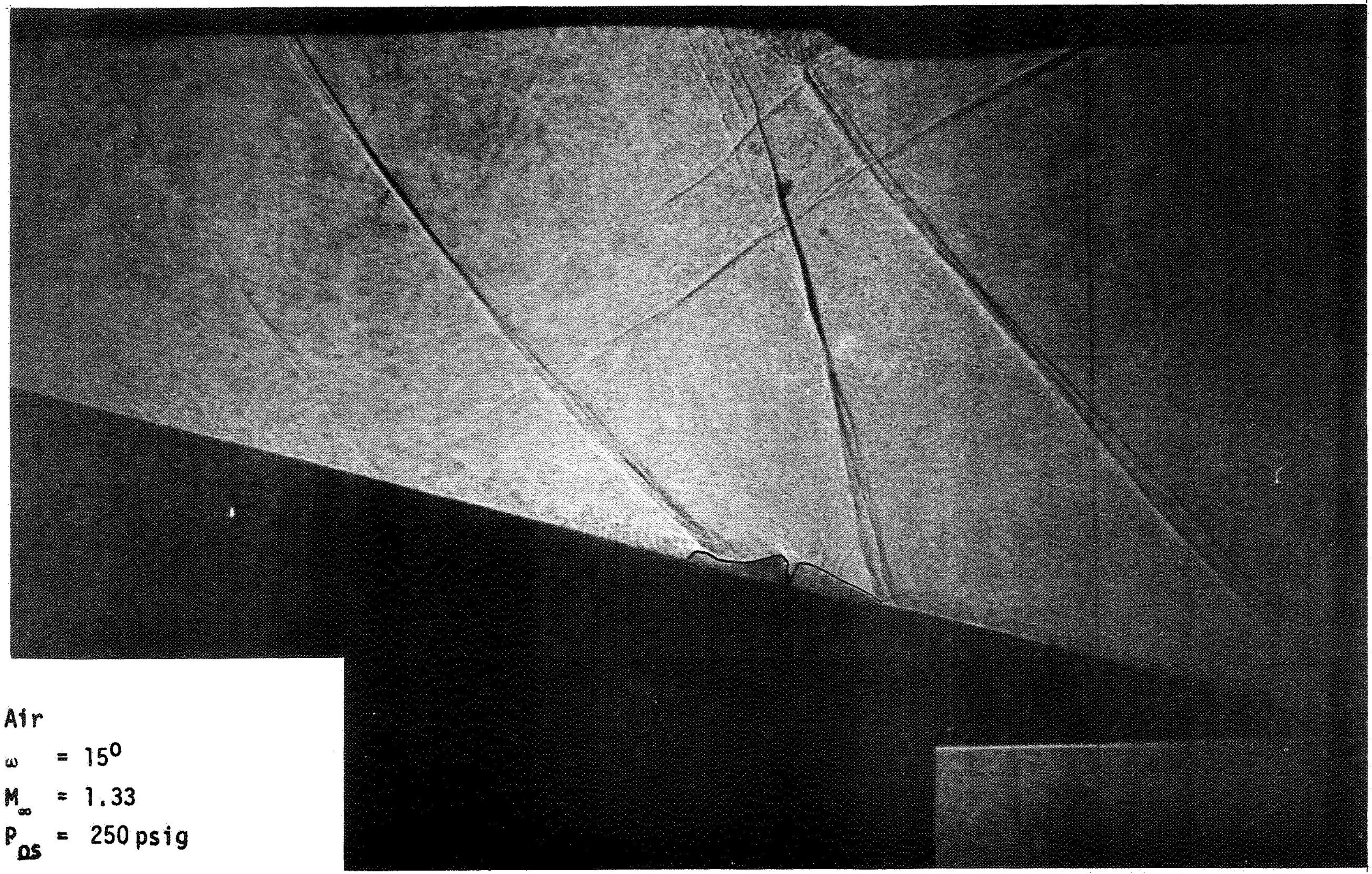

Air

$\omega = 15^{o}$

$M_{\infty} = 1.33$

$P_{os} = 250$ psig

Figure 6. Shadowgraph

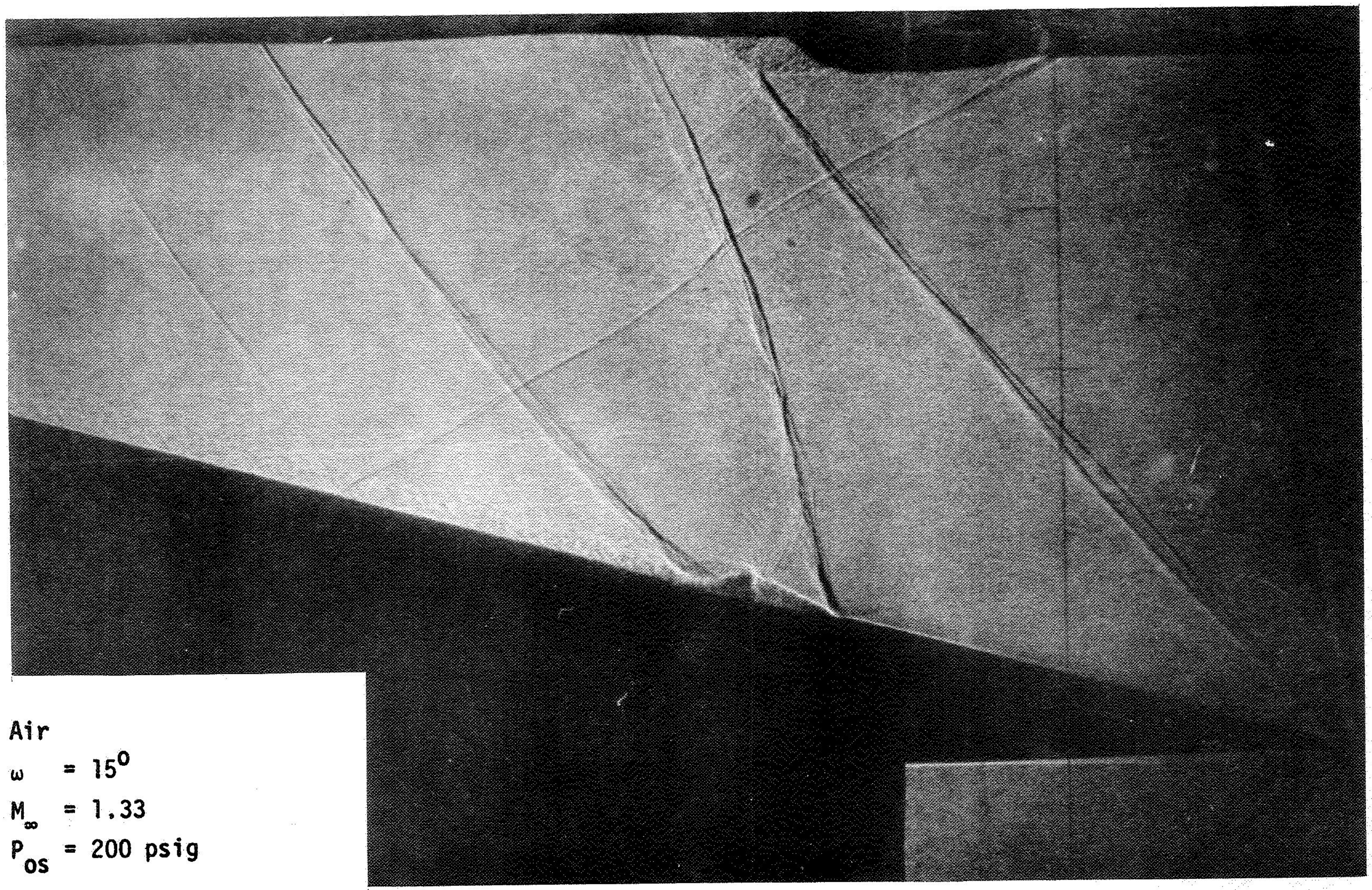

Air

$\omega = 15^{o}$

$M_\infty = 1.33$

$P_{os} = 200$ psig

Figure 7. Shadowgraph

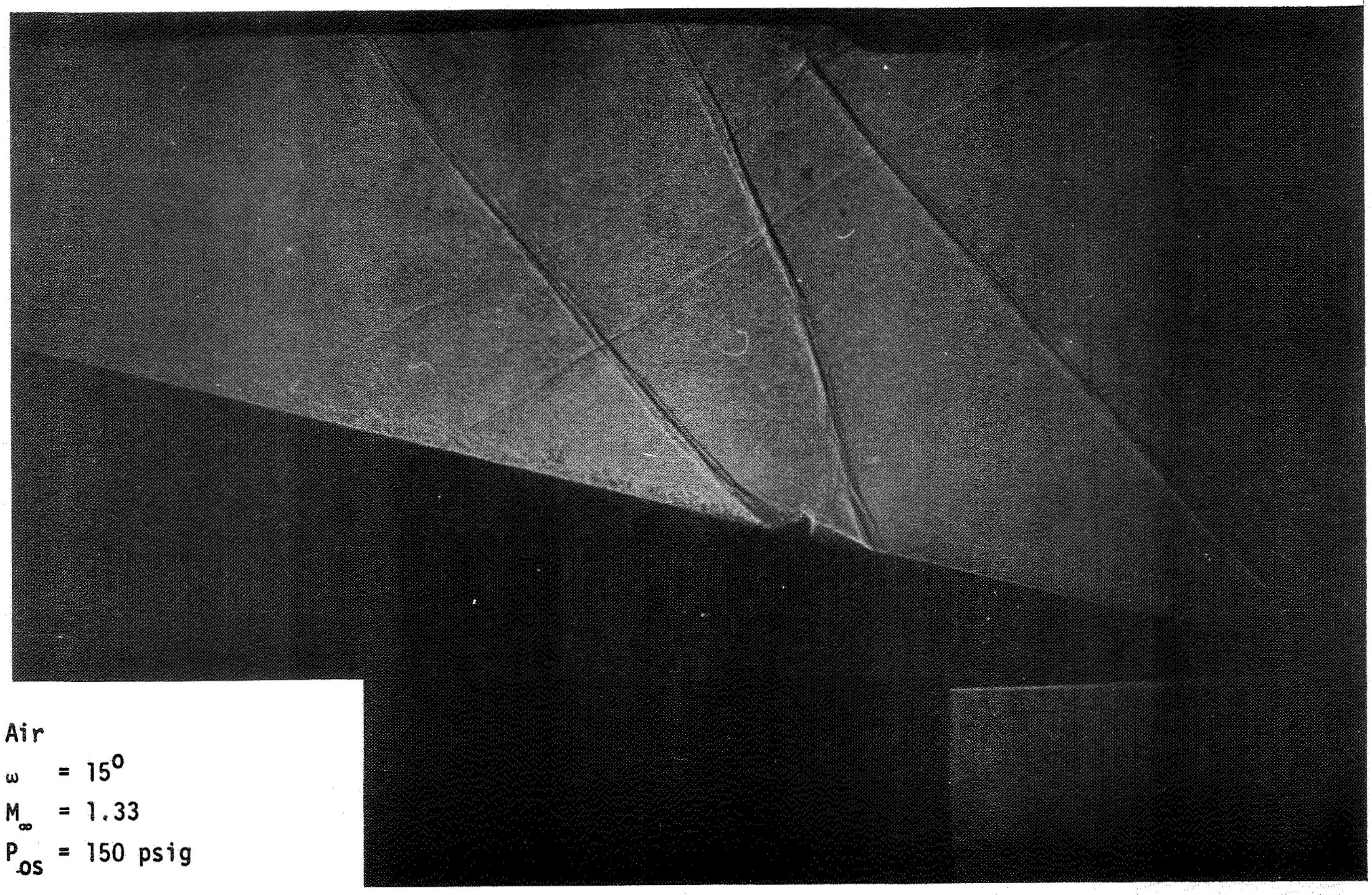

Air

$\omega = 15^{o}$

$M_{\infty} = 1.33$

$P_{os} = 150$ psig

Figure 8. Shadowgraph

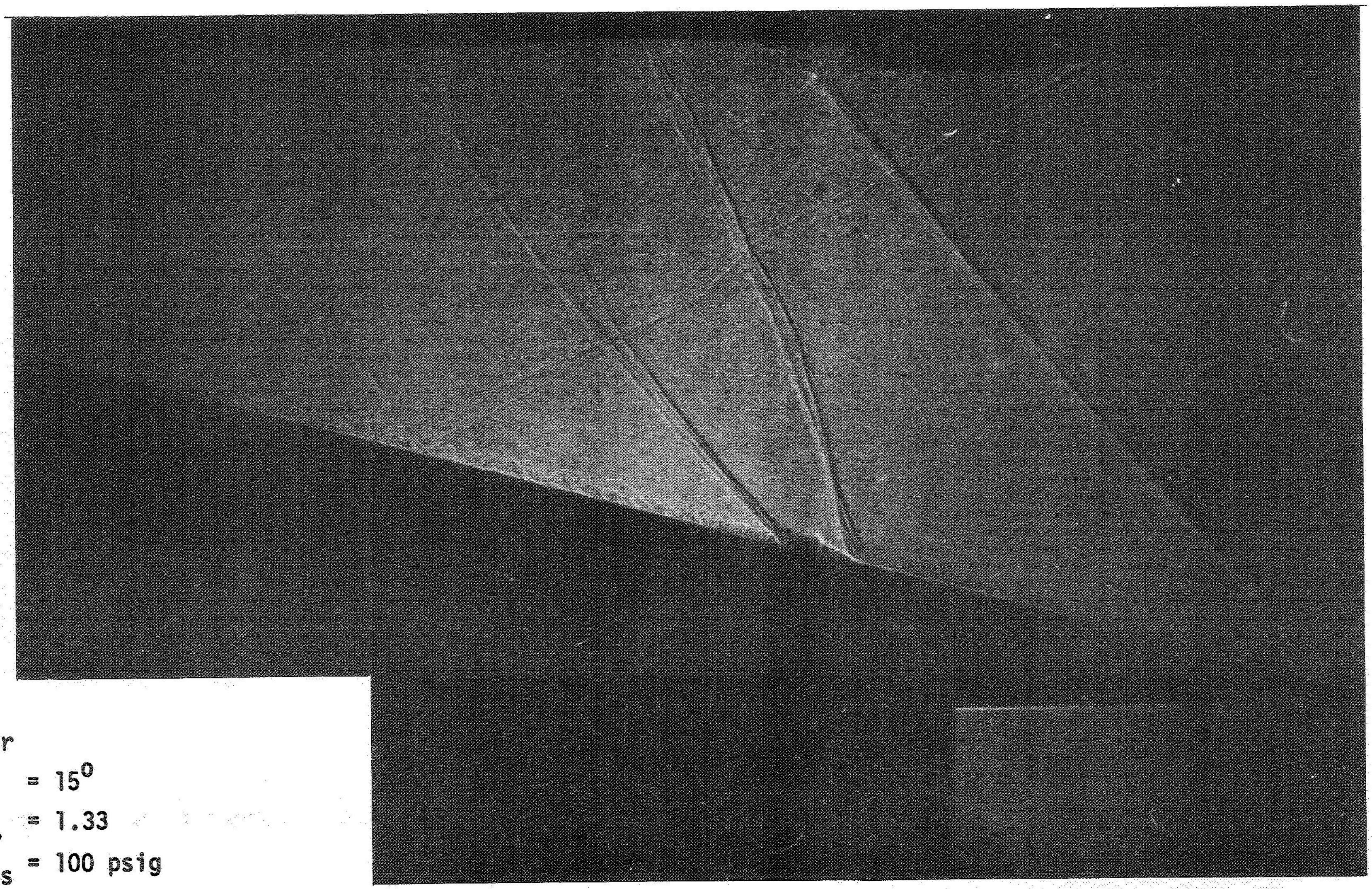

Air

$\omega = 15^{o}$

$M_{\infty} = 1.33$

$P_{os} = 100$ psig

Figure 9. Shadowgraph

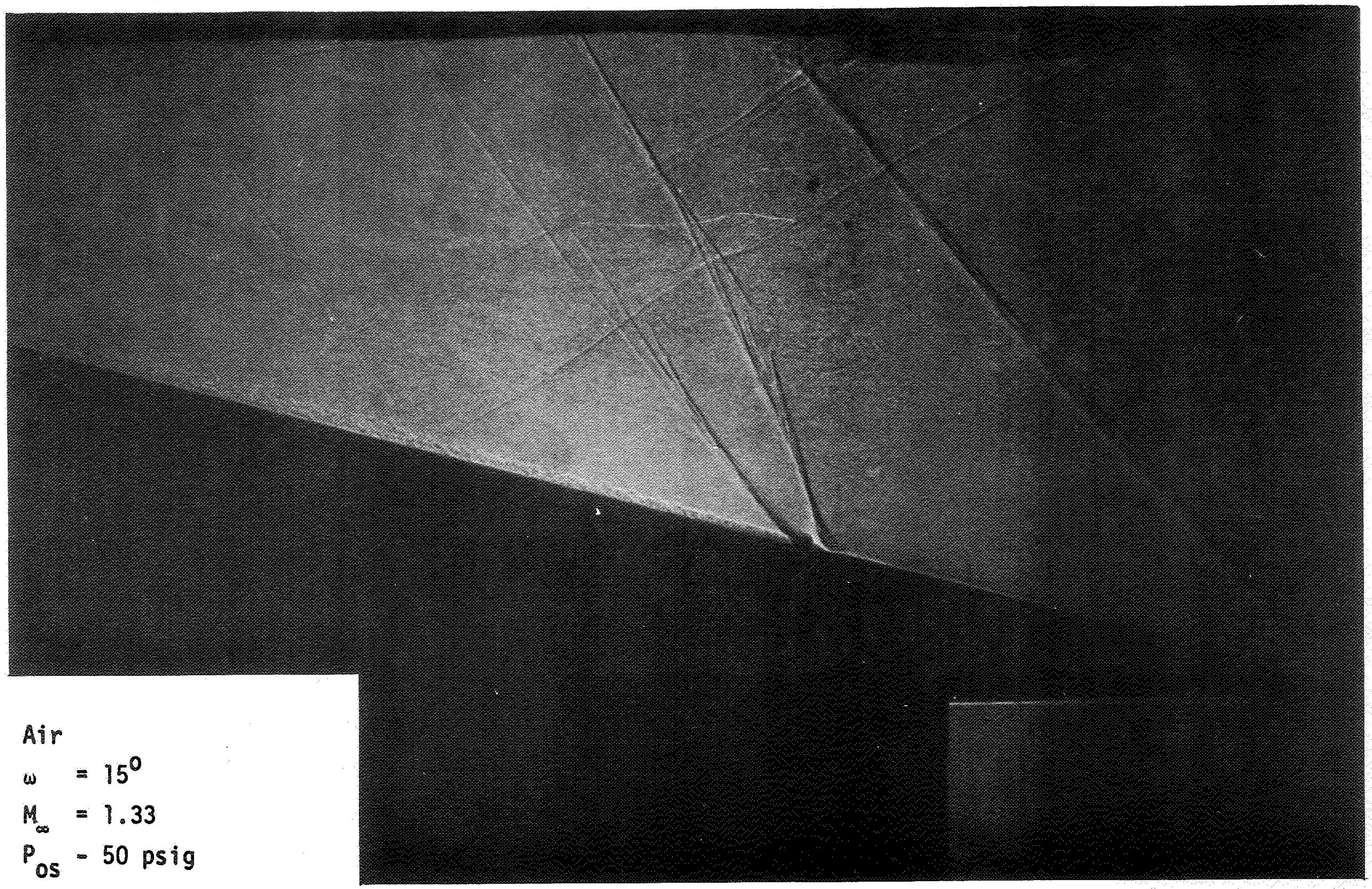

Air

$\omega = 15^{o}$

$M_{\infty} = 1.33$

P_{os} - 50 psig

Figure 10. Shadowgraph

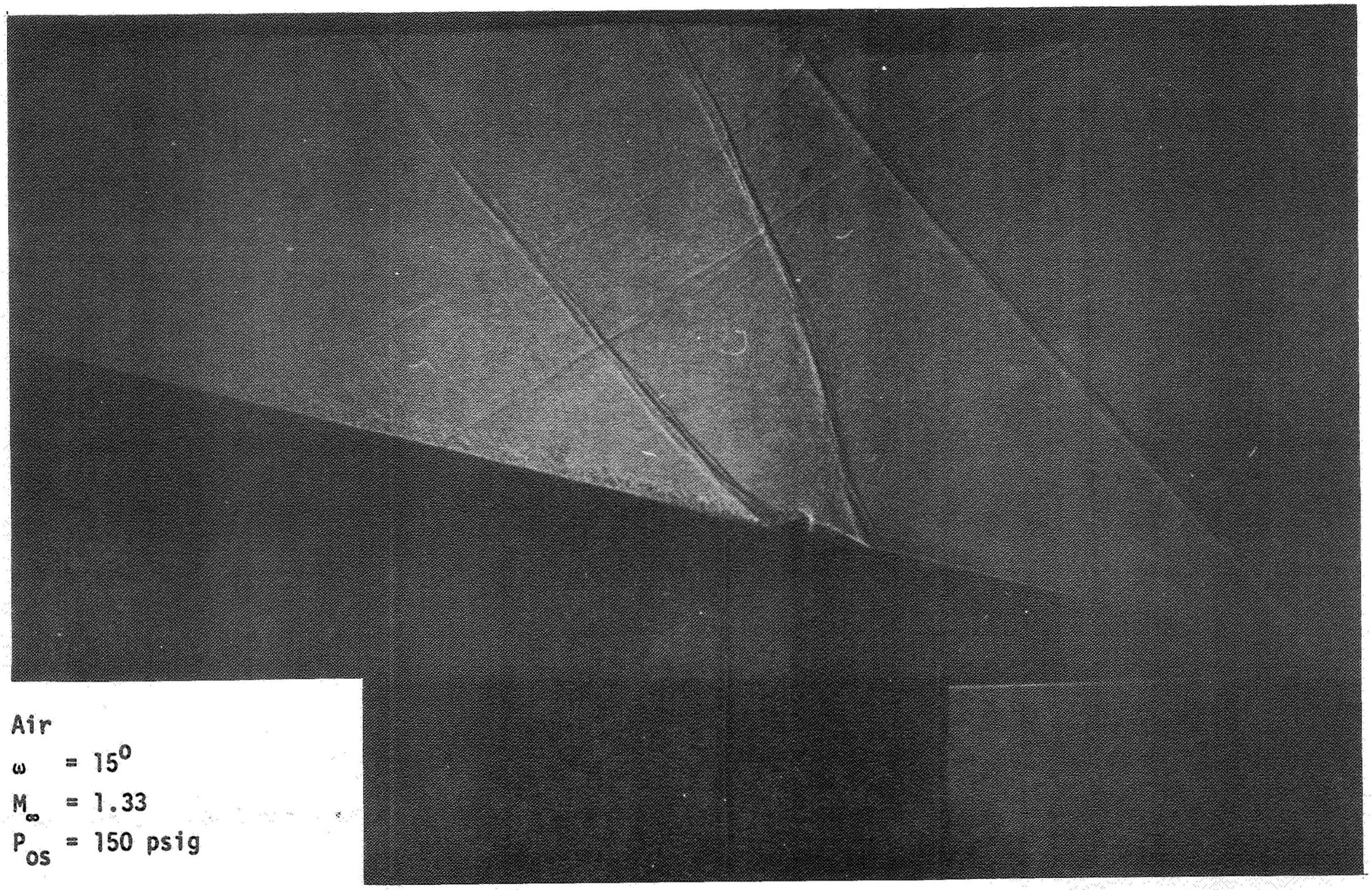

Air

$\omega = 15^{o}$

$M_{\infty} = 1.33$

$P_{os} = 150$ psig

Figure 11. Shadowgraph

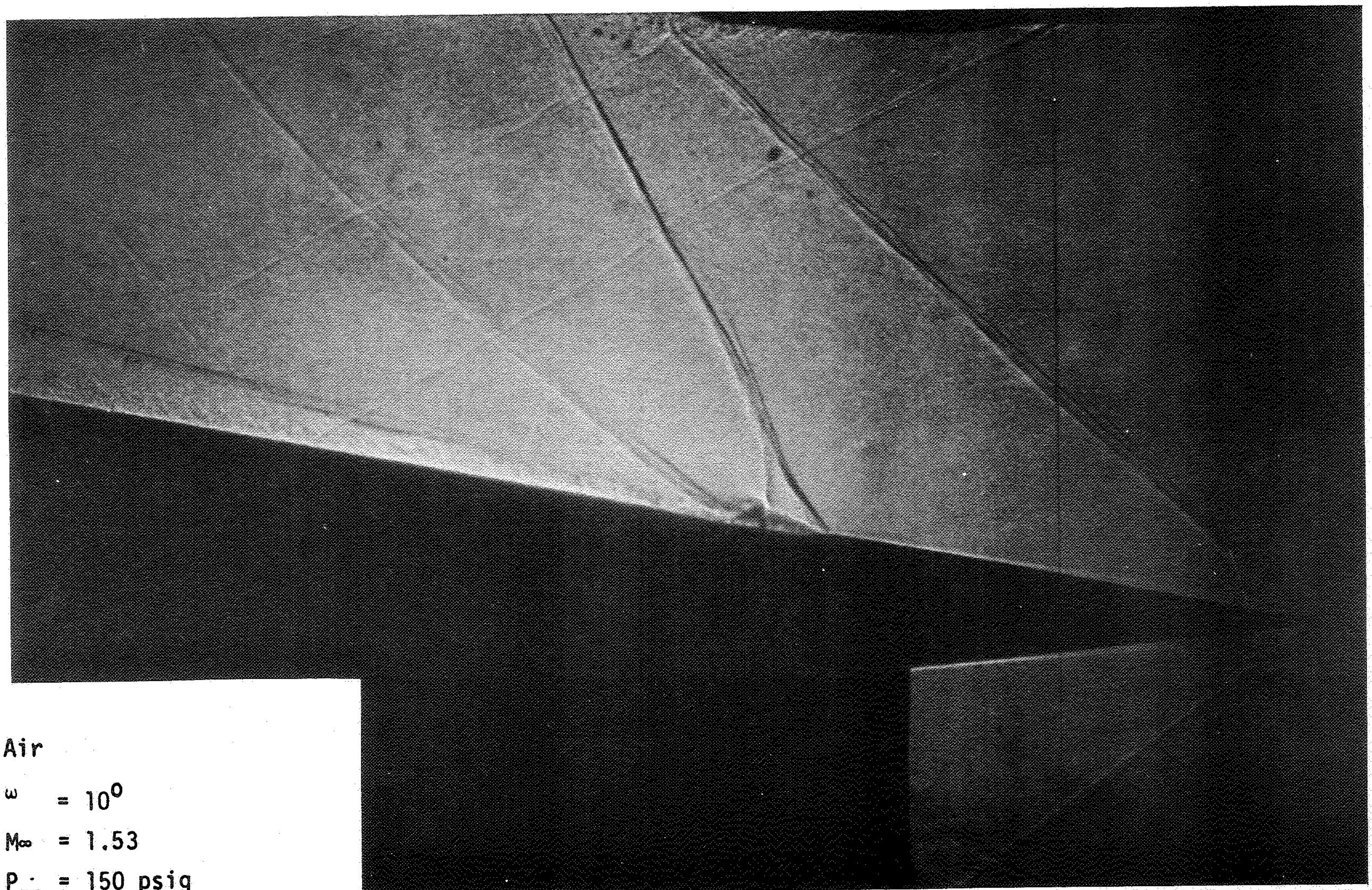

Air

$\omega = 10^{o}$

$M_\infty = 1.53$

$P_{os} = 150$ psig

Figure 12. Shadowgraph

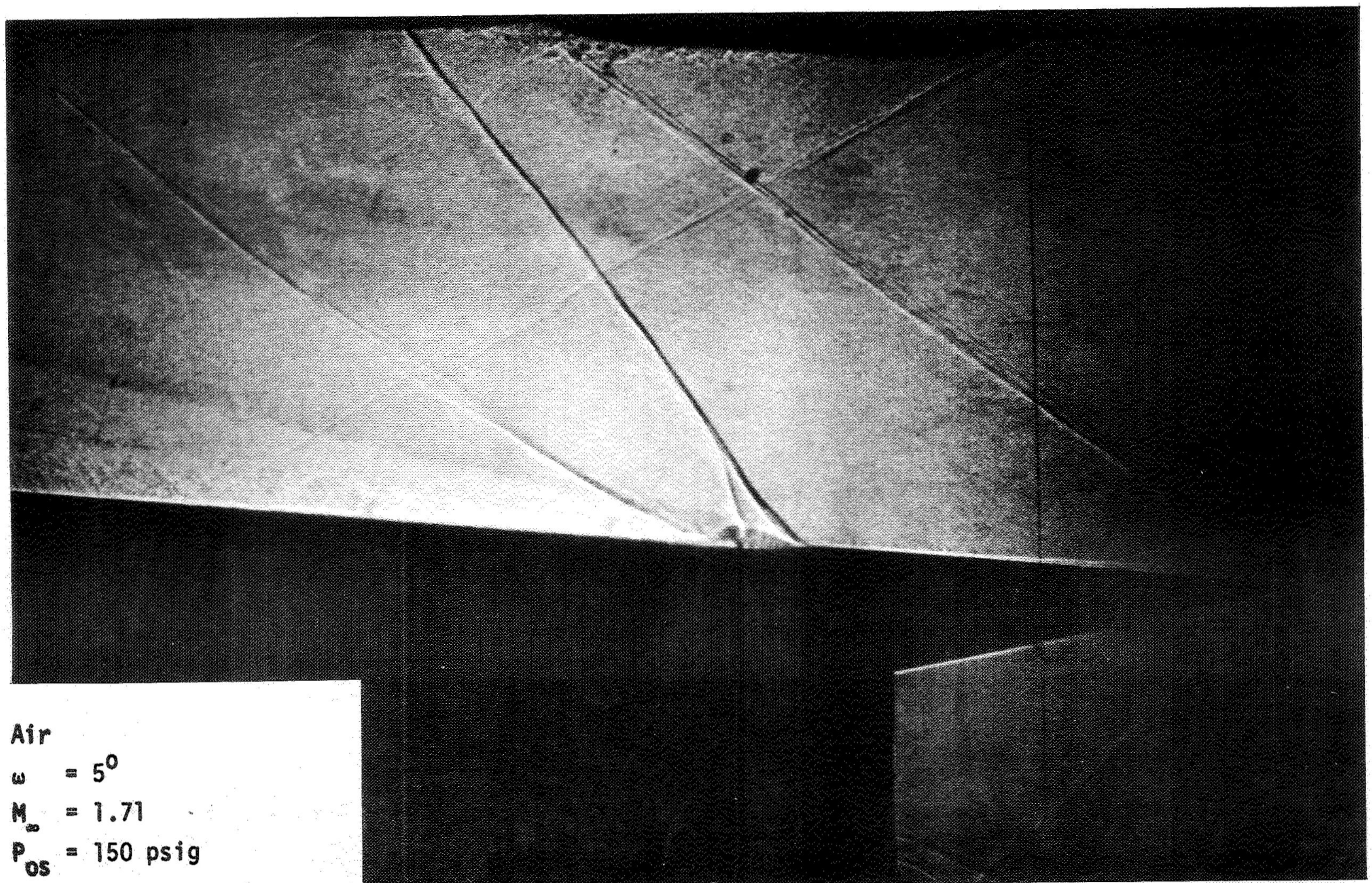

Air

$\omega = 5^{o}$

$M_{\infty} = 1.71$

$P_{os} = 150$ psig

Figure 13. Shadowgraph

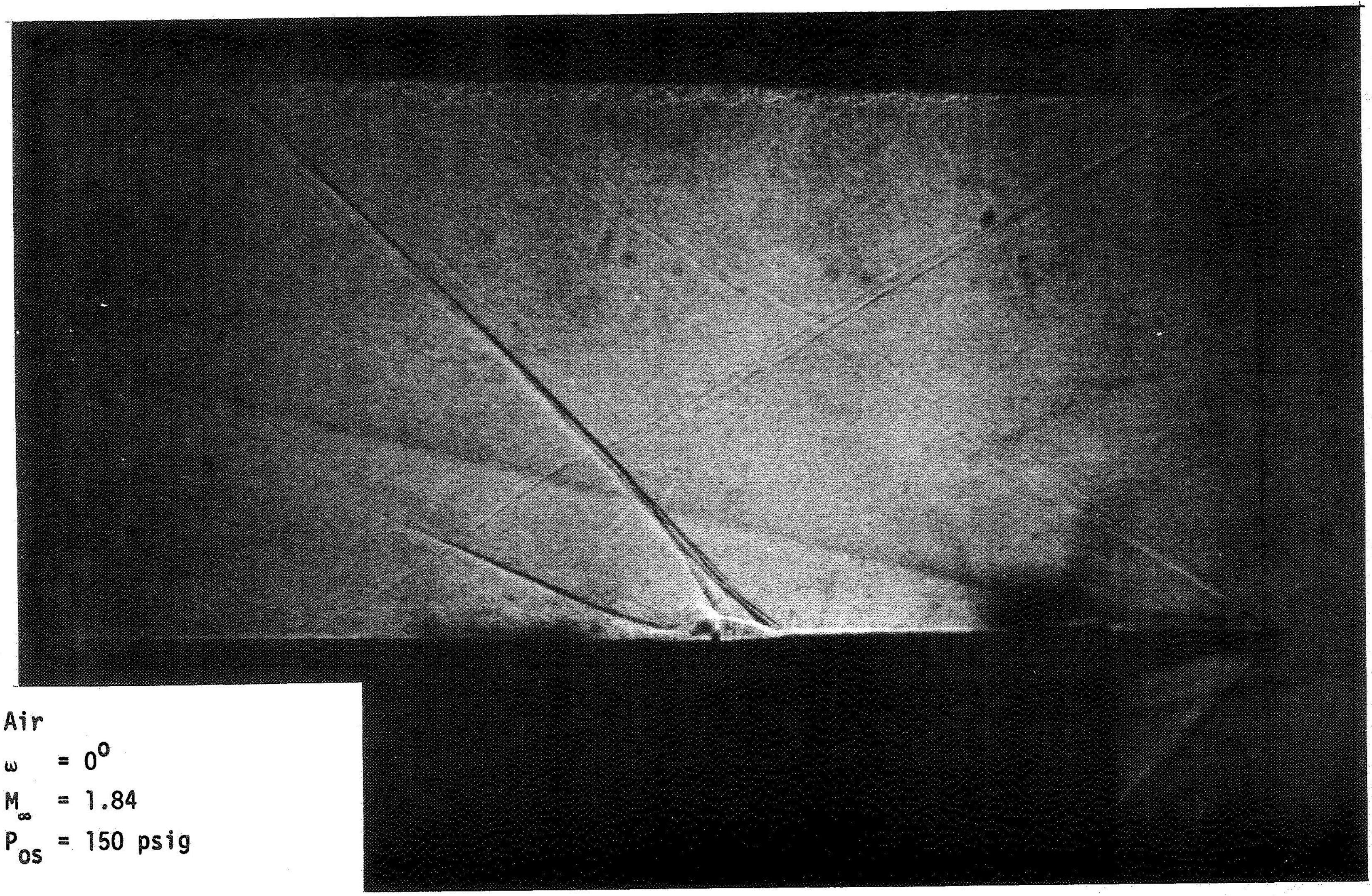

Air

$\omega = 0^{o}$

$M_{\infty} = 1.84$

$P_{os} = 150$ psig

Figure 14. Shadowgraph

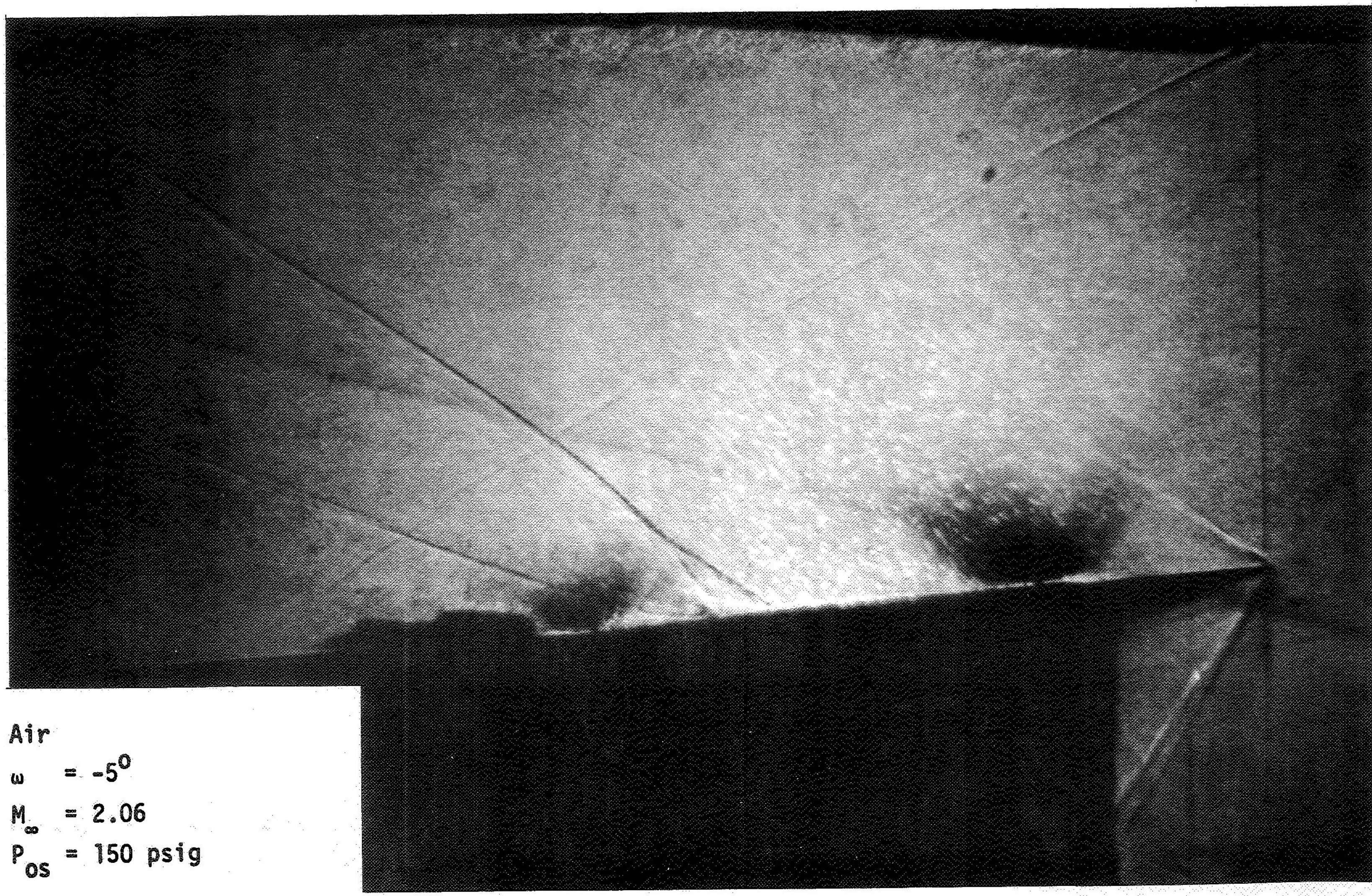

Air

$\omega = -5^{o}$

$M_{\infty} = 2.06$

$P_{os} = 150$ psig

Figure 15. Shadowgraph

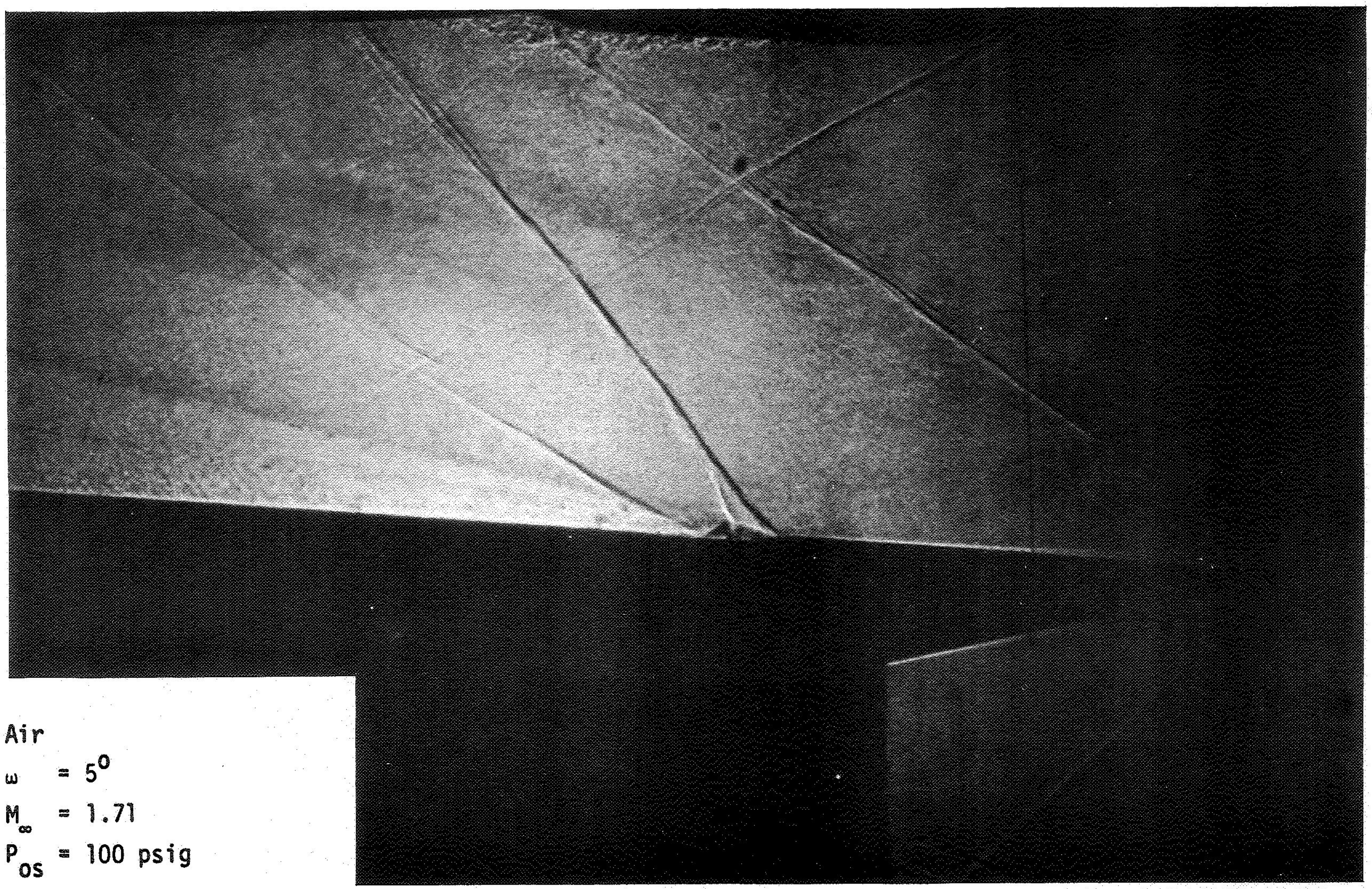

Air

$\omega = 5^{o}$

$M_{\infty} = 1.71$

$P_{os} = 100$ psig

Figure 16. Shadowgraph

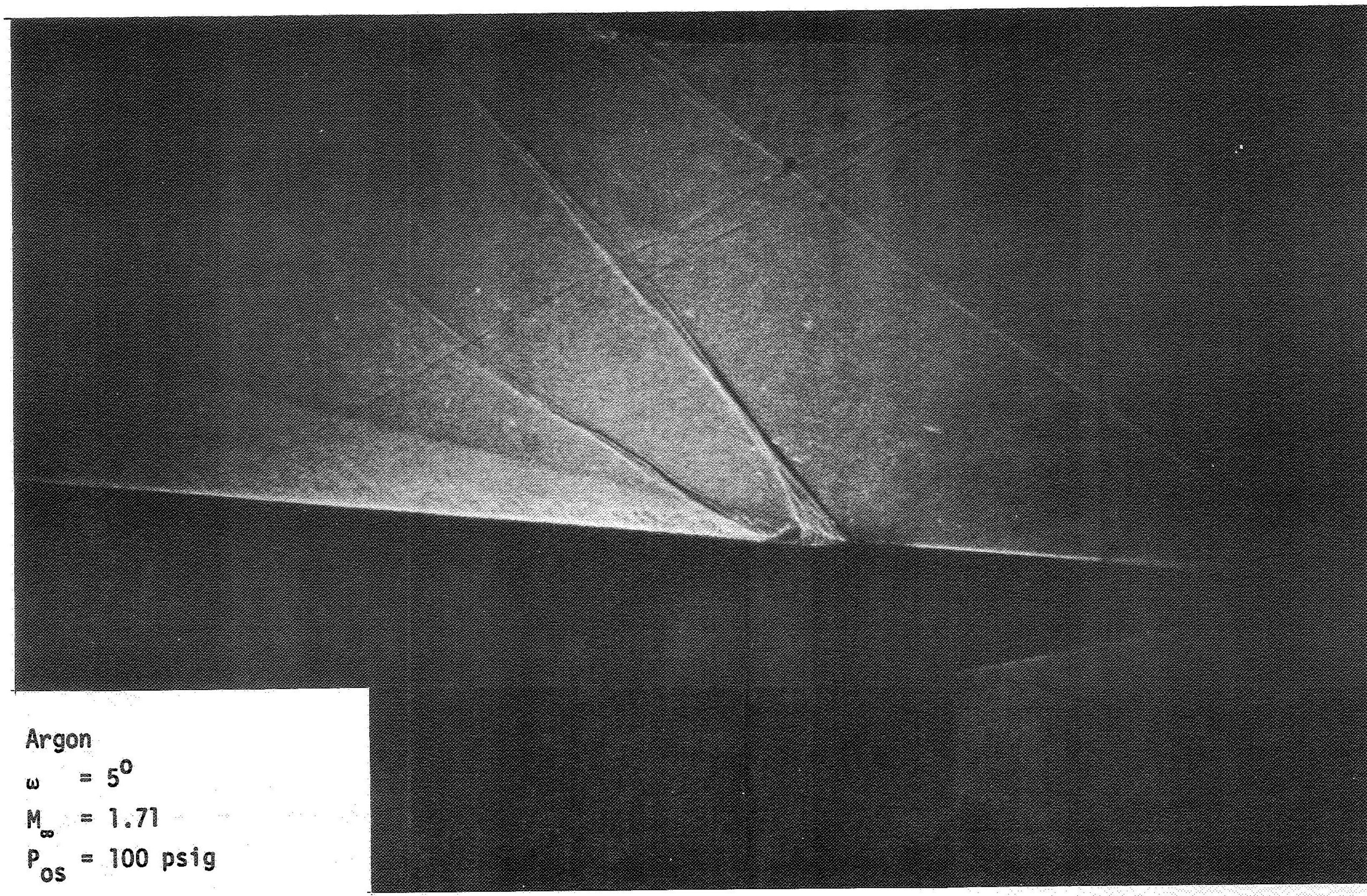

Argon
$\omega = 5^{o}$
$M_{\infty} = 1.71$
$P_{os} = 100$ psig

Figure 17. Shadowgraph

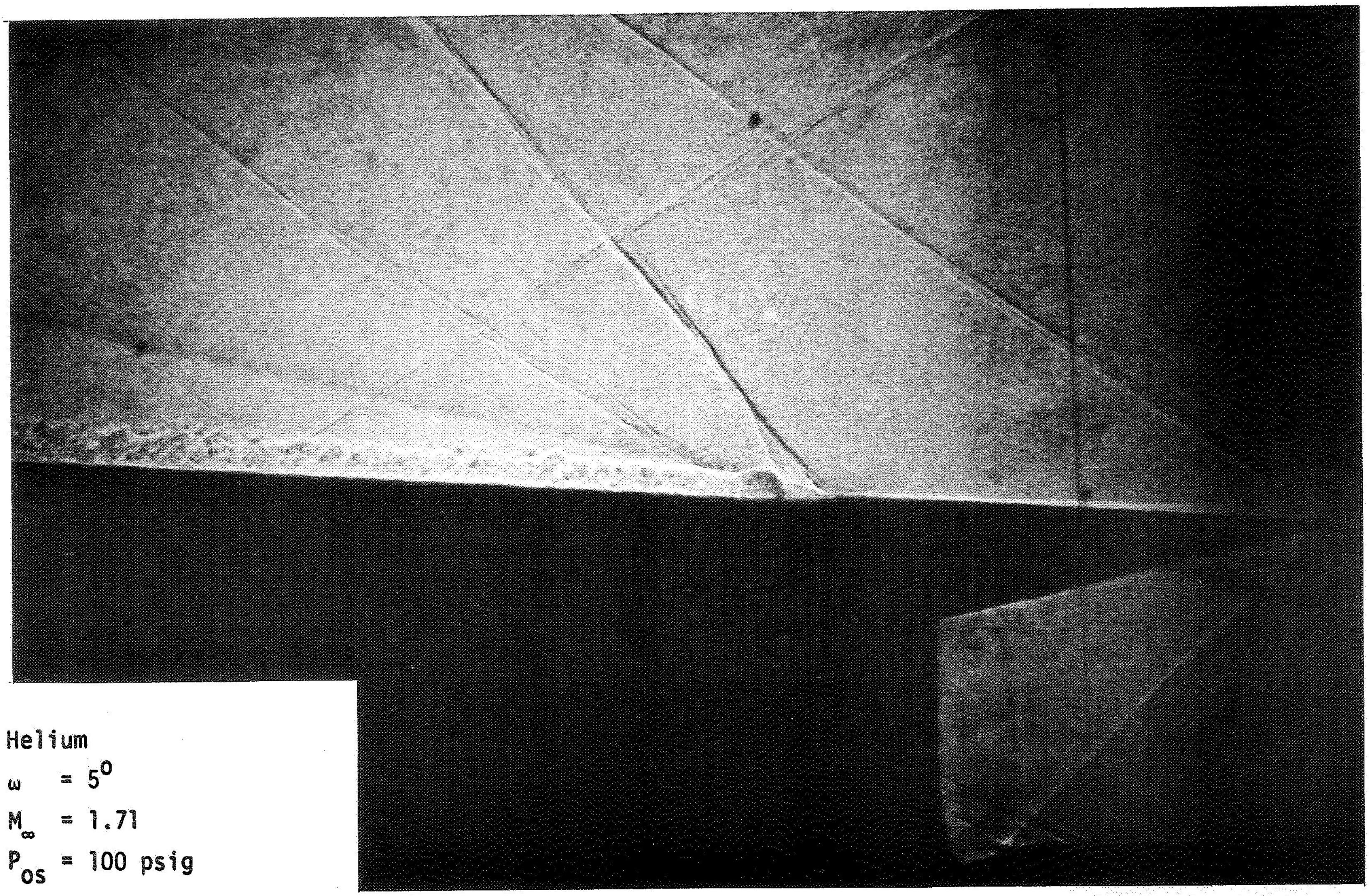

Helium
$\omega = 5^{\circ}$
$M_{\infty} = 1.71$
$P_{os} = 100$ psig

Figure 18. Shadowgraph

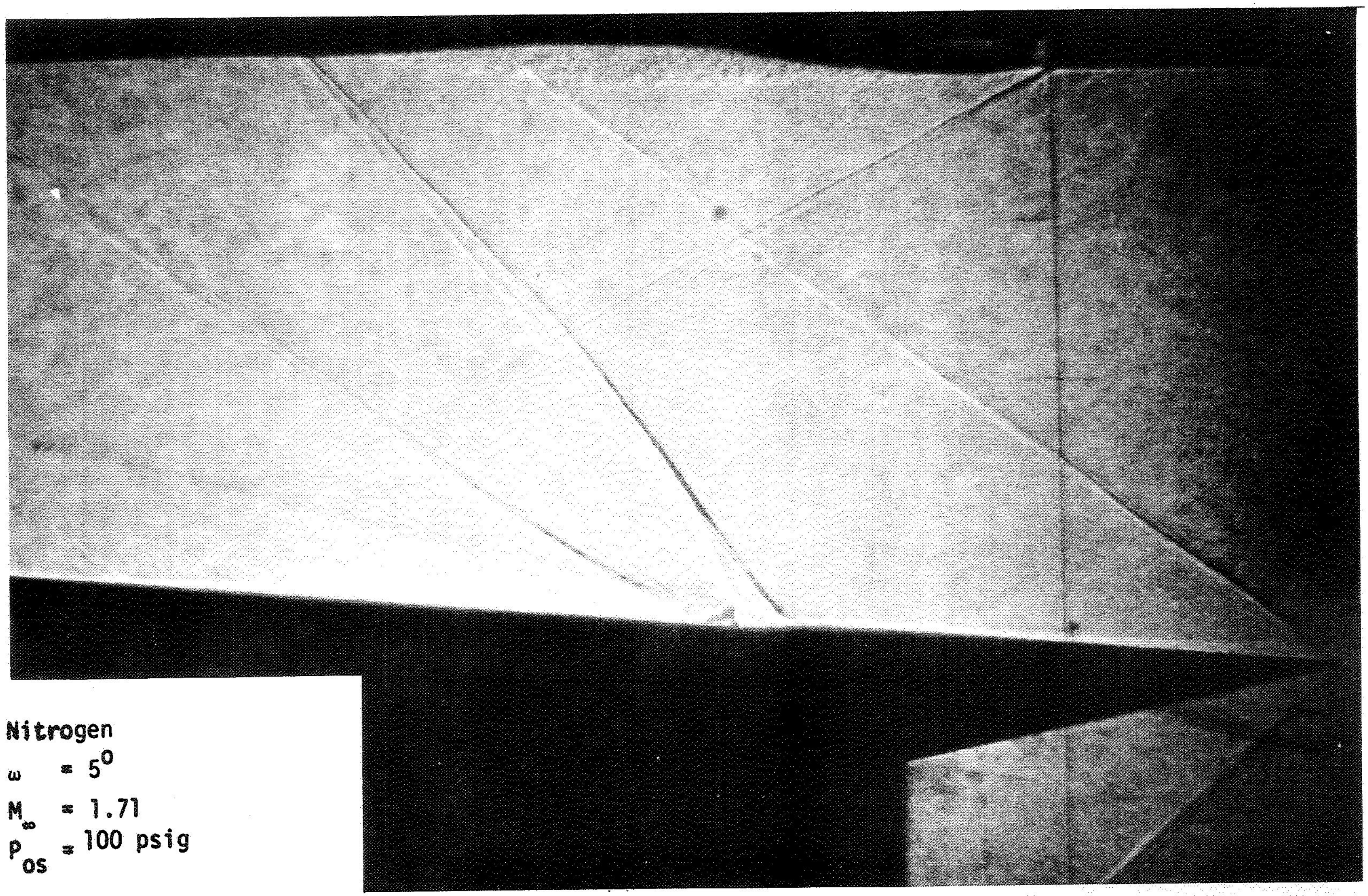

Nitrogen

$\omega = 5^{o}$

$M_{\infty} = 1.71$

$P_{os} = 100$ psig

Figure 19. Shadowgraph

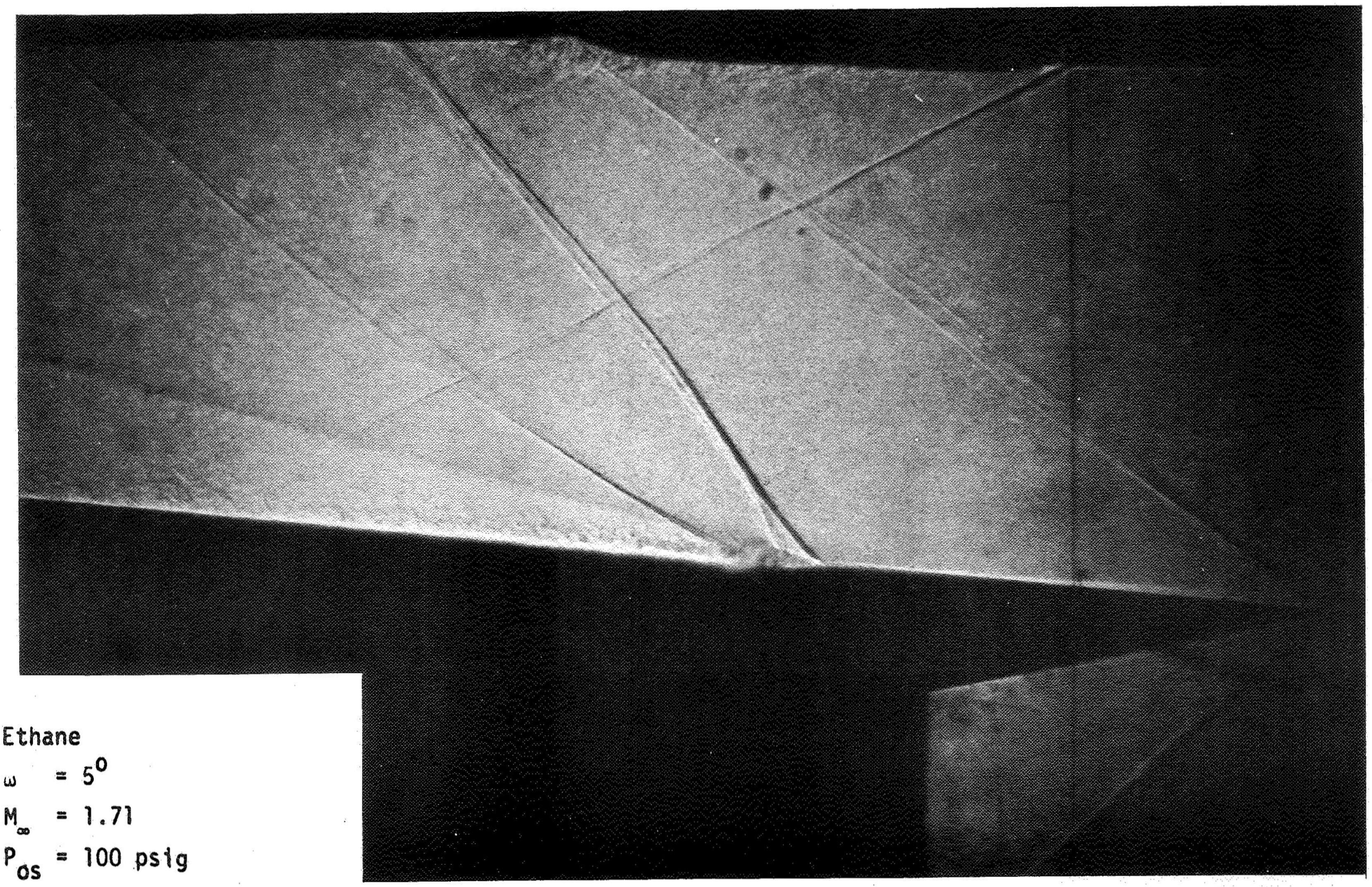

Ethane

$\omega = 5^{o}$

$M_{\infty} = 1.71$

$P_{os} = 100$ psig

Figure 20. Shadowgraph

3.2 Pressure Data

The pattern of pressure measurements was changed slightly for the various series of experimental runs to obtain a finer coverage in the areas of flow interaction. The variation is detailed in the tables in Appendix F. The actual experiment was conducted in three successive series. In the first, at a slot width of 0.012 inches, a complete set of variable angle-of-attack and secondary injection pressure experiments were run with air as the injectant to provide a basis for the determination of the effect of mass flow rate and to gain experience in operating the tunnel. In general, the shocks were too close together to separate photographically and thus determine the fine variations in the flow field. A second series of experiments were conducted with air as the secondary gas at a slot width of 0.024 inches. In this case, the flow disturbance was large enough to photograph well, but not so large as to react with the boundaries of the tunnel. Besides results on the effect of mass flow, this series was used for the evaluation of the effect of the variation secondary pressure with respect to angle-of-attack. The last series was run at constant angle-of-attack (+5 degrees) with various secondary gases.

As seen from the results tabulated in Appendix F, considerable more scatter is evident in the pressure field upstream of the onset of separation during the experiments conducted at a slot width of 0.012 inches than is the case for the runs at the 0.024 slot width. The increased scatter is attributed to small changes in model geometry caused by the "balloon effect" of the high gas pressure inside the model. When the model was disassembled for the purpose of enlarging the slot, distortions were noted on the wedge surface commencing approximately 1.5 inches upstream and downstream of the slot. Therefore, the internal structure was reinforced and no distortion was encountered in subsequent experiments. No structural deformation was noted in the vicinity of the injection slot in any of the experiments.

Mercury leaks and the partial plugging of the pressure taps by dessicant were problems that existed throughout the experiment. A loss of data from a manometer tube was attributed one or the other of these faults in every case. On the average, four manometer tubes out of 56 failed to register properly during any given run.

The criterion employed to locate the separation upstream of the slot was to select as the point of separation the pressure tap location just prior to the large pressure increased caused by the point of separation, as shown in Fig. 22. Figure 22 presents the surface pressure as a function of length for the condition shown on the figure. The separation determined from pressure measurements was in good agreement with scaled measurements from the shadowgraph, e.g., within 0.05 inches. The location of the reattachment position downstream of the slot was more difficult to determine. The shadowgraph pictures were, on the whole, less distinct because of the turbulence. The criterion used to designate the reattachment location was to select the first peak pressure in the manometer data after the slot as labeled in Fig. 22. For values of $w = 15^o$, 10^o, 5^o the first peak pressure was within the integration length used to derive the interaction force. For values of $w = 0^o$ and -5^o, the pressure data do not permit establishing a consistent criterion for determining reattachment. Pressure maps of the normalized pressure ($P_s + P\infty$), as a function of X for the 0.024 slot, air as the injectant and P_{os} = 150 psia, are presented in Figs. 21-25. This is plotted as $(P_s + P_{os})/P_{os}$ vs X.

3.3 Calculations

The calculated flow parameters were obtained using isentropic tables for air, in the case of air; and isentropic perfect gas tables in the case of other gases. The secondary jet momentum thrust was calculated by assuming isentropic flow with a discharge coefficient of unity and the measured wedge surface pressure as the back pressure.

3.4 Influence of Selected Parameters

The parameters influencing the side force produced by the secondary gas injection and the nature of the flow disturbances are:

a. the secondary gas flow rate, W_s.

b. the secondary stagnation pressure, P_{os}.

c. the secondary gas properties, P_s, T_s, $_k$, molecular weight.

d. the angle-of-attack.

3.5 The Effect of A Change in Weight Flow Rate

The weight flow rate was changed by changing the area of the slot. The ratio of the areas of the two slot widths employed in this experiment was 1.93. In the second series of experimental runs the slot width was expanded from 0.012 inches to 0.024 inches, however, the span was decreased in order to strengthen the model and to insure against bowing due to the high internal pressures. The additional force, $F_i + F_j$, attributed to the change in weight flow rate increased with increasing P_{os}; the increase was less at either positive or negative angle-of-attack than at 0^o angle-of-attack. There was considerable scatter in the data and no correlation or prediction parameter was obtained. The scatter is attributed primarily to the small scale of the interaction effects at the small slot width. The average increase in the force, $F_i + F_j$ due to the approximate doubling of the secondary weight flow rate was 1.40 at 0^o angle-of-attack.

3.6 The Effect of A Change in Molecular Weight

There were minor changes in the character of the flow field and the pressure field due to changing the injectant from air to argon, nitrogen or ethane. Figure 26 presents the sum of the jet thrust and interaction force as a function secondary gas pressure for air, argon, helium, nitrogen and ethane. The total force for helium averaged about 20% higher than the other gases. This was most evident in the downstream pressure distributions. This is in good agreement with the results obtained by Newton and Spaid (12).

In an as yet unpublished experiment at the Jet Propulsion Center, R.D. Guhse alternately injected hot and cold air through a slot transverse to a Mach 2.6 free stream. The interactions in both cases were almost identical. A comparison of the Allan and Guhse experiments indicates that the composition of the mixture downstream of the injector may be more important than the density.

3.7 The Effect of Charge of Specific Heat Ratio

An experiment was conducted at an angle-of-attack of 5^o and secondary stagnation pressures of 50 and 100 psig with nitrogen and ethane. The molecular weight and specific heat at constant pressure for nitrogen are 28.02 and 0.245 (399^oR); and for ethane, 30.07 and 0.367

(421^oR) respectively.

There was no discernable difference in the flow structure or the pressure fields for the alternate injection of nitrogen and ethane. This would indicate that a variation in the specific heat ratio has little or no effect on the interaction between the jet and the free-stream for the conditions of the experiment where the difference between the static temperature of the primary and secondary stream was approximately 130^oF.

3.8 The Effect of Changes in Angle-of-Attack

Figure 27 presents the sum of the jet and interaction force, $F_i + F_j$ as a function of the secondary injection pressure P_{os} for various angles-of-attack. Variations in the angle-of-attack produced the most dramatic changes in the results of all the parameters investigated. The following results were observed:

a. The resultant force, $F_i + F_j$ increased with increasing values of P_{os} for all angles-of-attack.

b. The resultant force, $F_i + F_j$ decreased between $\omega = 0^o$ and $\omega = -5^o$ for each value of P_{os}.

c. The resultant force, $F_i + F_j$ initially decreased for positive angle-of-attack ($+5^o$), increased at $\omega = 10^o$, and decreased for $\omega = 15^o$ for each value of P_{os}.

d. The flow interaction for values of $\omega = 0^o, -5^o$ extended downstream past the point of Mach line interaction from the nozzle exit plane. This resulted in considerable scatter in the data obtained during these experiments.

e. The length of the region of boundary layer separation upstream and downstream of the slot increased for increasing values of P_{os} and decreased with increasing angles-of-attack, starting at $\omega = -5^{o}$. The jet was sonic for all other experiments except for $\omega = 15^{o}$, both slot widths, and $P_{os} = 50$ psig, the secondary jet was subsonic.

A prediction factor was derived for values of $= 15^{o}, 10^{o}, 5^{o}$ such that the interaction force F_i could be predicted from the known values of F_a and F_j. This can be stated as:

$$C^{n} (F_j + F_a) = (F_i + F_j + F_a) = F_t$$

where n is an integer 0, 1, 2, 3 .... corresponding to values of P_{os} = 0, 50, 100, ... psig and C is a constant equal to 1.023. The curves in Fig. 28 are calculated from the above expression. The data points are experimental results. As can be seen the agreement is satisfactory.

3.9 Comparison of Results

A direct comparison of the results of this experiment with previously published results is difficult. Most of the published wind tunnel data were obtained at much lower values of the primary stagnation pressure than those employed in this experiment. No results were found in the literature to compare with the experimental results of this study in either the flow visualization and pressure distribution at angle-of-attack. The only generally accepted model is for flat plate conditions and this model is based principally on a inviscid or inertial interaction. The "scaling" parameters that have proved the most effective in correlating results are the scale height of the secondary jet (12) and the vacuum force coefficient (3). As mentioned earlier in 3.1, in some of of the shadowgraph pictures it was not possible to identify the penetration envelope of the secondary flow. Therefore no attempt was made to correlate these results with previously published data on scale heighth. An attempt at correlation was made using the vacuum force coefficient, C_{n_v} where:

$$C_{n_v} = \frac{\left(\frac{WV_s}{g} + P_s A_s\right)}{1/2\ P_{os} V_{os}^{2}\ (\text{Planform Area})}$$

The planform area was taken as the sum of the upstream and downstream separation distances multiplied by the width of the wedge model. A plot of the interaction force F_i vs C_{n_v} was made and it was approximately linear for each experimental run, however, there was no discernable correlation between the several runs. The region of the interaction has been considered to be effectively terminated by the downstream recompression wave. For the higher value of stagnation pressure of the primary stream employed in this investigation, it appears that viscous effects predominate and that the interaction is terminated well downstream of the recompression wave. The interaction upstream of the injection slot appears to be similar in both this and other investigations, except that the onset of separation is much more abrupt.

The reported result of a relative increase in the force effectiveness near 10^{o} angle-of-attack is similar to a result reported by Boeing (80) in an external burning experiment. Correlation between the two results is pure conjecture because of the diverse nature of the experiments.

The qualitative results of the investigation of the effect of mass flow rate and molecular weight agree with the published literature (3).

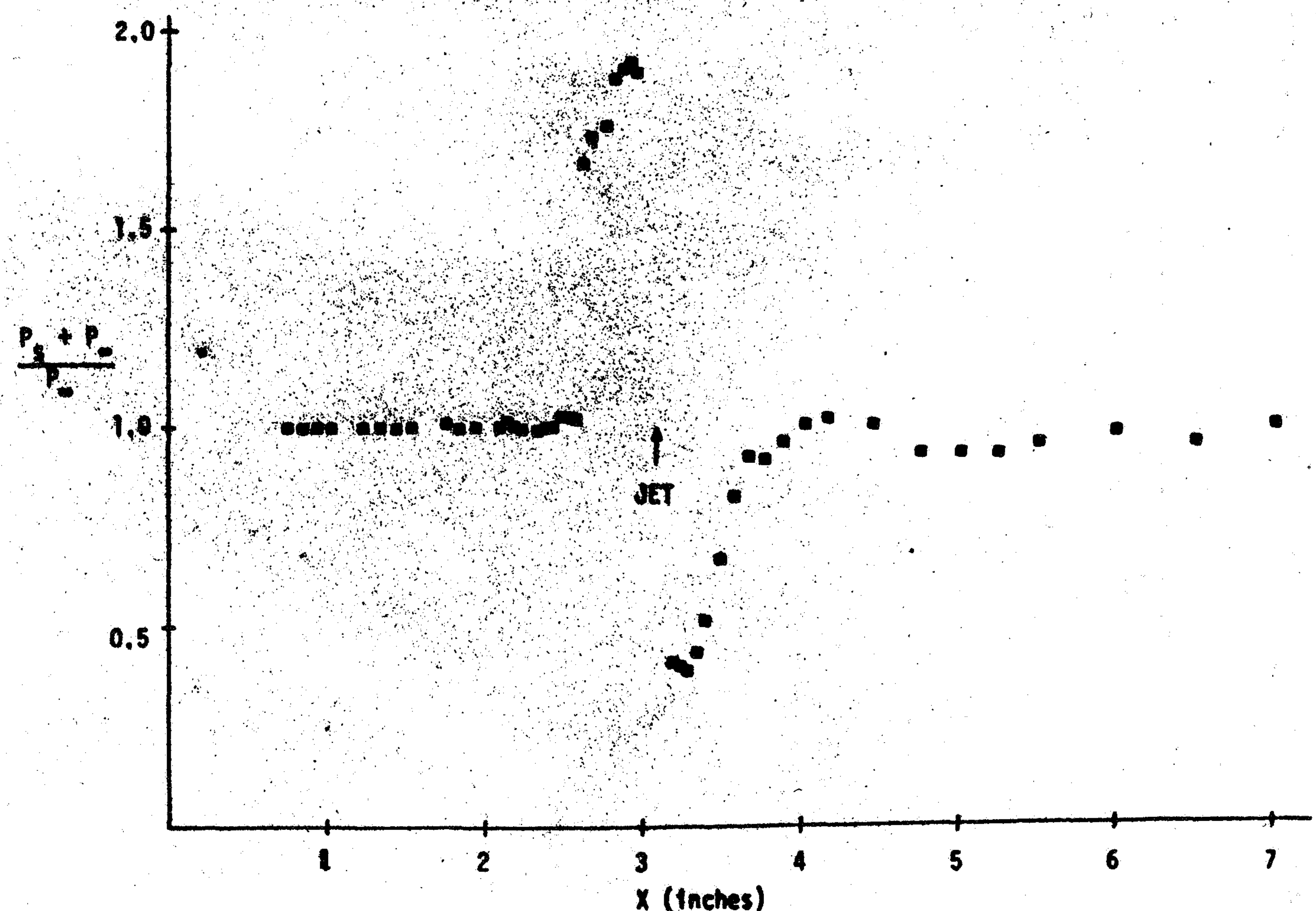

Figure 21. NORMALIZED SURFACE PRESSURE DISTRIBUTION, $\omega = -5^0$, $M_\infty = 2.06$, $P_{os} = 150$ psia

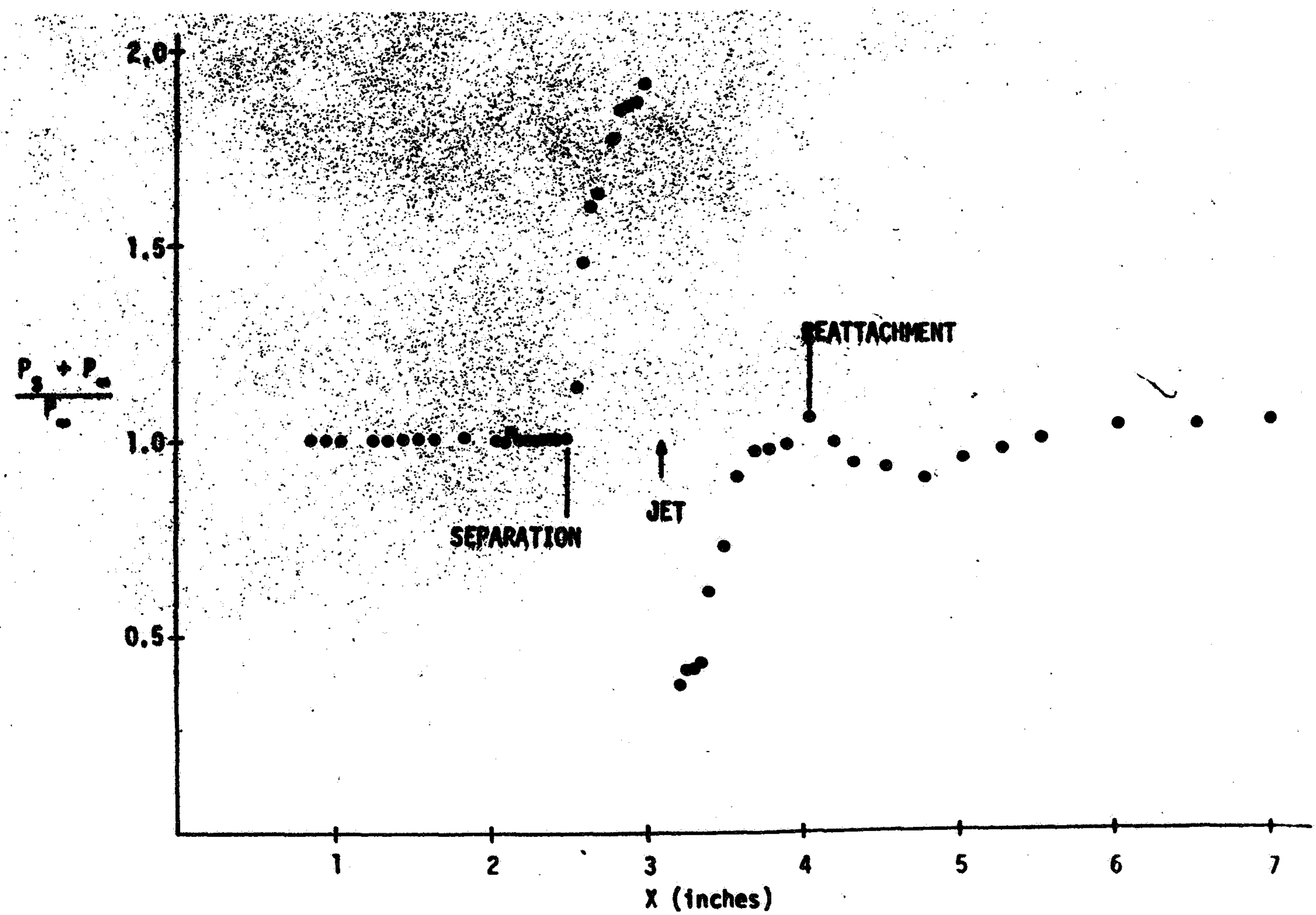

Figure 22. NORMALIZED SURFACE PRESSURE DISTRIBUTION, $\omega = 0^{0}$, $M_\infty = 1.84$, $P_{os} = 150$ psig

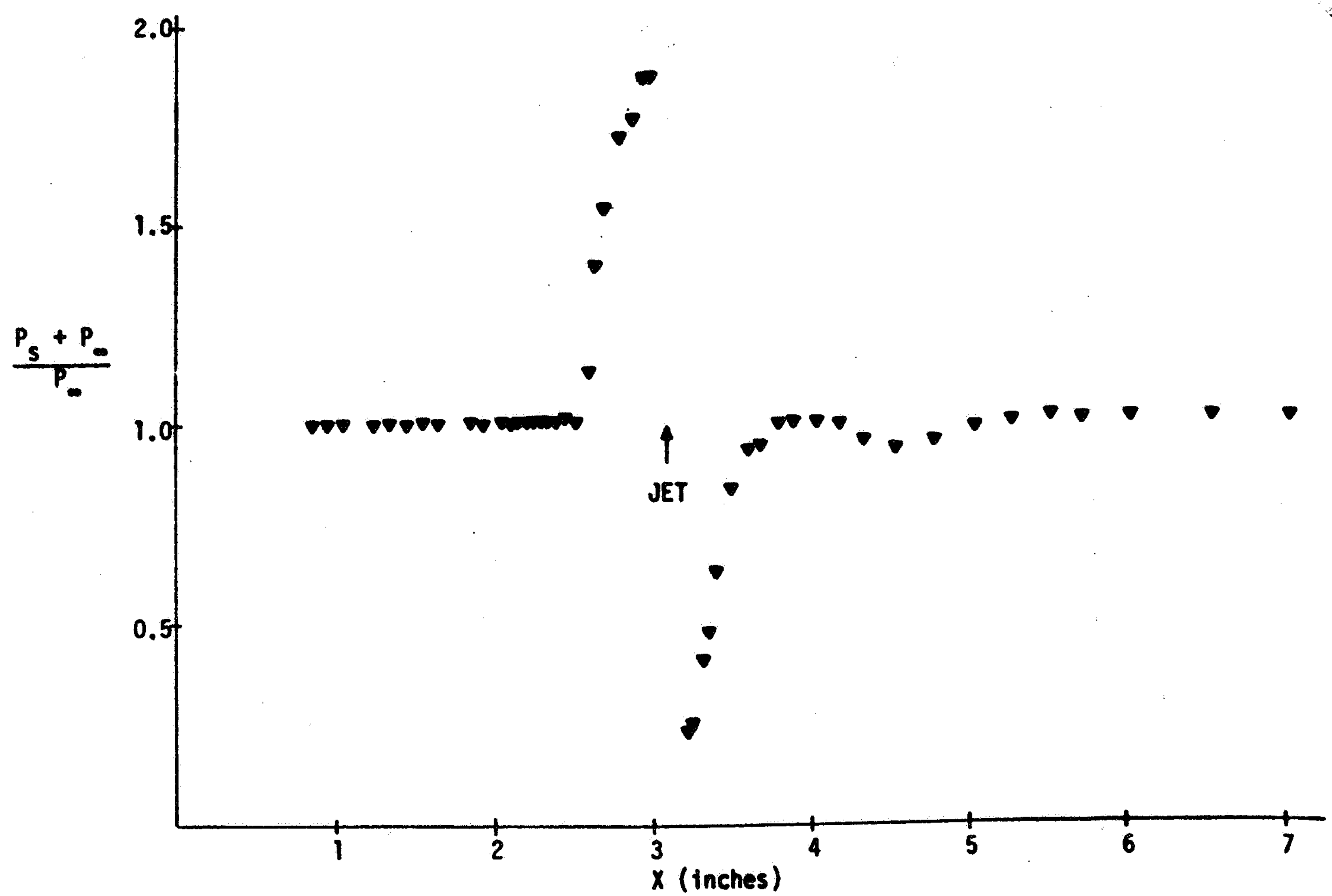

Figure 23. NORMALIZED SURFACE PRESSURE DISTRIBUTION, $\omega = 5^0$, $M_\infty = 1.71$, $P_{os} = 150$ psig

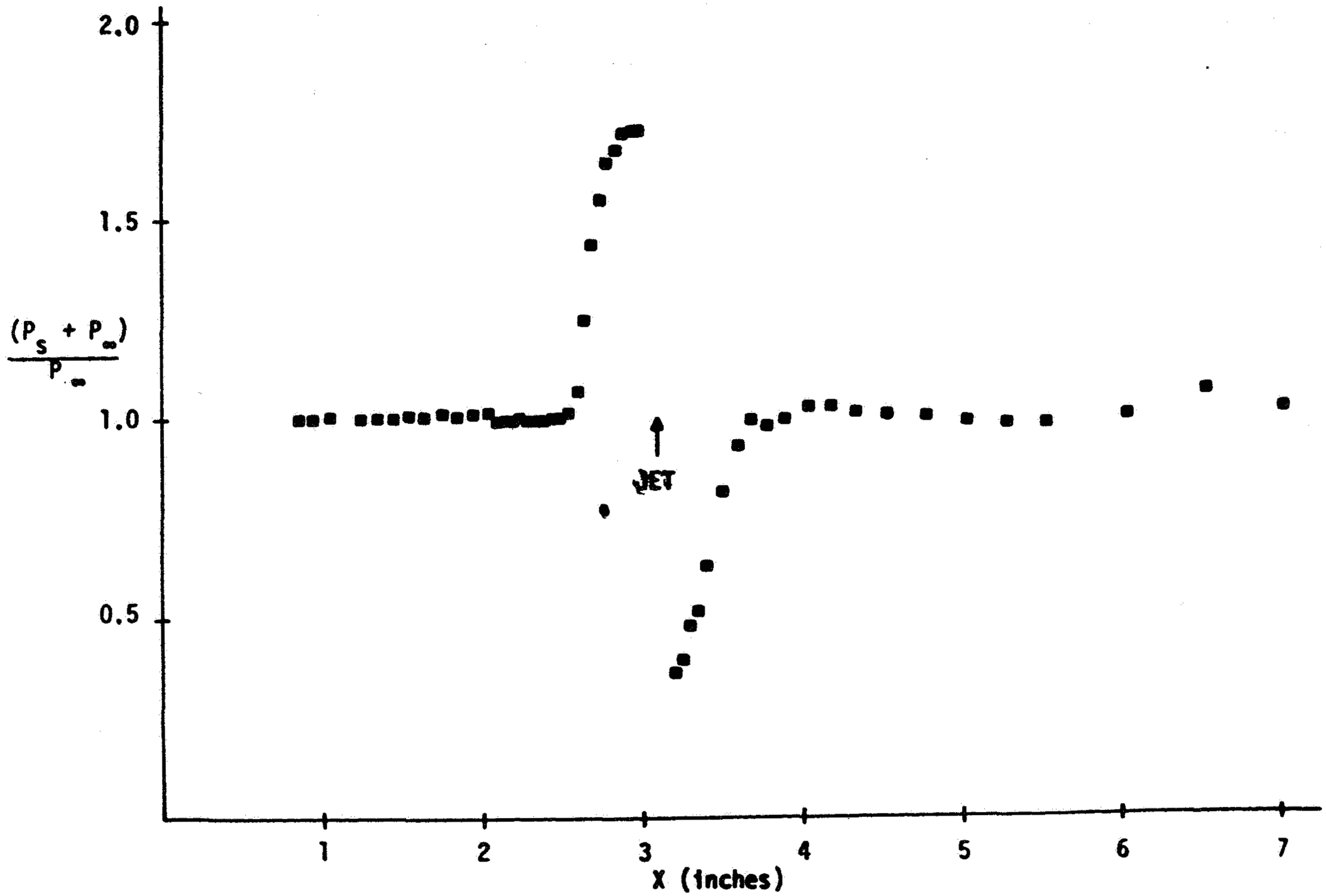

Figure 24. NORMALIZED SURFACE PRESSURE DISTRIBUTION, $\omega = 10^{o}$, $M_\infty = 1.53$, $P_{os} = 150$ psig

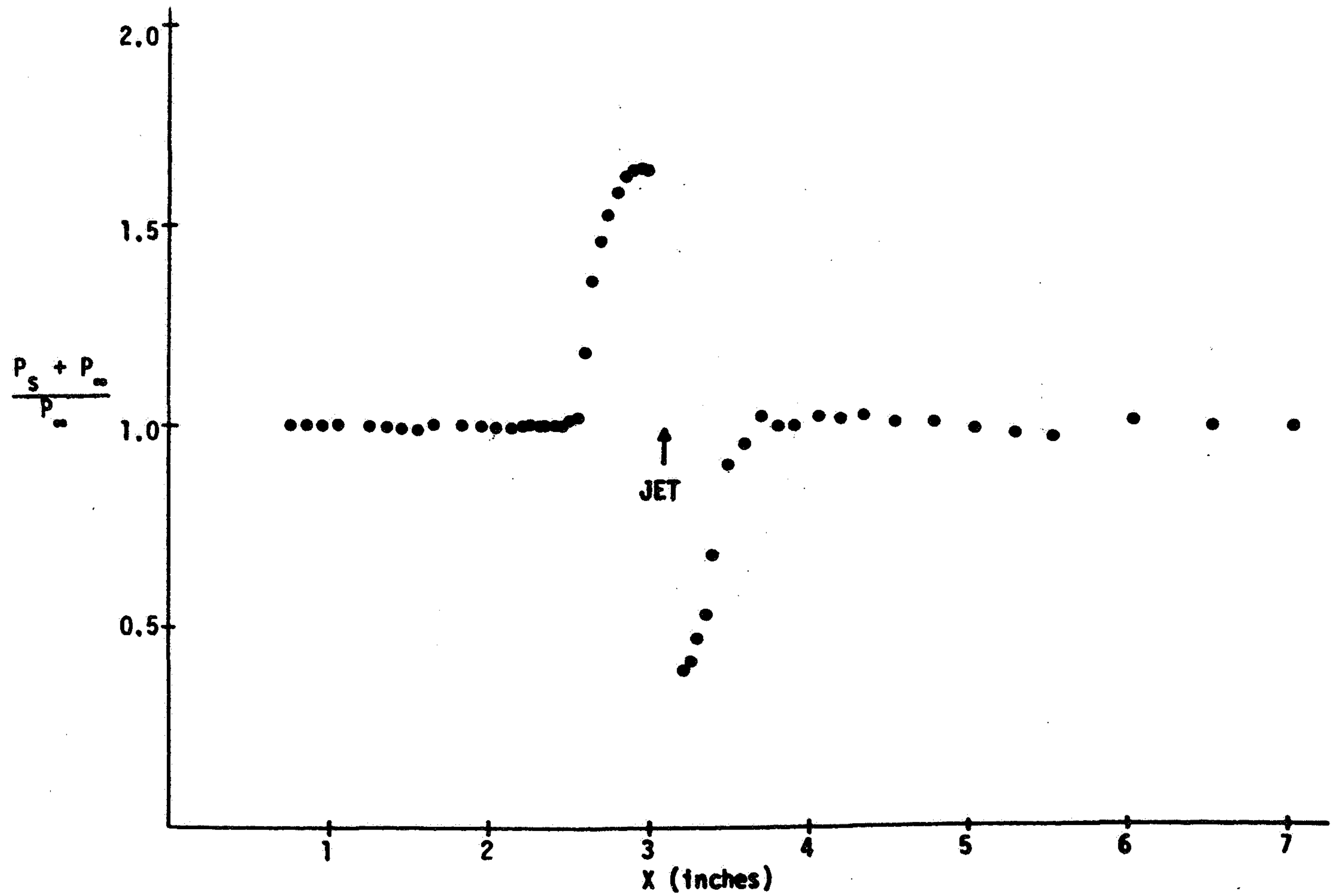

Figure 25. NORMALIZED SURFACE PRESSURE DISTRIBUTION, $\alpha = 15^{\circ}$, $M_\infty = 1.33$, $P_{os} = 150$ psig

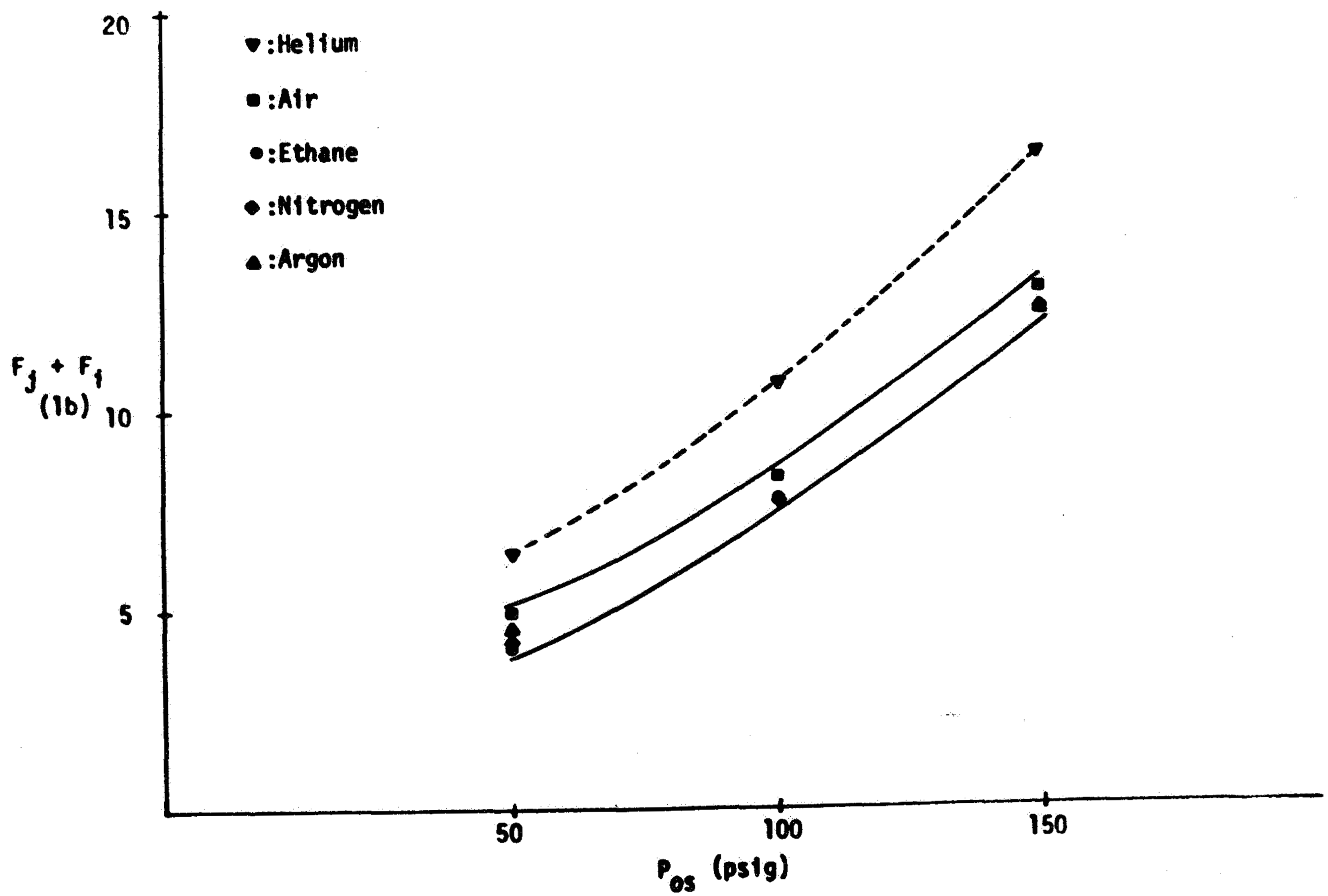

Figure 26. COMPARISON OF $(F_j + F_i)$ FOR DIFFERENT GASES

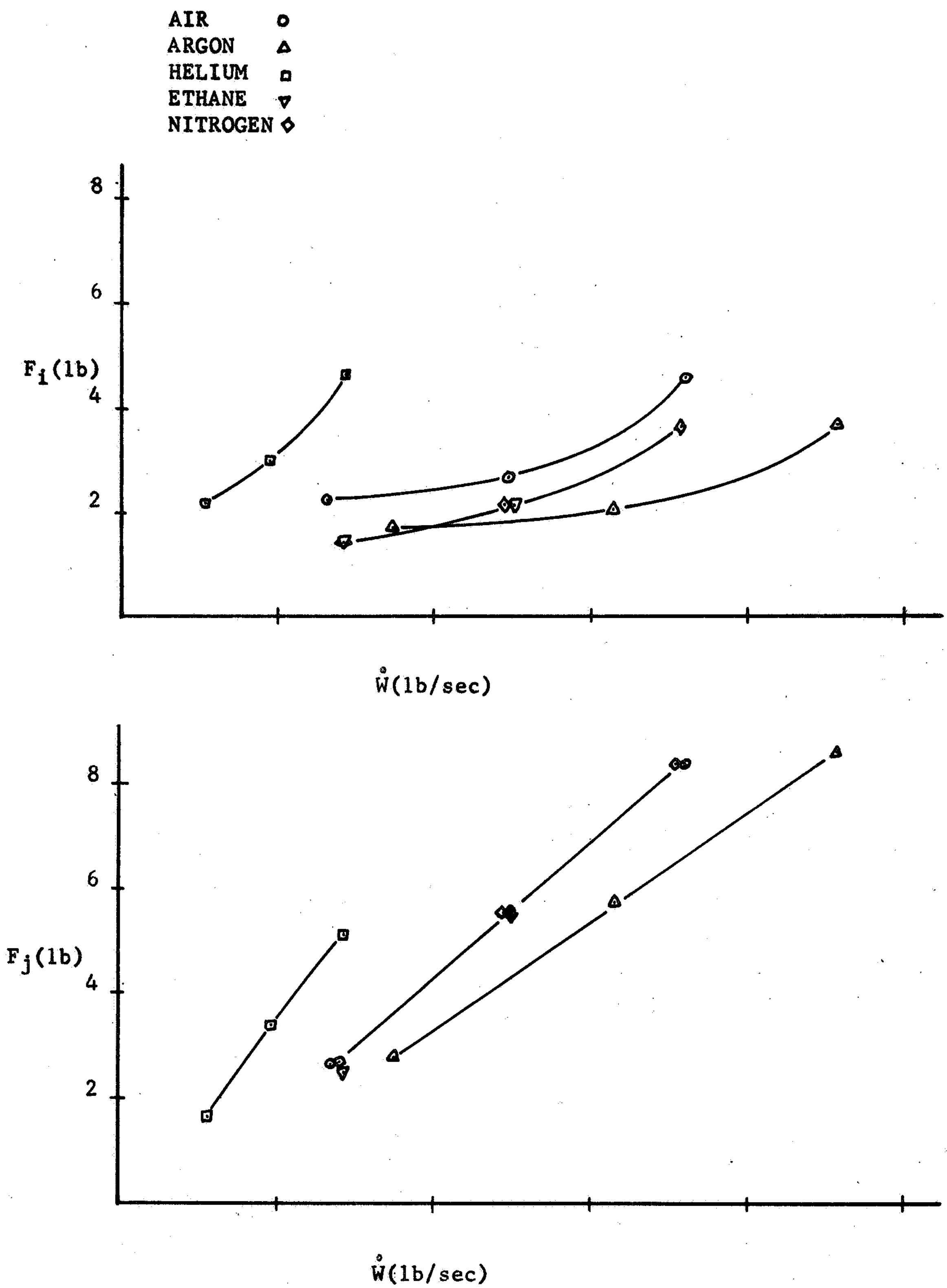

Figure 26a. F_i & F_j vs $\dot{W}$, Various Gases

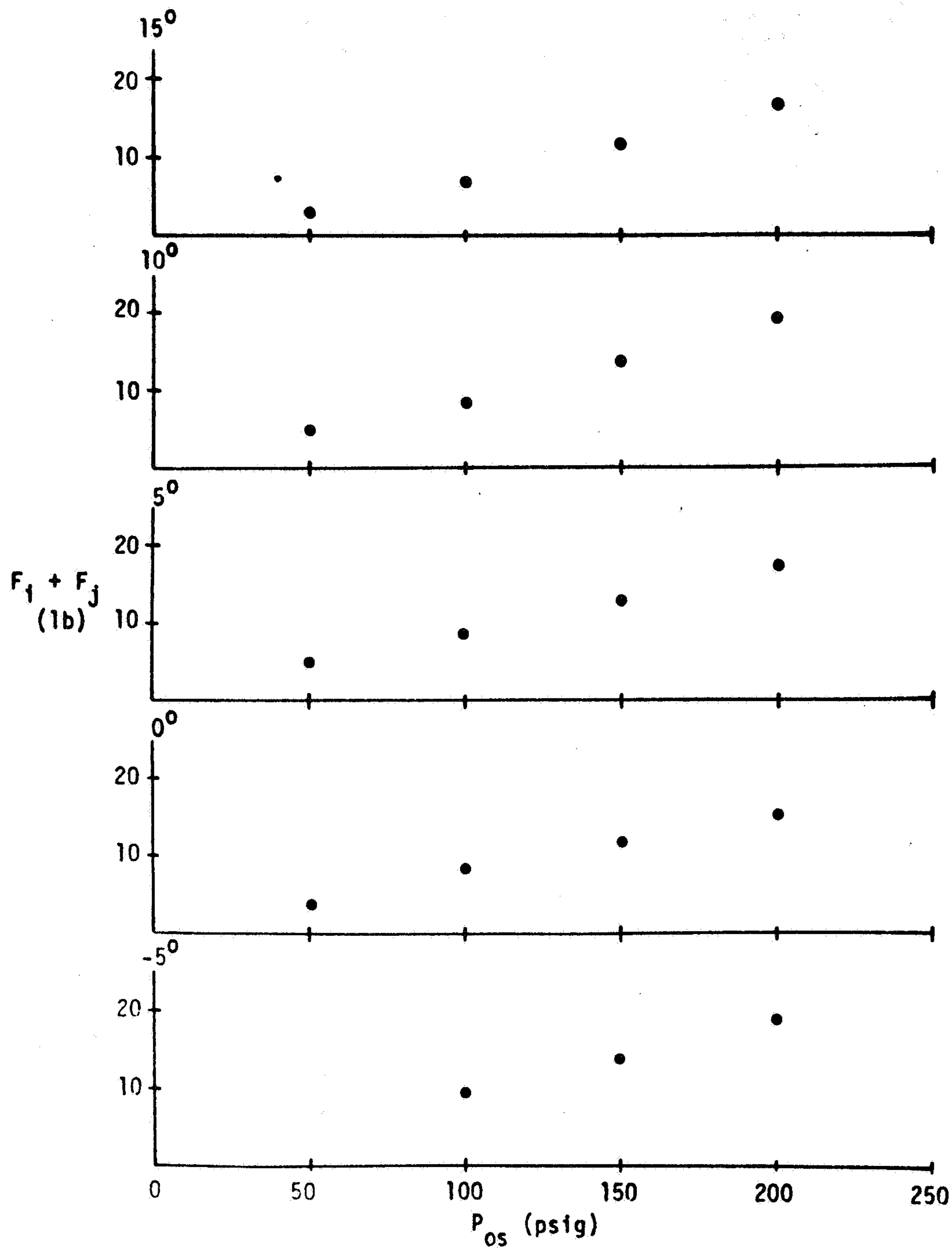

Figure 27. $(F_i + F_j)$ vs P_{os}

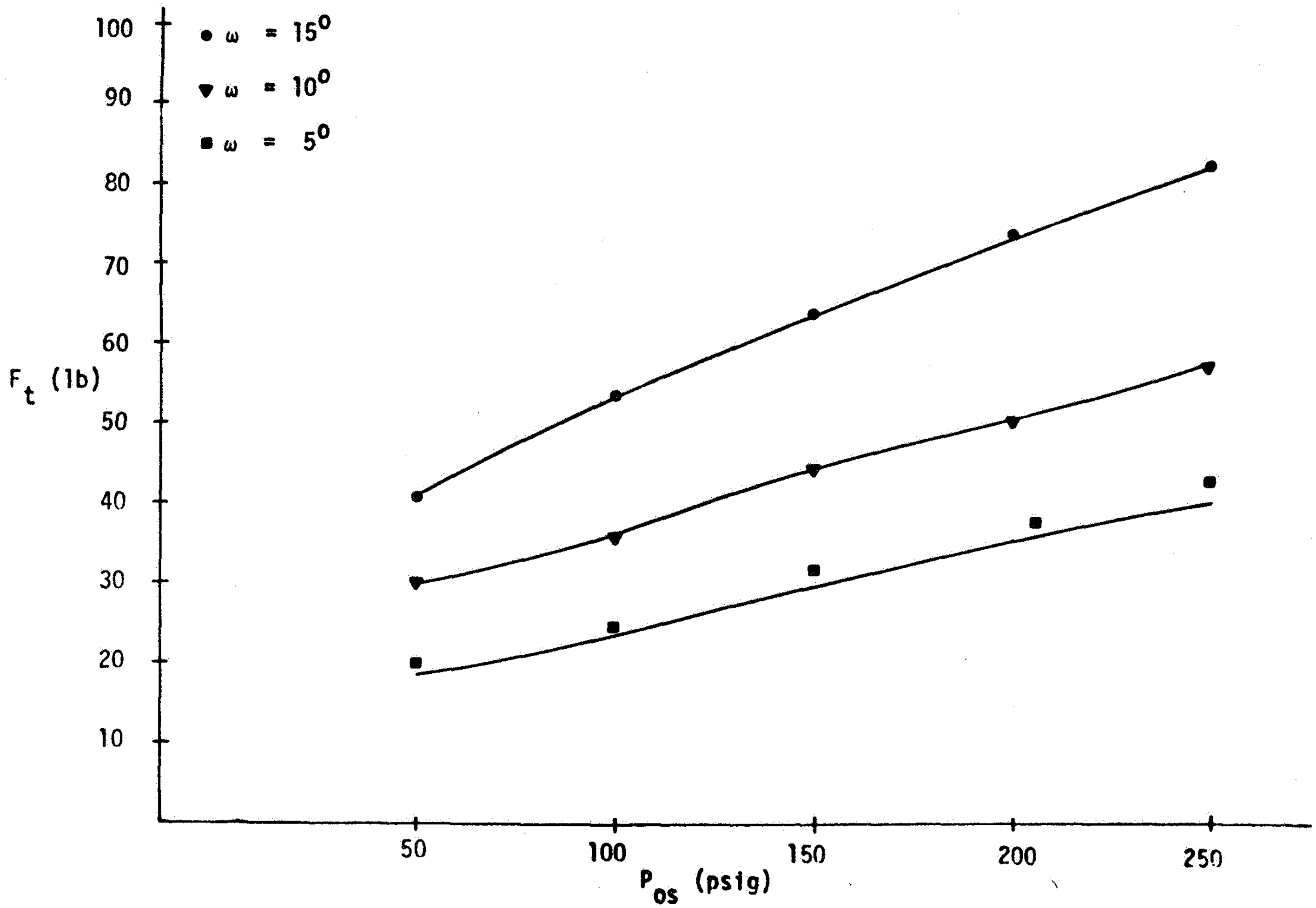

Figure 28. COMPARISON OF PREDICTED VALUES OF F_t AND ACTUAL VALUES OF F_t.

4. SUMMARY AND CONCLUSIONS

The aerodynamic interaction of a sonic jet issuing from a 15^{o} wedge with a transverse supersonic stream produces a side force due to flow interaction in addition to the jet thrust. The magnitude of this interaction force equals or even exceeds the value of the jet thrust. There is a substantial lack of agreement in the literature as to the effect of the flow parameters on the jet interaction; the prediction of the flow interaction for any given set of circumstances is in terms of empirical "scaling" laws.

The results of this study employing flow visualization and the measurement of surface pressure distributions on the wedge do not agree with previously published flat plate results. The results from these experiments show a more abrupt separation ahead of the slot, a shorter separation region and a thicker boundary layer or wake downstream of the "reattachment" point than the previous flat plate experiments. These differences may be all attributed to the higher viscous forces; in previous published experiments at lower values of free stream static pressure, the inviscid or inertial effects were considered dominant.

The results of the experiment may be summarized as follows:

a. As the angle-of-attack is increased from 0^{o} the magnitude of the jet interaction is decreased for fixed free stream conditions and jet stagnation pressure.

b. The effect of angles-of-attack between $+5^{o}$ and $+15^{o}$ and a range of values for the secondary stagnation pressure of 50 to 250 psig is predicted by the following expression:

$$F_t = (F_i + F_j + F_a) = 1.023^n(F_j + F_a)$$

where n is a function of jet stagnation pressure.

c. An increase in weight flow rate of the injectant increases the interaction force. This effect is a maximum at 0^o angle-of-attack and is diminished by both positive or negative angles-of-attack, and is enhanced by an increase in secondary stagnation pressure.

d. A moderate change in the molecular weight of the secondary injectant as the air is changed to argon, nitrogen or ethane, does not significantly affect the interaction. A large change in molecular weight, air to helium increased the force, $F_i + F_j$, by approximately 20%.

e. A 50% change in the specific heat ratio, k, did not affect the interaction for conditions of approximately equal molecular weight (ethane and nitrogen) and with an average temperature differential of 120^oF between the primary and secondary stream static temperature.

5. RECOMMENDATIONS

As indicated in the introductory remarks, this parametric analysis is the beginning of a comprehensive research program designed to explore in depth the feasibility and utility of a combined jet reaction and external burning control system. It is recommended that this program be continued; the recommended program can be conveniently discussed under two headings: hot flow studies with an inert injectant, and hot flow studies with a combustible injectant.

5.1 Hot Flow Studies, Inert Injectant

This series of experiments would parallel the preceeding cold flow experiments except that both the primary flow and the injectant would be heated to simulate conditions encountered in a potential flight envelope. The heating of the primary air could be accomplished by a pebble bed heater, a vitiating system with oxygen addition, or with synthetic air. The basic experimental design should be such that the apparatus will accommodate the use of combustible injectants. The operating design points would be determined by parameter values required to achieve the chosen flight envelope.

5.2 Hot Flow Studies, Combustible Injectant

These experiments would reproduce the preceeding hot flow, inert injectant studies. The major change in the experimental apparatus would be to replace the secondary flow system by a gas generator. The series of experiments would be expanded to include a variety of combustible mixtures and the relative proportion of combustion that takes place in the gas generator.

LIST OF CITED REFERENCES

1. "ARPA project defender - terminal defense activities - interim technical summary report"(U), Cornell Aeronautical Laboratory Report BM-1526-G-9, Section 3.1 (31 December 1964) (SECRET).

2. Billig, F. S., "A review of external burning ramjets", Applied Physics Laboratory, The Johns Hopkins University, TG 801 (December 1965) (CONFIDENTIAL).

3. Spring, D. G., Street, T. A., and Amick, J. L., "Transverse jet experiments and theories", U.S. Army Missile Command, Report No. RD-TR-67-4 (June 1967).

4. Walker, R. E., and Shandor, M., "Theoretical performance of selected fluid injectants for thrust vector control", The Johns Hopkins University, Applied Physics Laboratory, Silver Spring, Maryland, Report No. CM-1027 (November 1962).

5. Walker, R. E., and Shandor, M., "Influence of injectant properties for fluid injection thrust vector control," AIAA Solid Propellant Conference Preprint 64-112 (January 1964).

6. Walker, R. E., Stone, A. R., and Shandor, M., "Interaction between sonic sidejets and supersonic duct flow", The Johns Hopkins University, Applied Physics Laboratory, Silver Spring, Maryland, Bumblebee Series Report No. 316 (December 1962).

7. Walker, R. E., Stone, A. R., and Shandor, M., "Secondary gas injection in a conical rocket nozzle", AIAA Journal, Vol. 1, No. 2, (January 1963), pp. 334-338.

8. Walker, R. E., Stone, A. R., and Shandor, M., "Secondary gas injection into a conical rocket nozzle. I. Effect of orifice diameter and molecular weight of injectant," The Johns Hopkins University, Applied Physics Laboratory, Report CM-1010 (February 1962).

9. Broadwell, J. E., "An analysis of the fluid mechanics of secondary injection for thrust vector control (revised)", Space Technology Labs. Report 6120-7744-MU-000 (March 1962).

10. Broadwell, J. E., "Correlation of rocket nozzle gas injection data", AIAA Journal, Vol. 1, No. 8 (August 1963) pp. 1911-1913.

11. Rodriguez, C. J., "An experimental investigation of jet-induced thrust vector control methods", Bulletin 17th Meeting, JANAF-ARPA-NASA Solid Propellant Group, Vol. III (May 1961).

12. Spaid, F. W., Zukowski, E. E., and Rosen, R., "A study of secondary injection of gases into a supersonic flow", Jet Propulsion Laboratory, Technical Report No. 32-834 (August 1966).

13. Zukoski, E. E., and Spaid, F. W., "Secondary injection of gases into a supersonic flow", AIAA Journal, Vol. 2, No. 10 (October 1954), pp. 1689-1696.

14. Wu, Jain-Ming, Chapkis, R. L., and Mager, A., "Approximate analysis of thrust vector control by fluid injection", ARS Journal (December 1961), pp. 1677-1685.

15. Charwat, A. R., and Allegre, J., "Interaction of a supersonic stream and a transverse supersonic jet", AIAA Journal, Vol. 2, No. 11 (November 1964), pp. 1965-1972.

16. Hsia, Henry Tao-Sze, Siefert, Howard S., and Karamcheti, Krishnamurty, "Shocks inducted by secondary fluid injection", J. Spacecraft and Rockets, Vol. 2, No. 1 (January-February 1965), pp. 66-72.

17. Guhse, R. D., "An experimental investigation of thrust vector control by secondary injection", Jet Propulsion Center, Purdue University, Report No. TM-65-3 (March 1965).

18. Sanlorenzo, E. A., Chinitz, W., and Spadaccini, L., "Forced induced by air injection on a flat plate in supersonic flow"(U), GASL Technical Report No. 407 (January 1964) (CONFIDENTIAL).

19. Sanlorenzo, E., and Spadaccini, L., "Experimental study of control forces produced by air injection from an axisymmetric model"(U), GASL TR No. 444 (June 1964) (CONFIDENTIAL).

20. Spadaccini, L., "Investigation of secondary air injection techniques used to produce forces on a flat plate in supersonic flow"(U) GASL TR No. 353 (April 1964) (CONFIDENTIAL).

21. Amick, J. L., Bond, C. E., and Liepman, H. P., "An experimental investigation of the forces and flow field produced by a jet exhausting laterally from a cone-cylinder in a mach 2.84 stream", University of Michigan, Department of Aero Engineering WTM-255 (November 1955).

22. Vinson, P. W., Amick, J. L., and Liepman, H. P., "Interaction effects produced by a jet exhausting laterally near the base of ogive-cylinder model in a supersonic main stream", NASA Memo 12-5 58W (February 1959).

23. Amick, J. L., and Hays, P. B., "Interaction effects of side jets issuing from flat plates and cylinders aligned with a supersonic stream", Wright Air Development Division TR 60-329 (June 1960).

24. Amick, J. L., Stubblebine, W., and Chen, P. C. Y., "Experimental interaction effects of forward located side jets on a body of revolution", University of Michigan, WTM-276 (15 March 1963).

25. Amick, J. L. and Carvalho, G. F., "Interaction Effects of a jet flap on a 60 deg. delta wing at mach number 4, and comparison with two-dimensional theory", University of Michigan, Department of Aerospace Engineering Report APL/JHU CM-1031 (February 1963).

26. Amick, J. L. and Hawk, N. E., "Jet interaction studies on a body of revolution at angle of attach", University of Michigan, Department of Aerospace Engineering, WTM 279 (March 1964).

27. Hawk, N. E. and Amick, J. L., "An experimental and theoretical investigation of two-dimensional jet-flap aerodynamic at supersonic speeds", University of Michigan, Department of Aerospace Engineering Report APL/JHU CR-23 (October 1965).

28. Amick, J. L., "Circular-arc jet flaps at supersonic speeds - two-dimensional theory", University of Michigan, Department of Aerospace Engineering Report APL/JHU CR-24 (July 1966).

29. Barnes, J. W., Spaid, F. W., and Davis J. G., "Maneuvering reentry control and ablation studies (MARCAS)"(U), Final Report, Vol. I, Jet Interaction Controls, Douglas Aircraft Company Technical Report BSD-TR-65-310 (July 1965) (SECRET).

30. Baker, W. T., Davis, T. and Matthews, S. E., "Reduction of drag of a projectile in a supersonic stream by the combustion of hydrogen in the turbulent wake"(U), The Johns Hopkins University, Applied Physics Laboratory, CM-673 (June 1951) (CONFIDENTIAL).

31. Scanland, T. S. and Hebrank, W. H., "Drag reduction through heat addition to the wake of supersonic missiles"(U), Ballistic Research Laboratories, Memo Rep. No. 596 (June 1952) (CONFIDENTIAL).

32. Davis, F., Forney, H. B., Smith, E. H., Typson, T. L. and Wolf, R. L., "Two-dimensional expternal combustion airfoil"(U), Experiment Incorporated, Report TM 704 (July 1955).(CONFIDENTIAL).

33. Fletcher, E. A., Dorsch, R. G. and Gerstein, M., "Combustion of aluminum borohydride in a supersonic wind tunnel", NACA RM E55D07a (June 1955).

34. Dorsch, R. G., Serafini, J. S. and Fletcher, E. A., "A preliminary investigation of static-pressure changes associated with combustion of aluminum borohydride in a supersonic wind tunnel", NACA RM E55F07 (August 1955).

35. Dorsch, R. G., Serafini, J. S. and Fletcher, E. A., "Exploratory investigation of aerodynamic effects of external combustion of aluminum borohydride in airstream adjacent to flat plate in mach 2.46 tunnel", NACA RM E57E16.(March 1959).

36. Dorsch, R. E., Allen, H., Jr., and Dryer, M., "Investigation of aerodynamic effects of external combustion below flat-plate model in 10- by 1-foot wind tunnel at mach 2.4, NASA D-282 (April 1960).

37. Serafini, J. S., Dorsch, R. G. and Fletcher, E. A., "Exploratory investigation of static- and base-pressure increases resulting from combustion of aluminum borohydride adjacent to body of revolution in supersonic wind tunnel", NACA RM E57E15 (October 1957).

38. Dorsch, R. G., Serafini, J. S., Fletcher, E. A., and Pinkel, I. I., "Experimental investigation of aerodynamic effects of external combustion in airstream below two-dimensional supersonic wing at mach 2.5 and 3.0", NASA 1-11-59E (March 1959).

39. Allen, H. J., and Fletcher, E. A., "Combustion of various highly reactive fuels in a 3.84-by-10-inch mach 2 wind tunnel", NASA memo 1-15-59# (April 1959).

40. Dugger, G. L., Deklau, B., Billig, F. S. and Matthews, S. E., "Summary report on external ramjet program"(U), The Johns Hopkins University, Applied Physics Laboratory, TG-419 (October 1961) (CONFIDENTIAL).

41. Billig, F. S., "A study of combustion in supersonic streams", The Johns Hopkins University, Applied Physics Laboratory, BB 321 (July 1964).

42. Billig, F. S., "SCRAM combustor development and related supersonic combustion experiments"(U), Minutes of 31st Meeting of the Bumblebee Propulsion Panel, Applied Physics Laboratory, TG 63-53 (June 1964) (CONFIDENTIAL).

43. Billig, F. S., "Supersonic combustion of storable liquid fuels for hypersonic ramjets"(U), Applied Physics Laboratory Accomplishments for Fiscal Year 1964, The Johns Hopkins University, Applied Physics Laboratory, TG 277-8 (CONFIDENTIAL).

44. Grubman, D. H., "Applied research program, aerospace vehicle interception propulsion program - phase II"(U), The Marquardt Corporation Report S-346A, ARPA No. 278-62/6-28-62 (October 26, 1963) (Revised March 30, 1964) (CONFIDENTIAL).

45. "ARPA project upSTAGE - study phase final report, volume II - study results, book 2 preliminary design"(U), Douglas Missile & Space Systems Division Report SM-48545, Section 6 (March 1965) (SECRET).

46. Kranz, P. C. and Pelky, D. A., "Experimental investigation of external burning on an 8° half-angle cone at mach 5.0 and 6.1", No. D2-36037 (August 1964).

47. Chinitz, W. and Economos, C., "Study of hypersonic interceptor controls"(U), General Applied Science Laboratories, TR 440 (May 1964) (CONFIDENTIAL).

48. Chinitz, W., "Study of hypersonic interceptor controls" Final Report Phase II(U), General Applied Science Laboratories, TR 526 (April 1965) (CONFIDENTIAL).

49. Chinitz, W., Spadaccini, L., and Stein, H., "The effect of fuel injection parameters on forces produced by external burning on the surface of an axisymmetric body"(U), GASL Technical Report No. 536 (May 1965) (CONFIDENTIAL).

50. Chinitz, W., Spadaccini, L., and O'Neill, J., "An experimental investigation of forces produced by combustion on the surface of an axisymmetric body"(U), GASL TR 517 (March 1965) (CONFIDENTIAL).

51. Chinitz, W. and Spadaccini, "Force production due to combustion on a flat plate in supersonic air stream"(U), General Applied Science Laboratories, TR 512 (March 1965) (CONFIDENTIAL).

52. Chinitz, W. and Spadaccini, L., "Heat transfer due to combustion on a flat plate in supersonic flow", GASL TR 486 (December 1964).

53. Chinitz, W., "Forces induced by combustion on a flat plate in supersonic flow"(U), General Science Laboratires, TR 434 (April 1964) (CONFIDENTIAL).

54. Hicks, Bruce L., "Addition of heat to a compressible fluid in motion", NACA ACR No. E4A29 (1945).

55. Hicks, B. L., Montgomery, D. J. and Wasserman, R. H., "The one-dimensional theory of steady compressible fluid flow in ducts with friction and heat addition", NACA TN 1336 (July 1947).

56. Hicks, B. "Diabatic flow of a compressible fluid", Quarterly of Applied Mathematics, Vol. VI, No. 3 (1948).

57. Shapiro, Ascher H., "The Dynamics and Thermodynamics of Compressible Fluid Flow" (The Ronald Press Co., New York 1953).

58. Pinkel, I. I. and Serafini, J. S., "Graphical method for obtaining flow field in two-dimensional supersonic stream to which heat is added", NACA TN 2206 (November 1950).

59. Chu, Boa-Teh, "Pressure waves generated by addition of heat in a gaseous medium", NACA TN 3411 (June 1955).

60. Gazley, Carl, Jr., "Linearized solution for heat addition at the surface of a supersonic airfoil", Project Rand Rept. RM-1892 AD 133025 (November 1956).

61. "ARPA project UpSTAGE - study phase final report, volume I - study results, part 2 - appendixes"(U), The Boeing Company Report D2-23881-1, Section 10 (March 1965) (SECRET).

62. Willmarth, W. W., "The production of aerodynamic forces by heat addition on external surfaces of aircraft", Project Rand Rept. RM 2078, ASTIA AD 150681 (December 1957).

63. Woolard, H. W., "Tables of properties of some oblique deflagrations in supersonic flow", The Johns Hopkins University, Applied Physics Laboratory, TG 382 (September 1960).

64. Woolard, H. W., "An approximate analysis of the two-dimensional supersonic flow past a plane wall with super-critical heat addition in a normal plane", The Johns Hopkins University, Applied Physics Laboratory, APL/JHU CM 954 (July 1959).

65. Woolard, H. W., "Analytical approximations for stationary conical detonations and deflagrations in supersonic flow", The Johns Hopkins University, Applied Physics Laboratory, TG 446 (May 1963).

66. Chinitz, W., Bohrer, L. C. and Foreman, K. M., "Properties of oblique detonation waves", Fairchild Engine Division, Deer Park, New York, AFOSR TN 59-462 (ASTIA) AD 215-267 (April 1959).

67. "Applied research program aerospace vehicle interception propulsion program - phase II"(U) Marquardt Corporation, Rept. S-346, ARPA No. 278-62/6-28-62 (25 October 1963), Revised 30 March 1964 (CONFIDENTIAL).

68. "Applications for external burning propulsion"(U), Marquardt Corporation, Report Nol MR 20, 258 (December 1963) (CONFIDENTIAL).

69. Lindley, C. A., "Preliminary estimate of the feasibility of maneuvering a missile by external burning"(U), The Marquardt Corporation, MR 20, 175 (March 1962) (CONFIDENTIAL).

70. "Applied research program aerospace vehicle interception propulsion program - phase I"(U), Marquardt Corporation, Report No. S-283 (July 1962) (CONFIDENTIAL).

71. Pelkey, D. A., Brunner, D. W., and Field, R. E., "Experimental investigation of external burning on a flat plate at mach 5.0, using aluminum borohydride and triethylaluminum", The Boeing Company Report D2-90812-1 (To be issued).

72. Brunner, D. W., Pelkey, D. A., and Curulla, J., "HiBEX external burning experiment"(U), The Boeing Company Report D2-99604-1 (March 1966)(CONFIDENTIAL).

73. "Preliminary results of flat plate tests - ARPA project EBBO"(U), Boeing Company Report No. D2-125129-11 (March 1967) (CONFIDENTIAL).

74. Chinitz, W., "A survey of fuels suitable for external combustion applications", GASL TM 109 (June 1964).

75. Decker, D. D., Nichtenhauser, A., and Popolow, R. H., "External burning technology - a review of recent ARPA sponsored studies"(U), Columbia University, Electronics Research Laboratories Technical Report T-1/319 (December 1965) (CONFIDENTIAL).

76. "Project defender - terminal defense activities - interim technical summary report"(U), Cornell Aeronautical Lab Report No. BM-1526-G-12 (31 December 1965) (SECRET - RESTRICTED DATA).

77. Harmon, D. B., Jr., Barnes, J. W., and Johnson, G. P., "Maneuvering re-entry controls and ablation studies (MARCAS) first quarterly progress report"(U), Douglas Aircraft Company, AF-BSD-TR-64-173 (December 1964) (SECRET).

78. Harmon, D. B., Jr., "Maneuvering re-entry control and ablation studies (MARCAS) final report - volume II - external burning controls"(U), Technical Report BSD-TR-65-311, Douglas Aircraft Company, Santa Monica, California (July 1965) (SECRET).

79. "ARPA project upSTAGE - study phase final report, volume III - technical appendices"(U), Hughes Aircraft Company, Appendix B.4-5 (15 April 1965) (SECRET).

80. "Final report, analytical and experimental investigation of external burning ARPA project EBBO"(U), Boeing Company Report No. D2-125129-15 (June 1967) (CONFIDENTIAL).

81. Harvey, D. W., "Longtudinal waves on a liquid jet in a high velocity gas stream", Douglas Aircraft Company, Report No. SM-49287 (November 1965).

82. "ARPA project defender - final report - cold flow experimental studies of the break-up of non-reactive fluid jets injected into a supersonic cross flow", Douglas Report SM-48213, (April 1966) (CONFIDENTIAL).

83. "Penetration of a liquid jet injected into a gas stream", Douglas Aircraft Company, Report No. SM-47782R (October 1965).

84. "ARPA project preSTAGE, an analysis of the breakup characteristics of a liquid jet injected into a supersonic cross flow"(U),

Douglas Aircraft Company, Report No. 60610 (March 1967) (CONFIDENTIAL).

85. "Final report - combustion kinetics of pentaborane droplets falling into atmospheres of varying composition and temperature"(U), Douglas Aircraft Company, Report No. DAC-59317 (August 1966) (CONFIDENTIAL).

86. "ARPA project preSTAGE - the combustion rate of pentaborance droplets falling through air"(U), Douglas Aircraft Company, Report No. DAC-60574 (July 1967) (CONFIDENTIAL).

87. "Final report, ARPA preSTAGE - experimental investigation of the performance obtained from combustion of pentaborance on wedge and cone models in a hypersonic flow"(U), Douglas Aircraft Company, Report No. DAC-60544R (March 1967) (CONFIDENTIAL).

88. "PreSTAGE round one detailed flight test performance report"(U), Douglas Aircraft Company, Report No. DAC-60613 (March 1967) (CONFIDENTIAL).

89. "PreSTAGE round two detailed flight test performance report"(U), Douglas Aircraft Company, Report No. DAC-58855 (April 1967) (CONFIDENTIAL).

90. "PreSTAGE round three detailed flight test performance report"(U), Douglas Aircraft Company, Report No. DAC-58858 (May 1967) (CONFIDENTIAL).

91. "PreSTAGE round four detailed flight test performance"(U), Douglas Aircraft Company, Report No. DAC-58860 (July 1967), (CONFIDENTIAL).

92. "PreSTAGE round five detailed flight test performance report"(U), Douglas Aircraft Company, Report No. DAC 58863 (August 1967) (CONFIDENTIAL).

93. "PreSTAGE round six detailed flight test performance report"(U), Douglas Aircraft Company, Report No. DAC-58861 (July 1967) (CONFIDENTIAL).

94. "PreSTAGE round eight detailed flight test performance report"(U), Douglas Aircraft Company, Report No. DAC-58872 (September 1967) (CONFIDENTIAL).

95. "ARPA project preSTAGE external burning control analysis methods" (U), Douglas Aircraft Company, Report No. DAC-58862 (August 1967) (CONFIDENTIAL).

96. "ARPA project preSTAGE external burning control design handbook"(U), Douglas Aircraft Company, Report No. DAC-60680 (Uune 1967) (CONFIDENTIAL).

97. Chapman, D. R., Kuehn, D. N. and Larson, H. K., "Investigation of separated flows in supersonic and subsonic streams with emphasis on the effect of transition," NACA Report 1356 (1958).

98. Sterrett, J. R. and Emery, J. C., "Extension of boundary layer separation criteria to a mach number of 6.5 by utilizing flat plates with forward facing steps", NASA Tech. Note D-618 (December 1961).

99. Cubbison, R. W., Anderson, B. H., and Ward, J. J., "Surface pressure distributions with a sonic jet normal to adjacent flat surfaces at mach 2.92 to 6.4", NASA TN D-580 (February 1961).

100. Romeo, D. J. and Sterrett, J. R., "Aerodynamic interaction effects ahead of a sonic jet exhausting perpendicularly from a flat plate into a mach number 6 free stream", NASA Tech. Note D-743 (April 1961).

101. Zukowski, E. E., "Turbulent boundary-layer separation in front of a forward facing step", AIAA Journal, Vol. 5, No. 10 (October 1967), pp. 1746-1753.

102. Thompson, H. D., "Design procedure for optimization of rocket motor nozzles", Purdue University, Jet Propulsion Center Report No. TM-63-6 (May 1965).

103. Jordan, D. P. and Mentz, M. D., Air Tables (McGraw-Hill Book Co., New York 1965).

104. Pope, A. and Goin, K. L., High-Speed Wind Tunnel Testing (John Wiley and Sons, Inc., New York, 1965), pp. 357-359.

LIST OF GENERAL REFERENCES

1. Attas, J.E., "Interaction effects produced by a vaporizing liquid injected into a high energy supersonic gas stream", McGill University Report No. 63-2 (April 1963).

2. Bankston, L.T., and Larsen, H.M., "Thrust vectoring experiments with gas injection", NAVORD Rep. 6548, China Lake (May 1959).

3. Bankston, L.T., and Larsen, H.M., "Thrust vectoring by secondary injection in the nozzle exhaust cone", Bulletin 15th Meeting, JANAF Solid Propellant Group, Silver Spring, Maryland, SPIA 7, (June 1959) pp 151-169 (CONFIDENTIAL).

4. Bankston, L.T., and Barnes, G.G., "Gas injection thrust vectoring", NOTS Rep. IDP 662, China Lake (July 23, 1959).

5. Bankston, L.T., and Barnes, G.G., "Thrust vectoring: Shock wave and pressure effects of cold air injection in a two-dimensional nozzle", U.S. Naval Ordnance Test Station, NAVWEPS Rpt. 7611 (January 1961).

6. Bankston, L.T., "Thrust vectoring methods"(U), U.S. Naval Ordnance Test Station, NAVORD Rpt. 6423, NOTS 2123 (December 2, 1962) (CONFIDENTIAL).

7. Billig, F.S., "Supersonic combustion of storable liquid fuels in mach 3.0 to 5.0 air streams", Tenth Symposium (International) on Combustion, The Combustion Institute (1965), pp 1167-1178.

8. Broadwell, J.E., "Analysis of the fluid mechanics of secondary injection for thrust vector control", AIAA Journal, Vol. 1, No. 5 (May 1963), pp 1067-1075.

9. Browne, H.N. and Williams, M.M., "The theoretical computation of equilibrium compositions, thermodynamic properties and performance characteristics of propellant systems", U.S. Naval Ordnance Test Station, NAVWEPS Rep. 7043 (June 8, 1960).

10. Carvalho, C.F., and Hays, P.B., "Jet interference experiments employing body alone and body-fin configuration at supersonic speeds", University of Michigan, CM-979 (December 1960).

11. Chinitz, W. and Spadaccini, L., "The effects of free stream conditions on force generation by external combustion on a flat plate in mach 3.1

flow"(U), General Applied Science Laboratories, TR 472,(CONFIDENTIAL) (October 1964).

12. Clark, B.J., "Breakup of a liquid jet in a transverse flow of a gas", NASA TN D-2424 (August 1964).

13. "Control jet effectiveness in the subsonic and transonic flight regimes", Aeronutronic Division, Philco, Report No. U-2932 (December 1964).

14. Cuadra, E., "Applications for external burning propulsion"(U), The Marquardt Corporation, MR 20, 258 (December 1963)(CONFIDENTIAL).

15. Dowdy, M.W., and Newton, J.F., Jr., "Investigation of liquid and gaseous secondary injection phenomena on a flat plate with M = 2.01 to M = 4.54", Jet Propulsion Laboratory, Pasadena, California, TR 32-542 (December 1963).

16. Drewry, D.G., Hnatiuk, B.T., Kallmeyer, T.E., Harmoning, H.D., Hanely, D.P., and Hug, D.P., "Propellant gas injection for thrust vector control of solid propellant rockets", Bulletin 17th Meeting, JANAF-ARPA-NASA Solid Propellant Group, Vol. II (May 1961).

17. Dugger, G.L. and Monchick, L., "External burning ramjets"(U) Preliminary Feasibility Study, Applied Physics Laboratory, The Johns Hopkins University, CM-948 (June 1959)(CONFIDENTIAL).

18. Dugger, G.L., "Comparison of hypersonic ramjets with subsonic and supersonic combustion", Combustion and Propulsion, Fourth AGARD Colloquim, Pergamon Press, London (1961).

19. Eschenroeder, A.Q., "Combustion in the boundary layer on a porous surface", J. Aerospace Sciences, Vol. 27, No. 12 (December 1960), pp 901-906.

20. Falanga, R.A., and Janes, J.J., "Pressure loads produced on a flat plate wing by rocket jet exhausting in a spanwise direction below the wind and perpendicular to a free stream flow at mach number 2.0", NASA TN D-893 (May 1961).

21. Falconer, F.L., "External burning performance characteristics", The Marquardt Corporation, MR 20, 270 (March 1964).

22. Feldman, S., "Hypersonic gas dynamic charts for equilibrium air", AVCO Research Laboratory, Res. Report 40 (January 1957).

23. Ferrari, C., "Interference between a jet issuing laterally from a body and the enveloping supersonic stream", The Johns Hopkins University, Applied Physics Laboratory, Bumblebee Series Report No. 286 (April 1959).

24. Ferri, A., "Review of problems in applications of supersonic combustion", J. Royal Aero. Soc., Vol. 68, No. 645 (1964)pp 575-585.

25. Foa, Joseph V. and Rudinger, George, "On the addition of heat to a gas flowing in a pipe at supersonic speed", Cornell Aeronautical Laboratory, Report No. HF-534-A-2 (February 1949).

26. General Electric Company, "Properties of combustion gases/system: C_NH_{2N}---air", Vols. I and II (McGraw-Hill, New York, 1955).

27. Green, C.J., and Benham, C.B., "Parameters controlling the performance of secondary injection", U.S. Naval Ordnance Test Station, China Lake, NAVWEPS 7743, NOTS 2710 (December 1961).

28. Green, C.J., and McCullough, Foy, "Liquid injection thrust vector control", AIAA Journal, Vol. 1, No. 3 (March 1963), pp 573-578.

29. Gross, R.A., "Exploratory studies of combustion in supersonic flow", AFOSR TN 59-587 (June 1959).

30. Harvey, D.W., "Longitudinal waves on a liquid jet in a high velocity air stream", Douglas Aircraft Company Report No. SM-49287 (November 1965).

31. Nausmann, G.F., "Thrust axis control of supersonic nozzles by airjet shock interference", United Aircraft Corporation, Dept. Rep. R-63143-24 (May 2, 1952).

32. Hayman, L.D. and McDearman, R.W., "Jet effects on cylindrical afterbodies housing sonic and supersonic nozzles which exhaust against a supersonic stream at angles of attack from 90^o to 180^o", NASA TN D-1016 (March 1962).

33. Hicks, B.L., "On the characteristics of fields of diabatic flow", Quarterly of Applied Mathematics, Vol. IV, No. 4 (1949).

34. Hicks, B.L., Hebrank, W.H. and Kravitz, S., "On the characterization of fields of diabatic flow", Ballistic Research Laboratory Report No. 720 (July 1950).

35. Hicks, B.L., Hebrank, W.H. and Kravitz, "Comment on heat source in a uniform flow", Journal of the Aeronautical Sciences, Vol. 17, No. 9 (September 1950).

36. Hill, D.E., "Penetration of a liquid injected into a gas stream", Douglas Aircraft Company Report No. SM-47782 (December 1964) Revised October 1965.

37. Hilsenrath, J., et al, "Tables of thermal properties of gases", NBS Circular 564 (November 1965).

38. Hirschfelder, J.O., Curtiss, C.F. and Bird, R.B., "Molecular theory of gases and liquids", John Wiley and Sons, Inc., New York (1954).

39. Ingebo, R. and Foster, H., "Drop size distribution for cross-current

break-up of liquid in airstreams", NASA TN 4087 (October 1957).

40. Janos, J.J., "Loads induced on a flat-plate wing by an air jet exhausting perpendicularly through the wing and normal to a free-stream flow of mach number 2.0", NASA TN D-649 (March 1961).

41. Jeffreys, H., "On the formation of water waves by winds", Philosophical Magazine, Vol. 42, pp 368-370 (1871)

42. Kaufman, L.G., "Hypersonic flows past transverse jets", Grumman Research Dept. Report, RE 263 (August 1966).

43. Kuehn, D.M., "Experimental investigation of the pressure rise required for incipient separation of turbulent boundary layers in 2-D supersonic flow", NASA Memo. 1-21-59A (October 1958).

44. Kuiper, R.A., "Control jet effectiveness in the subsonic and tr transonic flight regimes", Philco Pub. No. U-2932 (1 December 1964).

45. Kummerer, K.R., "Jet induced boundary layer separation", Lockheed Missiles and Space Company, Internal Report (1966).

46. Lamb, H., "Hydrodynamics", Sixth Edition, Dover Publications, New York (1945).

47. LeCount, R., and Mikatarian, R., "An analysis of the physical and chemical aspects of liquid injection", Lockheed Missiles and Space Company, TR-55-12-6 (September 1964).

48. Lefko, W., "Loads induced on a flat plate at a mach number of 4.5 with a sonic or supersonic jet exhausting normal to the surface", NASA TN D-1935 (July 1963).

49. Libby, P.A., and Economos, C., "A flame zone model for chemical reaction in a laminar boundary layer with application to the injection of hydrogen-oxygen mixtures", Int. J. Heat and Mass Transfer, Vol. 6 (February 1963) pp 113-128.

50. Lien, Hwachii (Ed.), "Missile phenomenology studies", General Applied Science Laboratories, Inc., TR 615 (16 June 1966) pp 25-34.

51. Liepman, H.P., "On the use of side jets as control devices", ARS Journal, Vol. 29 (1959) pp 453-454.

52. Lingen, A., "Jet-induced thrust vector control applied to nozzles having large expansion ratios", United Aircraft Corporation, Rept. R-0973-33 (March 1957).

53. Lomax, H., "Two-dimensional, linearized flow with heat addition", NASA Memo 1-10-59A (February 1959).

54. Luidens, R.W. and Flaherty, R.J., "Analysis and evaluation of supersonic underwing heat addition", NASA Memo 3-17-59E (April 1959).

55. Mager, A., "On the model of free, shock-separated turbulent boundary layer", J. of Aero. Sci., Vol. 23, No. 2, pp 181-184 (Feb. 1956).

56. Mager, A., "Supersonic airfoil performance with small heat addition", Journal of the Aero/Space Sciences, Vol. 26, No. 2 (February 1959).

57. Marino, A., "Theoretical performance with external burning on surface", General Applied Science Laboratory, Rept. No. 506 (February 1965).

58. McAulay, J.E., and Pavli, A.J., "A cold flow investigation of jet-induced thrust vector control", NASA Tech Memo X-416 (December 1960).

59. McCloy, R.W., "Specific fuel consumption and over-all efficiency for external heating processes", Report CV-6, Convair Division of General Dynamics Corporation (March 7, 1958).

60. McCloy, R.W., "External heat addition for cases other than constant-pressure heat addition", Report CV-5, Convair Division of General Dynamics Corporation, San Diego, California (March 7, 1958).

61. McCloy, R.W., "Propulsion by supersonic heat addition", Report CV-1, Convair Division of General Dynamics Corporation, San Diego, California (March 7, 1958).

62. McCullough, F., Jr., "Thrust vector control by secondary injection" (U), Proceedings of the Symposium on Ballistic Missile and Space Technology, Space Technology Labs, Los Angeles, California, Vol. 1. (1959) pp 1-25 (CONFIDENTIAL).

63. McDonald, R.D., and Garbrick, M.W., "Research study to verify and extend high speed math model for jet reaction control effectiveness", Martin Marietta Corp., OR 8439 (August 1966).

64. Mitchell, J.W., "An analytical study of a two-dimensional flow field associated with some secondary injection into a supersonic stream", VIDYA Technical Note 9166-TN-2 (March 1964) (AD 450,742).

65. Mockel, W.E., "Approximate method for predicting form and location of detached shock waves ahead of plane or axially symmetric bodies", NACA TN 1921 (July 1949).

66. Monchick, L., Keirsey, J.L. and Dugger, G.L., "External burning ramjet - I preliminary analyses of two two-dimensional models with plane flame behind norman shock, and approximate weight-range and size comparisons with ramjets and rockets"(U), Applied Physics Laboratory, The Johns Hopkins University, CF 2705 (February 1959) (CONFIDENTIAL).

67. Nicholls, J.A., "Stabilization of gaseous detonation waves with emphasis on the ignition time delay zone", AFOSR TN 60-442 (June 1960).

68. "Otto fuel reaction control", Lockheed Missiles and Space Company, LMSC 805811 (April 1966 (CONFIDENTIAL).

69. Parker, G.H., and Edwards, S., "A theoretical and experimental investigation of a method of thrust vector control for solid rocket motors", Naval Ordnance Report NAVORD 5904, Vol. II (December 1959).

70. Pinkel, I.I., Serafini, J.S. and Gregg, J.L., "Pressure distribution and aerodynamic coefficients associated with heat addition to supersonic air stream adjacent to two-dimensional supersonic wing", NACA RM E51 K26 (February 1952).

71. "Project PreSTAGE - Quarterly Technical Summary Report"(U), Douglas Report SM-52035 (April 1966) (CONFIDENTIAL).

72. "Project defender system and technology studies - Quarterly Progress Report P-4/322, 7/1/65 to 9/30/65"(U), Columbia University Electronics Research Laboratories (October 1, 1965) p 10 (SECRET).

73. "Quarterly review of APL activities, July-September 1960, II. Space exploration and research and development", The Applied Physics Laboratory, The Johns Hopkins University, Bumblebee Report No. 299-B, pp 11-13 (CONFIDENTIAL).

74. Rhodes, R.P. and Chriss, D.E., "A preliminary study of stationary shock-induced combustion with hydrogen air mixtures", Arnold Engineering Development Center, AEDC TN 61-36 (July 1961).

75. Schulmeister, M., "Static evaluation tests of an oblique shock wave system for rocket exhaust deflection"(U) U.S. Naval Air Rocket Test Station, Lake Denmark, Dover, New Jersey, NARTS 77, TED-ARTS-51-5517 (December 1955) (CONFIDENTIAL).

76. Shankov, I.F., and Frost, V.A., "The flow of a supersonic ideal gas past a flat plate in the presence of volume heat release", AD 287708, reporduced by ASTIA from Trudy Moskovskogo Fisiko-Tekniches Kogo Instituta, No. 7, Issledovaniya po Mekhanike i Prikladnoy Matematike (1961) pp 110-123.

77. Slates, R.O., Geres, R.J., Benham, C.B., and Johanson, D.F., "Research on secondary gas injection for thrust vector control applications", U.S. Naval Ordnance Test Station TP 2856 (April 1962).

78. Smith, E.H. and Davis.T., "The creation of thrust and lift by combustion on external surfaces of airfoils"(U), Smith and Davis, Physicists, Silver Spring, Md.(1 September 1952)(BuOrd, Dept. Navy Contract NORD 12141) (CONFIDENTIAL).

79. Snyder, A.D., Robertson, J., Zanders, D.L. and Skinner, G.B., "Shock tube studies of fuel-air ignition characteristics", Monsanto Research Corporation, Tech. Report AFAPL-TR-65-93 (August 1965).

80. Spaid, F.W., Zukowski, E.E., and Rosen, R., "A study of secondary injection of gases into a supersonic flow", NASA TR 32-834 (1 August 1966).

81. Stanbrook, A., "An experimental study of the glancing interaction between a shock wave and a turbulent boundary layer", Royal Aircraft Establishment (Bedford), TN Aero 2701 (July 1960).

82. Strike, W.T., Schueler, C.J. and Deitering, J.S., "Interactions produced by sonic lateral jets located on surfaces in a supersonic stream", AEDC-TR-63-22 (April 1963).

83. Terry, J.E. and Caras, G.J., "Transpiration and film cooling of liquid rocket nozzles", Redstone Scientific Information Center, RSIC-535 (March 1966).

84. "Tests of the 10^{o}-20^{o} model external ramjet in the mach 5.00 free jet, in the blowdown facility for the applied physics laboratory, The Johns Hopkins University", General Dynamics Daingerfield Division, OAL Rept. 651,(CONFIDENTIAL)(August 1962).

85. Totten, J.K., Final Summary Report on the Calendar Year 1963 Ramjet Technology Program, Volume X, "New and novel engine concepts"(U), The Marquardt Corporation Report MR 25, 116 (June 1964) (CONFIDENTIAL).

86. Tsien, H.S. and Beilock, Milton, "Heat source in a uniform flow", Journal of the Aeronautical Sciences, Vol. 16, No. 12 (1949).

87. Wald, Q., "Reduction of drag at supersonic velocities by heating the external air stream", United Aircraft Corporation Research Dept. M-13362-2 (June 1950).

88. Woolard, H.W., "Some analytical considerations of the aerothermodynamic aspects of supersonic combustion"(U), Minutes of 44th Meeting of the Bumblebee Aerodynamics Panel, The Johns Hopkins University, Applied Physics Laboratory, TG 14-41 (CONFIDENTIAL) (August 1961).

89. Yen, S.M., "One-dimensional flow with heat addition", Report CV-4, Convair Division of General Dynamics Corporation, San Diego, California (March 7, 1958).

90. Zwick, E.E., Grubman, D.H., and Hardy, L., "Analysis of droplet evaporation and combustion in hypersonic streams", Paper presented at AIAA Aerospace Sciences Meeting (January 1964).

APPENDIX A

NOMENCLATURE

<u>Symbol</u>

A_s = Injection slot area

C = Coefficient

F_a = Aerodynamic side force due to angle-of-attack

F_i = Side force due to jet interaction

F_j = Momentum thrust of secondary jet

F_t = Total side force

I = Specific impulse

M = Mach number

P = Pressure

R = Degrees, Rankine Scale

SW = Slot width

T = Temperature

V = Gas velocity

$\dot{W}$ = Weight flow rate

X = Axial distance,reference located 0.79 inches from leading edge.

a = Acoustic velocity

c = Constant

h = Scaled heighth of injected gas

k = Specific heat ratio

$\dot{m}$ = Mass flow rate

v = Vacuum

x = Axial distance along wedge surface

y = Heighth above wedge surface

z = Transverse distance across wedge surface

Greek Symbols

α = Oblique shock angle

ω = Angle-of-attack

Subscripts

a = Ambient

i = Interaction

j = Jet

n = Normal

o = Stagnation conditions

p = Primary

s = Secondary

t = Total

x = Conditions before oblique shock

y = Conditions after oblique shock

∞ = Free stream conditions

Superscripts

$*$ = Sonic conditions

Pages 70-93 are contained in APPENDIX B which is classified CONFIDENTIAL and is issued separately.

APPENDIX C

Description of Apparatus

1. Supersonic Nozzle Design

A uniform discharge, Mach 2.0, two dimensional nozzle was employed in the design of the wind tunnel facility. The nozzle was designed by R. D. Guhse (17) to produce an exit section with a heighth of 6.000 inches and a uniform width of 1.981 inches.

For design purposes, the nozzle was divided into three regions:

a. Subsonic to sonic contour by Friedrich's method, (102).

b. Initial expansion to obtain radial source flow at the inflection point by simple wave theory.

c. The straightening portion to obtain parallel uniform Mach 2.0 flow at the exit section by Foelsch's method (102).

The calculations were carried out on the IBM 7090 computer with the results being obtained in the form of the X coordinate (axial) as the independent variable; with the Y coordinate, design Mach number and slope with respect to the X axis as dependent variables.

The analytical results were used as the basis for fabrication of a model block which was then employed with a profile mill to produce a series of identical blocks machined from stainless steel stock.

2. Supersonic Wind Tunnel

The side plates which are the main structure of the tunnel were fabricated from 1/2 inch mild steel and 1/2 inch plexiglas. The nozzle blocks were sandwiched between the plexiglas and the steel sidewalls. The blocks were positioned by employing dowels inserted through the steel side walls into the blocks; the entire assembly was bolted together by a series of 1/2 inch steel bolts arranged above and below the nozzle blocks. Because of this arrangement, the blocks were essentially floating within a rigid structure. The alignment was accomplished by means of a Bridgeport vertical mill bed and dial indicators. The blocks were aligned with respect to the centerline coordinate to within .0005 inches at three points - the entrance coordinate, the throat, and the exit plane. This entire assembly was bolted to a plenum chamber in a cantilever fashion.

The wedge model was held in the tunnel by dowels inserted through the steel sidewalls. The positioning of the holes was referenced to the centerline of the nozzle. The model could be positioned at various angles of attack by inserting dowel pins into a series of matching holes in the side plates of the wedge model. Fig. 3 shows the model installed in the tunnel.

3. The model was a 15 degree wedge. The model was fabricated from mild steel and was made up of four basic parts - two side plates, the front section, and the aft section. This is shown in Fig. 4. A 0.012 inch wide slot for injecting the secondary gas was formed by the abutment of the front and aft sections. The side plates were relieved at the slot so that the actual slot extended well into the

region of the wall boundary layer. Prior to assembly the internal faces of the slot were ground to insure uniformity in width. After assembly, both the upper and lower faces were ground flat and the entire model was flash chrome plated. Static pressure taps on the upper surface of the model were fabricated from stainless hypodermic needle material, 0.020 inches I.D. The needle material was hydrogen brazed in position prior to grinding the upper surface. The pressure tap hole pattern was in the form of staggered rows of five along the upper surface of the wedge with a longitudinal distance between centers of .050 inches. The hypodermic needle material extended from the downstream end of the model and was terminated in an array of fittings. The model was disassembled and the slot re-ground to a width of 0.024 inches for the second series of experimental runs.

4. Control System

The primary flow of air was controlled by means of an Askania regulator system. The secondary flow from the wedge slot was regulated by a remote dome loaded valve which was placed upstream of a secondary plenum chamber. The total pressure and temperature in the two plenum chambers were sensed by means of stagnation probes and iron-constantin thermocouples. The thermocouples were referenced to a common ice bath and the temperatures recorded on a Brown Recorder. All operations were accomplished at a location remote from the test cell. A schematic diagram of the flow system is shown in Fig. 5.

The following controls and displays were available to the operator:

a. Controls

(1) Hand operated control for the Askania regulator system

(2) Remote dome loaded valve for the secondary gas system

(3) Remote actuator valves for the multiple gas secondary system

(4) Camera trigger switch, coupled to a Brown recorder through a multiplex circuit to record simultaneously the primary and secondary total temperature.

b. Displays

(1) Heise gauge for primary stagnation pressure

(2) Heise gauge for secondary stagnation temperature

(3) U tube mercury manometer for surface pressure on the wedge upstream of the injection slot

(4) Pressure gauge for supply pressure

(5) Stop watch timer

(6) Brown recorder for stagnation temperatures

5. Instrumentation

a. The spark shadowgraph system consisted of a spark source, a parabolic mirror with a focal length of 64 inches, a ground glass screen, and an automatic Nikon F single lens reflex camera. A schematic representation of the system is presented as Fig. 29.

The spark source was manufactured from a set of drawings furnished to the Jet Propulsion Center by the Ballistics Research Laboratory, Aberdeen, Maryland. The design specifications for the spark duration was 1 microsecond. Tests of the device indicated an actual duration of 3 microseconds. The image on the ground glass screen was photographed with a f1.2, 55 mm Auto-Nikor lens on Kodak Tri-X film

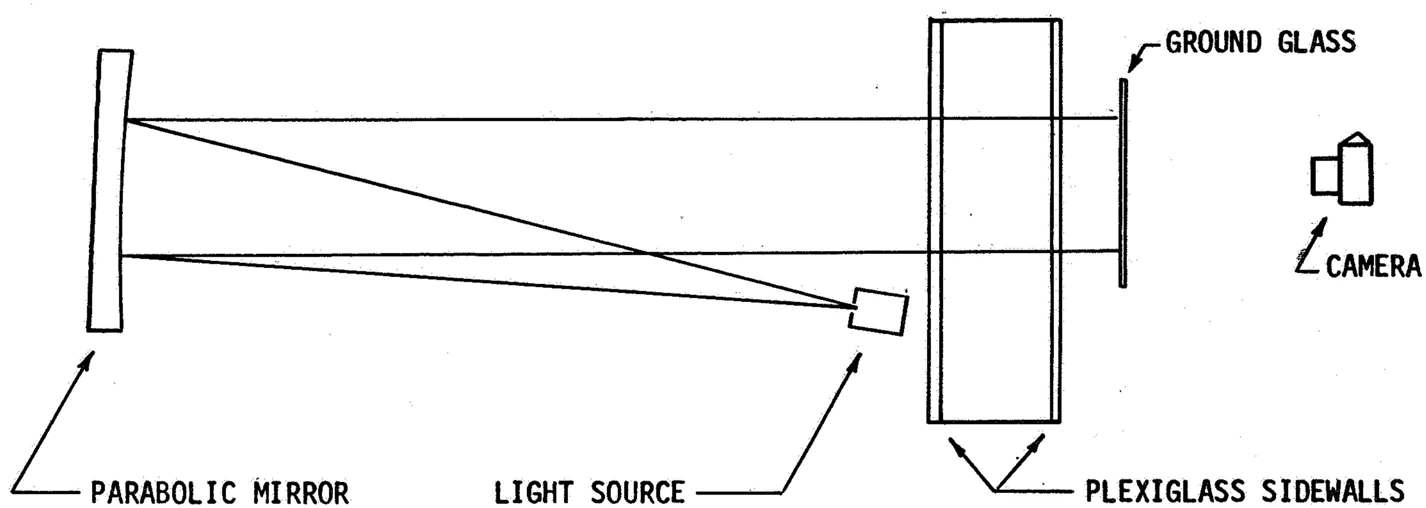

Figure 28. Schematic Diagram of Spark Shadowgraph System

upgraded to an A.S.A. speed of 1200.

b. The pressure field on the wedge model was determined from a bank of 58 mercury manometers which was photographically recorded. These manometers were arranged in two sets, with each set having a common reservoir. The reference pressure to the reservoirs was obtained by utilizing the first row of pressure taps on the wedge model. Shadowgraph pictures of the flow field and pictures of the manometers were taken simultaneously during the experimental runs. Fig. 29 is a photograph of the manometer bank.

6. Calibration

The Mach number at the exit plane of the nozzle was determined by means of a series of static pressure measurements taken along the sidewall of the tunnel and a corresponding set of total pressure measurements obtained from a pilot tube rake positioned in the tunnel at the exit plane. The results of these measurements are presented as Fig. 30 which presents Mach number at the exit plane as a function of theoretical distance from lower nozzle block. The local Mach number was determined using the relation:

$$\frac{P_{oy}}{P_x} = \left[\frac{k+1}{2} M_x^2\right]^{\frac{k}{k-1}} \Bigg/ \left[\frac{2k}{k+1} M_x^2 - \frac{k-1}{k+1}\right]^{\frac{1}{k-1}}$$

and the Air Tables (103).

The uniformity of the flow - the local Mach number in the vicinity of the wedge varied from 1.89 to 1.92 - is considered satisfactory. The lack of complete uniformity is assumed to be the result of the

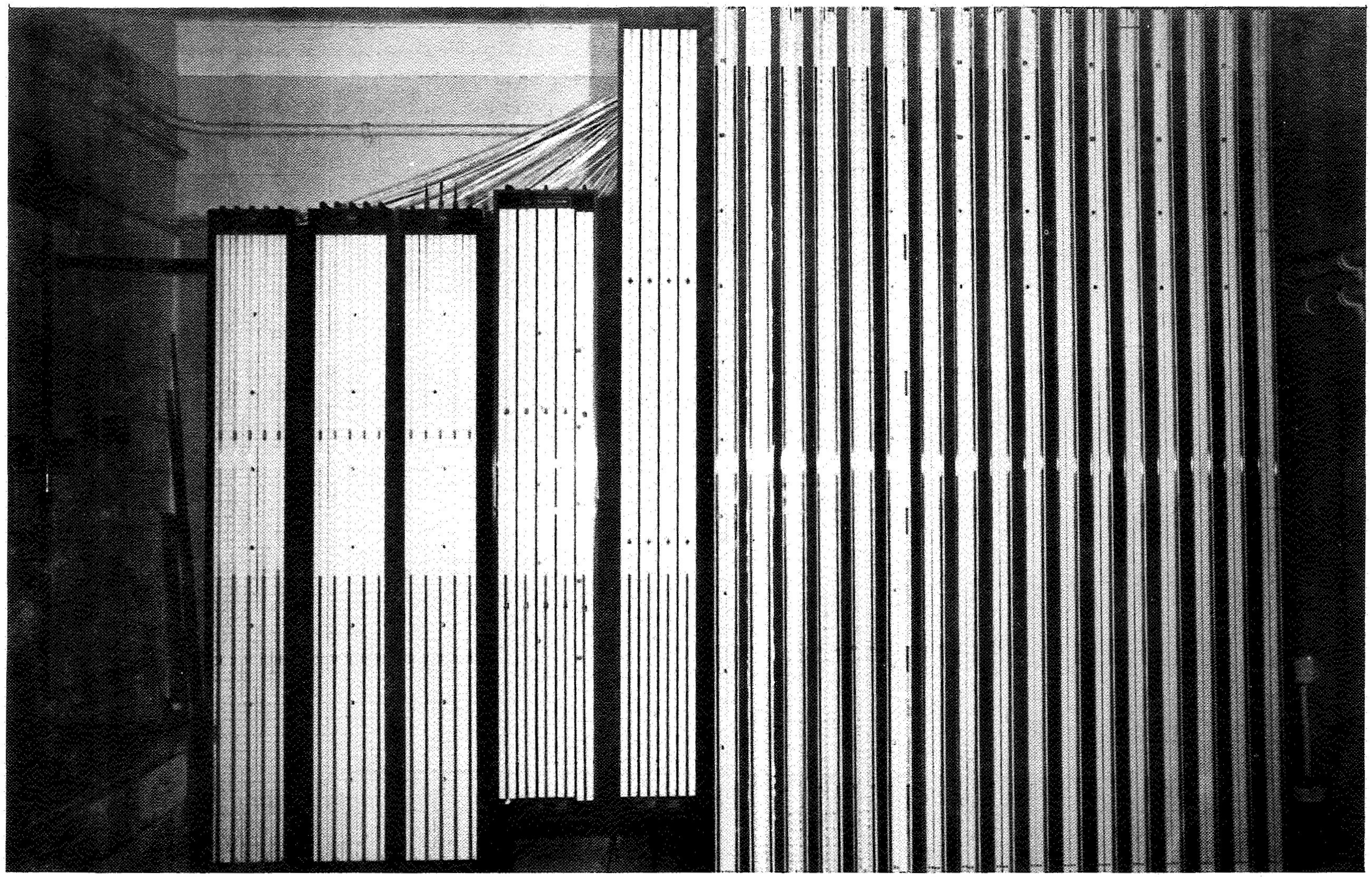

Figure 30. Manometer Bank

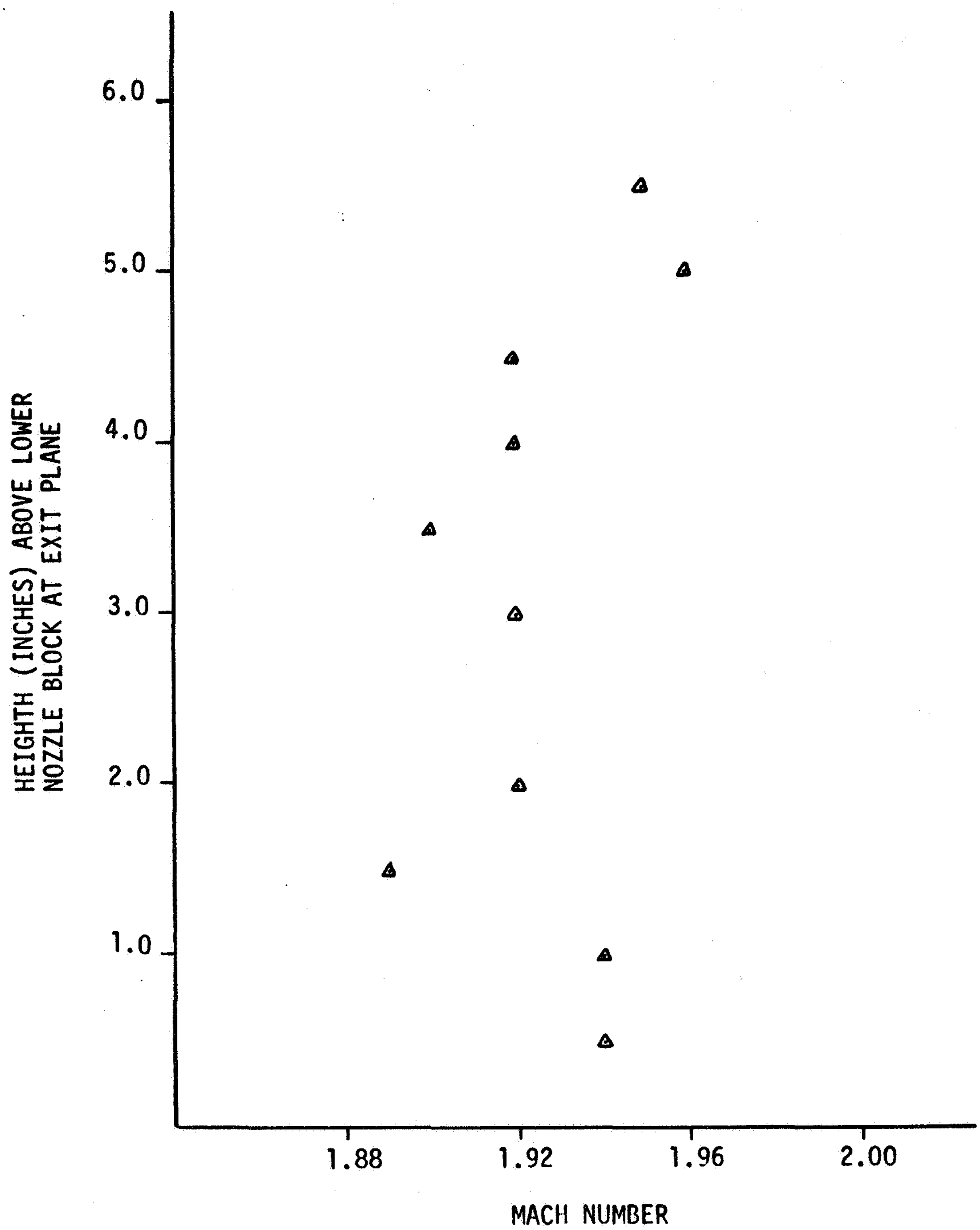

Figure 30. Mach Number Distribution at the Nozzle Exit Plane

following effects:

a. Early tests on the nozzle indicated that a series of shocks originated immediately downstream of the nozzle inflection point. These shocks were clearly visible in shadowgraphs. It was determined that during the polishing, a series of depressions were inadvertently made in the contour immediately downstream of the inflection point. Hand filing removed the depressions and eliminated the shocks.

b. During the design of the nozzle blocks, no boundary layer correction was made to the nozzle contour. Thus, based on an increasing thickness of the boundary layer there is a corresponding decrease in affective area ratio between the exit plane and the throat.

c. The static pressures measured on the sidewall do not correspond directly to the centerline static pressures. A variation of 1 to 2 percent of the Mach number may be present due to expansion waves between the wall and the centerline (104).

APPENDIX D

Experimental Procedure

1. Items to be completed at least one hour before initiation of run.
   a. Turn on Brown recorder.
   b. Fill thermocouple reference dewar with chipped ice.
   c. Check camera circuit to insure that it is wired for single frame.
   d. Turn all gauge manifold valves to proper position.
2. Items to be completed immediately before run (in order listed).
   a. Check voltage output of camera power supply (adjust if necessary to 12 v), load cameras (Tri-X for shadowgraph camera - Plus X for manometer cameras), focus, set proper aperature and speed (F 1.4 and 1/30 for shadowgraph camera and F4 and 1/4 for manometer cameras), and plug cameras in.
   b. Calibrate Brown recorder.
   c. Turn on 24 v power supply.
   d. Control panel should have switches in following positions.
      (1) two secondary "BLEED" switches off
      (2) "HIGH PRESSURE AIR" valve OPEN and "TO DOMES" valve CLOSED
      (3) "SECONDARY FLOW REGULATOR" off
      (4) if control wheel closed counter (clockwise to STOP) "PANIC" off, if control wheel open, "PANIC" on.
      (5) "SOLENOID" on.

(6) "CAMERA" off.

(7) "BROWN RECORDER" off

(8) 220 v "ASKANIA MOTOR" on

e. Open large valve at high pressure tanks

f. Remove "block" from No. 1 control valve in air control room

g. Turn on spark power supply and "camera shutter" motor

h. Operate camera switch for reference pictures

i. Sound "HORN" three times

3. Conduct of experiment

a. Open the Askania control and stabilize the primary stagnation pressure at 100 psig. Record wedge surface pressure from manometer.

b. "BROWN RECORDER" on.

c. After 30 seconds, "CAMERA" on for one second to record shadowgraph manometer bank, and primary stagnation temperature without secondary flow.

d. Open "SECONDARY FLOW REGULATOR" and stabilize the secondary stagnation pressure at 50 psig.

e. After 30 seconds, "CAMERA" on for one second to record shadowgraph, manometer bank, and primary and secondary stagnation temperatures.

f. Repeat steps 3d and 3f at secondary stagnation pressures of 100, 150, 200, 250 psig.

g. Shut down by turning "PANIC" on.

4. For that portion of the experimental program that involves multiple gases, between steps 3e and 3f above, operate selector switches.

APPENDIX E

Measurements and Data Reduction

1. Measurements

a. Shadowgraphs

The shadowgraph negatives were enlarged to 1:1 and 2:1 scale. The shock angles and points of intersection were scaled directly from the photographs using reference lines scribed on the Plexiglas side walls. The accuracy of measurement was 0.01 inches. The location of interaction points was within 0.05 inches.

b. Pressure measurements

(1) The accuracy of the wedge surface pressure downstream of the oblique shock was accurate to within 0.1 inch of mercury. Variations during the run did not exceed 0.2 inches of mercury. The recorded value was the mean value.

(2) The manometer pressures were allowed to stabilize for 30 seconds at each data point. The pressures were recorded photographically by Nikon cameras on Kodak Plus X film. The negatives were projected on a large scale screen. The values of the projected image were recorded to 0.1 inch of mercury. The error introduced by camera angle was determined to be a maximum of 0.1 inches of mercury. The overall error, a function of reading error, camera angle error, and meniscus determination was less than 0.3 inches of mercury.

2. Data Reduction

All calculations were carried out to two decimal points. The integration was carried out using a modified Simpsons rule.

APPENDIX F. DATA

TABLE F1.

Date: 22 October 1967

Test Conditions:

Angle of Attack 15 degrees
Slot Width 0.012 inches
Barometric Pressure 14.53 psia
Local Static Pressure 36.11 psia

Data:

Injectant	Air	Air	Air	Air	Air
P_{os} (psig)	50	100	150	200	250
T_{op} (^oR)	481	472	467	465	464
T_{os} (^oR)	513	506	499	496	494

X(in)	ΔP(inHg)	ΔP(inHg)	ΔP(inHg)	ΔP(inHg)	ΔP(inHg)
0.75	---	0,0	+ 1.1	+ 1.5	---
0.85	0.0	- 1.4	- 0.5	- 1.4	0.0
0.95	- 0.9	- 1.5	+ 0.21	- 1.5	---
1.05	- 0.2	- 1.3	+ 0.6	- 0.8	---
1.25	+ 0.4	- 1.1	+ 0.6	- 0.3	- 0.4
1.35	+ 0.7	- 1.2	- 0.3	- 0.3	- 0.4
0.45	+ 0.4	- 2.0	- 1.3	- 0.2	- 0.4
1.55	- 0.8	- 1.6	- 0.7	+ 0.4	- 1.3
1.65	- 0.9	- 1.4	- 0.5	- 0.6	- 0.8
1.75	=--	---	---	---	---
1.85	+ 0.3	- 1.5	+ 0.4	- 0.6	- 0.9
1.95	- 1.8	- 2.4	- 1.6	- 2.6	- 1.8
2.05	- 0.9	- 0.4	- 0.6	- 1.6	- 0.8
2.10	- 1.3	- 1.9	- 1.2	- 1.9	- 1.3
2.15	- 1.0	- 1.6	+ 0.2	- 1.7	- 1.1
2.20	- 0.8	- 1.4	- 0.8	- 1.6	- 0.9
2.25	- 0.9	- 1.4	- 0.9	- 1.6	0.0
2.30	- 0.3	0.0	- 0.2	- 1.2	- 0.2
2.35	- 0.2	- 0.5	+ 0.1	- 0.8	- 0.2
2.40	- 1.4	- 1.2	- 1.2	- 2.3	- 0.6
2.45	- 1.0	- 1.0	- 1.3	- 2.4	- 1.7
2.50	+ 1.1	0	- 0.4	+ 5.0	+28.6
2.55	- 0.2	- 0.9	- 0.9	+11.2	+32.9
2.60	+ 0.1	- 1.5	+ 1.5	+23.7	+36.5
2.65	- 0.1	+ 0.4	+11.9	+31.3	+39.9
2.70	+ 0.0	+ 0.1	+24.0	+36.7	+42.3
2.75	+ 0.7	+ 7.5	+31.8	+40.0	+43.6
2.80	- 0.3	+19.8	+37.2	+43.4	+46.5
2.85	+ 0.1	+29.7	+40.2	+45.5	+48.9
2.90	+ 2.5	+34.9	+42.9	+47.0	+49.9
2.95	+24.0	+38.3	+44.5	+47.3	+48.7
3.00	+31.1	+49.4	+44.9	+47.2	+48.1

TABLE F1 (Continued)

Data:

Injectant	Air	Air	Air	Air	Air
P_{os} (psig)	50	100	150	200	250
T_{op} (^oR)	481	472	467	465	464
T_{os} (^oR)	513	506	499	496	494

X(in)	ΔP(inHg)	ΔP(inHg)	ΔP(inHg)	ΔP(inHg)	ΔP(inHg)
3.20	-12.5	-40.9	-45.2	-47.5	-48.0
3.25	- 1.5	-29.3	-41.1	-45.0	-45.7
3.30	- 0.8	-12.1	-33.1	-40.1	-43.8
3.35	- 0.7	- 2.2	-19.4	-34.1	-37.1
3.40	- 0.8	+ 0.3	- 6.9	-19.3	-31.2
3.50	- 1.3	- 0.2	- 1.3	- 5.9	-12.9
3.60	- 0.4	+ 3.2	+ 0.4	- 1.8	- 6.1
3.70	---	---	---	---	---
3.85	- 1.0	- 0.4	0.0	0.0	- 0.6
4.00	- 1.2	- 0.5	0.0	+ 0.3	+ 0.2
4.15	---	---	---	---	---
4.30	- 1.8	- 1.7	+ 1.4	- 1.4	- 1.4
4.55	- 2.0	- 1.5	+ 1.1	- 1.5	- 2.0
4.80	- 1.3	- 0.8	+ 0.6	- 1.0	- 1.8
5.05	- 2.2	- 2.3	+ 2.6	- 3.2	- 3.8
5.30	- 3.1	- 3.5	- 4.0	- 4.7	- 5.2
5.55	- 4.9	- 5.2	- 5.4	- 5.9	- 6.4
5.80	- 7.0	- 6.5	- 5.6	- 7.5	- 7.5
6.05	- 5.5	- 1.9	- 4.6	- 6.9	- 6.3
6.30	- 5.3	- 5.4	- 5.6	- 7.2	- 8.0
6.55	- 7.0	- 6.8	- 6.8	- 8.7	- 9.0
6.80	- 4.3	- 3.8	- 3.6	- 5.6	- 5.5
7.05	- 3.9	- 3.5	- 3.3	- 5.0	- 5.1

TABLE F2.

Date: 3 November 1967

Test Conditions:

Angle of Attack 10 degrees
Slot Width 0.012
Barometric Pressure 14.42
Local Static Pressure 27.60

Data:

Injectant	Air	Air	Air	Air	Air
P_{os} (psig)	50	100	150	200	250
T_{op} (^oR)	478	466	457	453	451
T_{os} (^oR)	506	499	490	484	478
X(in)	ΔP(inHg)	ΔP(inHg)	ΔP(inHg)	Δp(inHg)	ΔP(inHg)
0.95	- 0.8	- 0.9	---	- 0.3	- 1.0
1.05	0	- 0.2	- 0.9	0	- 0.9
1.25	- 0.5	- 0.6	- 0.3	- 0.8	- 1.2
1.35	- 0.1	- 0.3	- 0.6	- 0.3	- 1.8
1.45	- 0.2	- 0.6	- 0.2	- 0.7	- 1.9
1.55	- 1.5	- 1.6	- 0.5	- 1.9	- 0.9
1.65	- 1.4	- 1.3	- 1.7	- 1.6	- 1.6
1.75	- 1.8	- 0.9	- 1.5	- 1.1	- 1.1
1.85	- 0.4	- 0.4	- 1.0	- 0.5	- 0.6
1.95	---	---	---	---	---
2.05	0	- 0.3	- 1.7	- 0.4	- 0.3
2.10	- 1.2	- 1.4	- 0.2	- 1.6	- 1.5
2.15	- 1.6	- 1.0	- 1.5	- 1.1	- 1.0
2.20	- 0.3	- 0.6	- 1.0	- 0.8	- 0.7
2.25	- 0.5	- 0.7	- 0.7	- 0.7	- 0.5
2.30	- 0.2	- 0.1	- 0.6	- 1.3	- 0.2
2.35	+ 0.5	+ 0.3	= 0.1	- 1.7	+ 0.1
2.40	- 0.5	- 0.6	+ 0.2	- 0.7	- 0.9
2.45	- 1.0	- 1.3	- 0.8	- 1.2	- 1.2
2.50	- 0.4	- 0.7	- 1.1	- 0.3	+ 0.6
2.55	- 0.6	- 1.1	- 0.3	- 0.6	+ 2.2
2.60	- 0.6	- 0.3	- 0.8	+ 0.4	+11.5
2.65	- 0.6	- 0.7	- 0.8	+ 4.7	+23.2
2.70	- 0.8	- 0.9	+ 0.1	+18.8	+30.3
2.75	- 0.6	- 0.5	+14.2	+28.9	+34.5
2.80	- 0.3	+ 1.6	+23.7	+33.5	+37.3
2.85	- 0.6	+16.1	+30.3	+37.2	+39.4
2.90	+ 1.9	+27.0	+34.7	+39.5	+41.1
2.95	+16.8	+34.0	+37.2	+40.5	+41.1
3.00	+25.9	+36.5	+39.0	+41.6	+41.6

TABLE F2. (Continued)

Data:

Injectant	Air	Air	Air	Air	Air
P_{os} (psig)	50	100	150	200	250
T_{op} (^oR)	478	466	457	453	451
T_{os} (^oR)	506	499	490	484	478
X(in)	ΔP(inHg)	ΔP(inHg)	ΔP(inHg)	ΔP(inHg)	ΔP(inHg)
3.20	-10.1	-33.2	-36.7	-38.0	-36.2
3.25	- 1.3	-22.0	-30.2 1	-33.4	-33.2
3.30	- .8	- 8.2	-21.3	-27.4	-31.4
3.35	+ .6	- 1.0	-10.1	-18.5	-25.9
3.40	+ 1.2	_ 2.0	- 1.2	- 8.8	-16.6
3.50	- 1.5	= 0.6	- 0.9	- 4.0	- 8.0
3.60	+ 0.8	+ 2.1	+ 2.3	_ 1.4	- 0.6
3.70	---	---	---	---	---
3.85	+ 0.5	+ 1.4	+ 1.2	+ 1.4	+ 0.6
4.00	- 0.4	+ 1.2	+ 1.8	+ 2.1	+ 1.7
4.15	---	---	---	---	---
4.30	- 0.1	0.0	= 0.9	- 1.1	- 1.4
4.55	- 1.4	- 1.7	- 2.8	- 3.6	- 4.3
4.80	0.0	- 0.4	- 0.8	- 1.3	- 1.9
5.05	- 1.8	- 2.5	- 2.6	- 2.4	- 2.7
5.30	= 1.0	- 1.3	- 1.2	- 1.1	- 1.0
5.55	- 1.2	- 1.5	- 1.4	- 1.0	- 0.7
5.80	- 2.0	- 2.1	- 1.9	- 1.5	- 1.3
6.05	- 4.1	- 4.0	- 3.6	- 3.3	- 3.2
6.30	- 4.5	- 3.6	- 2.2	- 2.6	+ 0.1
6.55	+ 2.7	_ 0.9	+ 2.1	+ 1.8	+ 1.4
6.80	+ 0.2	= 0.2	- 0.5	- 0.7	- 0.8
7.05	- 0.8	- 0.2	- 1.2	- 1.6	- 1.1

TABLE F3

Date: 2 November 1967

Test Conditions:

Angle of Attack 5^{o}

Slot Width 0.012 inches

Barometric Pressure 14.45 psia

Local Static Pressure 22.10 psia

Data:

Injectant	Air	Air	Air	Air	Air
P_{os} (psig)	50	100	150	200	250
T_{op} (^{o}R)	482	470	465	462	459
T_{os} (^{o}R)	505	497	492	487	485

X(in)	ΔP(inHg)	ΔP(inHg)	ΔP(inHg)	ΔP(inHg)	ΔP(inHg)
0.75	---	+ 2.6	---	---	---
0.85	---	- 0.3	---	- 0.5	---
0.95	---	+ 0.2	- 0.6	- 0.2	- 0.4
1.05	- 0.5	+ 0.3	- 0.1	0	0
1.25	0	0	- 0.1	- 0.3	+ 0.1
1.35	+ 0.1	- 0.3	- 0.2	- 0.3	- 0.1
1.45	- 0.1	+ 0.3	- 0.3	- 1.3	- 0.3
1.55	- 0.3	- 1.0	- 1.1	- 1.2	- 0.9
1.65	- 1.0	- 0.6	- 1.1	- 1.3	- 1.0
1.75	---	---	---	---	---
1.85	- 0.7	- 0.2	- 0.2	- 0.5	- 0.5
1.95	- 0.3	- 1.5	- 1.8	- 1.9	- 1.7
2.05	- 1.7	+ 0.3	- 0.1	- 0.1	0
2.10	+ 0.1	- 0.5	- 0.9	+ 0.1	- 0.7
2.15	- 0.7	- 0.9	- 1.2	- 1.2	- 1.1
2.20	- 1.2	+ 0.2	0	- 1.3	- 0.2
2.25	- 0.1	+ 0.3	0	- 0.2	- 0.1
2.30	- 0.1	+ 0.6	+ 0.5	+ 0.5	+ 0.5
2.35	+ 0.4	+ 0.4	+ 0.1	+ 0.6	+ 0.5
2.40	_ 0.1	+ 0.2	+ 0.4	- 0.1	- 0.5
2.45	∓ 0.1	- 0.1	0	- 0.7	- 0.4
2.50	- 0.5	0	+ 0.5	+ 0.5	+ 0.1
2.55	+ 0.2	- 0.3	- 0.2	+ 0.3	+ 1.1
2.60	- 0.5	+ 0.1	0	+ 0.3	+ 4.3
2.65	+ 0.1	+ 0.3	+ 0.2	+ 3.2	+17.7
2.70	+ 0.3	+ 0.1	+ 0.8	+14.4	+25.1
2.75	+ 0.1	---	---	---	---
2.80	+ 0.5	+ 2.5	+18.8	+27.8	+32.5
2.85	+ 0.5	+16.3	+28.4	+32.6	+35.5
2.90	+ 1.4	+24.7	+32.0	+34.4	+36.8
2.95	+18.4	+28.8	+32.6	+36.3	+37.9
3.00	+24.3	+30.5	+32.1	+37.3	+38.3

TABLE F3. (Continued)

Data:

Injectant	Air	Air	Air	Air	Air
P_{os} (psig)	50	100	150	200	250
T_{op} (^oR)	482	470	465	462	459
T_{os} (^oR)	505	497	492	487	485
X(in)	ΔP(inHg)	ΔP(inHg)	ΔP(inHg)	ΔP(inHg)	ΔP(inHg)
3.20	- 9.8	-26.3	-29.3	-28.6	-28.6
3.25	- 2.4	-18.7	-24.8	-26.7	-26.9
3.30	- 1.2	- 9.2	-17.7	-23.7	-25.9
3.35	+ 0.1	- 2.3	- 8.6	-16.6	-21.8
3.40	+ 0.4	+ 0.4	- 1.6	- 8.2	-13.0
3.50	0.0	+ 0.1	- 1.0	- 2.7	- 4.6
3.60	+ 0.6	+ 1.7	+ 2.2	+ 0.9	+ 0.2
3.70	---	---	---	---	---
3.85	+ 1.0	+ 1.9	+ 2.8	+ 3.0	+ 3.4
4.00	- 0.6	+ 0.4	+ 1.1	+ 1.4	+ 1.6
4.15	---	---	---	---	---
4.30	= 0.6	- 0.8	- 0.7	- 0.9	- 1.-
4.55	- 2.8	- 4.5	- 5.0	- 5.4	- 6.0
4.80	- 1.8	- 3.8	- 4.8	- 6.3	- 7.7
5.05	+ 0.2	- 0.6	- 2.6	- 4.4	- 5.2
5.30	- 0.4	- 019	- 1.3	- 1.9	- 1.0
5.55	- 0.5	- 0.7	- 0.8	- 0.7	- 0.4
5.80	- 0.9	- 0.6	- 0.8	- 0.3	+ 0.1
6.05	- 0.9	- 0.8	- 0.5	+ 0.2	+ 0.6
6.30	- 1.8	- 1.3	- 1.2	- 0.6	- 0.5
6.55	- 3.1	- 1.8	- 3.5	- 1.8	- 4.3
6.80	- 0.2	+ 3.4	- 1.4	+ 1.3	- 1.0
7.05	+ 0.2	+ 0.7	- 1.6	- 0.1	- 1.9

TABLE F4

Date: 9 November 1967

Test Conditions:

Angle of Attack 0 degrees
Slot Width 0.012 inches
Barometric Pressure 14.52 psia
Local Static Pressure 16.10 psia

Data:

Injectant	Air	Air	Air	Air	Air
P_{os} (psig)	50	100	150	200	250
T_{op} (^oR)	487	478	472	468	467
T_{os} (^oR)	510	501	495	490	488
X(in)	ΔP(inHg)	ΔP(inHg)	ΔP(inHg)	ΔP(inHg)	ΔP(inHg)
.75	- 0.1	+ 0.1	---	---	---
.85	+ 0.8	- 1.6	---	---	---
.95	+ 0.3	- 0.1	0.0	0.0	0.0
1.05	+ 0.5	- 0.3	- 0.7	- 0.7	- 0.7
1.25	- 2.3	- 1.8	- 0.3	- 0.2	- 0.2
1.35	- 0.8	- 0.4	- 0.5	- 0.6	- 0.4
1.45	- 0.8	- 0.5	- 1.7	- 2.1	- 1.8
1.55	- 1.6	- 1.4	- 0.5	- 0.9	- 0.8
1.65	- 0.8	- 0.5	- 0.7	- 0.8	- 0.8
1.75	---	---	---	---	---
1.85	- 0.5	- 0.2	- 1.6	- 1.8	- 0.8
1.95	- 1.3	- 0.9	- 0.5	- 2.1	- 0.3
2.05	+ 1.4	+ 2.0	- 0.9	- 3.4	- 1.4
2.10	- 1.0	- 0.3	+ 2.0	- 0.3	+ 1.7
2.15	- 1.3	- 0.5	- 0.3	- 2.6	- 0.4
2.20	- 1.3	- 1.1	- 0.6	- 3.1	- 0.4
2.25	- 0.2	0	- 1.4	- 3.7	- 1.7
2.30	+ 1.8	+ 2.3	- 0.1	- 2.4	- 0.3
2.35	+ 1.2	+ 1.8	+ 2.4	+ 0.1	+ 2.3
2.40	- 1.0	---	+ 1.9	- 0.4	+ 1.7
2.45	---	- 0.9	- 0.9	- 3.5	- 1.3
2.50	- 0.7	- 0.8	- 0.2	- 0.1	+ 0.2
2.55	+ 0.1	+ 0.9	+ 1.0	+ 0.8	+ 1.2
2.60	+ 0.9	+ 1.4	- 1.3	+ 1.0	+ 1.4
2.65	+ 0.6	+ 0.9	+ 0.8	+ 0.6	+ 3.3
2.70	- 1.1	- 1.7	- 0.7	- 0.3	+ 7.2
2.85	---	---	---	---	---
2.80	- 0.1	+ 0.7	+ 0.6	+17.0	+22.9
2.85	+ 0.7	+ 6.8	+19.5	+24.0	+27.4
2.90	+ 1.3	+17.4	+23.7	+26.2	+28.3
2.95	+11.0	+21.9	+25.8	+27.5	+29.2
3.00	+17.7	+25.2	+28.5	+29.9	+31.6

TABLE F4 (Continued)

Data:

Injectant	Air	Air	Air	Air	Air
P_{os} Ipsig)	50	100	150	200	250
T_{op} (^oR)	487	478	472	468	467
T_{os} (^oR)	510	501	495	490	488
X(in)	ΔP(inHg)	ΔP(inHg)	ΔP(inHg)	ΔP(inHg)	ΔP(inHg)
3.20	- 9.6	-19.7	-22.5	-23.0	-23.0
3.25	- 2.3	-12.6	-17.5	-20.2	-20.8
3.30	- 0.4	- 4.2	- 9.7	-14.4	-18.0
3.35	+ 1.6	+ 0.7	- 1.1	- 6.6	-10.4
3.40	+ 2.4	+ 0.4	- 1.0	- 2.4	- 4.4
3.50	0	- 0.2	- 1.2	- 1.7	- 1.3
3.60	+ 2.5	+ 2.3	+ 2.4	+ 2.2	+ 3.2
3.70	---	---	---	---	---
3.85	+ 1.9	+ 2.6	+ 3.7	+ 4.1	+ 4.1
4.00	- 3.8	+ 1.9	+ 2.8	+ 3.1	+ 3.1
4.15	---	---	---	---	---
4.30	+ 0.9	+ 2.2	+ 2.6	+ 2.3	+ 1.7
4.55	- 1.6	- 2.4	- 3.1	- 3.7	- 4.5
4.80	- 2.9	- 4.9	- 6.2	- 6.9	- 7.7
5.05	- 3.2	- 4.8	- 6.3	- 7.4	- 8.5
5.30	- 3.0	- 3.8	- 4.5	- 5.0	- 5.7
5.55	- 3.8	- 4.5	- 4.7	- 4.7	- 5.1
5.80	- 2.3	- 3.1	- 3.5	- 2.1	- 3.1
6.05	0	- 0.1	- 0.3	+ 1.0	+ 0.8
6.30	+ 1.1	+ 1.0	+ 1.6	+ 2.4	+ 3.7
6.55	+ 1.3	+ 1.5	+ 1.9	+ 3.2	+ 3.5
6.80	+ 1.4	+ 1.7	+ 2.0	+ 3.3	+ 3.5
7.05	+ 2.0	+ 2.2	+ 2.7	+ 3.5	+ 3.2

TABLE F5

Date: 8 November 1967

Test Conditions:

Angle of Attack -5 degrees
Slot Width 0.012
Barometric Pressure 14.52 psia
Local Static Pressure 13.10 psia

Data:

Injectant	Air	Air	Air	Air	Air
P_{os} (psig)	50	100	150	200	250
T_{op} (^oR)	463	458	454	452	452
T_{os} (^oR)	492	488	485	482	480

X(in)	ΔP(inHg)	ΔP(inHg)	ΔP(inHg)	ΔP(inHg)	ΔP(inHg)
0.75	---	---	---	---	---
0.85	---	---	+ 0.7	+ 0.7	+ 0.8
0.95	+ 0.9	+ 0.8	+ 0.6	+ 0.6	+ 0.6
1.05	+ 0.6	+ 0.6	+ 0.5	+ 0.6	+ 0.4
1.25	+ 0.5	+ 0.5	+ 1.1	+ 1.1	+ 1.2
1.35	+ 1.4	+ 1.0	+ 0.4	- 0.3	- 0.4
1.45	- 1.4	- 1.4	+ 0.2	+ 0.1	+ 0.3
1.55	- 0.8	- 0.9	- 1.0	- 1.0	- 1.0
1.65	- 1.9	- 2.0	- 0.5	- 0.5	- 0.6
1.75	---	---	---	---	---
1.85	- 1.0	- 1.0	- 0.1	0	- 0.1
1.95	- 1.4	- 1.7	- 0.7	- 0.7	- 0.7
2.05	+ 0.7	+ 0.6	+ 1.5	+ 1.6	- 1.6
2.10	- 2.0	- 1.9	- 1.0	- 0.9	- 0.8
2.15	- 1.8	- 2.0	- 1.0	- 1.0	- 1.1
2.20	- 0.9	- 1.2	- 0.2	- 0.2	- 0.2
2.25	- 0.7	- 0.7	+ 0.2	± 0.2	+ 0.5
2.30	- 0.8	- 0.8	+ 0.2	∓ 0.2	+ 0.4
2.35	- 0.5	- 0.5	+ 0.6	+ 0.6	+ 0.6
2.40	- 1.2	- 1.3	- 0.2	- 0.1	- 0.1
2.45	- 0.4	- 0.8	+ 0.2	+ 0.2	+ 0.4
2.50	+ 0.6	- 0.4	+ 0.6	+ 0.4	+ 2.9
2.55	- 0.3	- 1.4	- 0.4	0	+10.9
2.60	+ 0.5	- 0.7	+ 0.3	+11.5	+19.6
2.65	+ 0.4	- 0.5	+ 4.3	+17.3	+22.0
2.70	- 0.7	- 1.4	+ 7.9	+17.7	+22.9
2.75	---	---	---	---	---
2.80	- 0.5	+12.5	+19.9	+22.6	+25.9
2.85	+ 3.3	+18.6	+22.7	+23.7	+27.0
2.90	+14.8	+21.3	+23.8	+24.1	+26.0
2.95	+18.7	+23.7	+25.7	+25.6	+28.6
3.00	+20.7	+24.5	+25.7	+25.5	+28.8

TABLE F5 (Continued)

Data:

Injectant	Air	Air	Air	Air	Air
P_{os} (psig)	50	100	150	200	250
T_{op} (^oR)	463	458	454	452	452
T_{os} (^oR)	492	488	485	482	480

X(in)	ΔP(inHg)	ΔP(inHg)	ΔP(inHg)	ΔP(inHg)	ΔP(inHg)
3.20	-13.9	-17.2	-17.0	-16.3	-16.8
3.25	- 8.7	-14.5	-15.6	-15.0	-15.6
3.30	- 3.4	-10.5	-14.8	-15.1	-15.6
3.35	- 0.6	- 4.7	-10.0	-13.1	-14.9
3.40	- 0.2	- 2.2	- 6.0	- 9.8	-12.1
3.50	+ 0.1	- 2.4	- 4.9	- 5.2	- 5.8
3.60	+ 0.4	- 0.9	- 1.0	- 1.5	- 3.6
3.70	---	---	---	---	---
3.85	+ 2.0	+ 2.6	+ 2.9	+ 2.1	+ 1.5
4.00	+ 0.6	+ 1.5	+ 2.4	+ 2.3	+ 1.9
4.15	---	---	---	---	---
4.30	+ 2.3	+ 2.2	+ 2.3	+ 1.6	+ 1.0
4.55	- 0.6	- 1.2	- 1.7	- 2.4	- 3.0
4.80	- 2.2	- 3.6	- 4.6	- 5.3	- 6.1
5.05	- 3.2	- 4.9	- 6.2	- 6.5	- 8.8
5.30	- 1.6	- 2.6	- 3.4	- 4.3	- 5.4
5.55	- 1.9	- 2.4	- 2.5	- 2.8	- 3.3
5.80	- 3.3	- 3.5	- 3.2	- 3.0	- 3.4
6.05	- 6.3	- 4.7	- 4.1	- 3.6	- 4.0
6.30	- 3.1	- 3.3	- 2.3	- 1.1	- 2.4
6.55	+ 1.1	+ 1.3	- 2.1	- 3.6	1.7
6.80	+ 1.3	+ 0.7	∓ 1.7	- 2.4	∓ 1.8
7.05	0.0	- 0.3	∓ 0.7	- 1.5	+ 0.9

TABLE F6

Date: 28 November 1967

Test Conditions:

Angle of Attack 15 degrees
Slot Width 0.024 inches
Barometric Pressure 14.58 psia
Local Static Pressure 34.23 psia

Data:

Injectant	Air	Air	Air	Air	Air
P_{os} (psig)	50	100	150	200	250
T_{op} (^oR)	450	444	441	440	440
T_{os} (^oR)	490	482	474	467	463

X(in)	ΔP(inHg)	ΔP(inHg)	ΔP(inHg)	ΔP(inHg)	ΔP(inHg)
0.75	- 0.1	- 0.3	0	+ 0.7	- 0.4
0.85	+ 0.2	0	+ 0.2	+ 0.9	+ 0.1
0.95	- 0.2	- 0.9	- 0.3	+ 0.4	- 0.5
1.05	+ 0.2	- 0.1	0	+ 0.7	- 0.2
1.25	- 0.1	- 0.2	- 0.2	+ 0.6	- 0.4
1.35	0.0	- 0.4	- 0.3	+ 0.4	- 0.5
1.45	- 0.2	- 0.5	- 0.4	- 0.6	- 0.7
1.55	- 0.2	- 0.5	- 0.7	- 0.7	- 0.8
1.65	0.0	0.0	+ 0.1	+ 0.9	- 0.1
1.75	---	---	---	---	---
1.85	- 0.2	- 0.7	- 0.4	+ 0.3	- 0.7
1.95	0.0	- 1.2	- 0.1	+ 0.7	- 0.3
2.05	- 0.1	- 0.3	- 0.2	+ 0.6	- 0.2
2.10	- 0.1	- 0.3	- 0.3	+ 0.5	- 0.5
2.15	- 0.2	- 0.6	- 0.3	+ 0.4	- 0.6
2.20	- 0.2	- 0.5	+ 0.4	- 0.7	
2.25	- 0.2	- 0.6	- 0.5	+ 0.4	- 0.2
2.30	- 0.1	- 0.4	- 0.1	+ 0.6	+ .7
2.35	- 0.3	- 0.7	- 0.5	+ 0.4	+ 5.9
2.40	- 1.4	- 0.8	- 0.8	0	+17.0
2.45	- 1.1	- 0.4	- 0.3	+ 5.4	+28.2
2.50	0.0	- 0.8	+ 0.3	+19.5	+34.9
2.55	- 0.2	- 0.6	+ 1.2	+26.9	+37.5
2.60	- 0.3	- 0.7	+12.2	+34.7	+40.6
2.65	- 0.1	- 0.3	+24.8	+38.9	+42.9
2.70	0.0	+ 1.7	+31.8	+41.6	+43.9
2.75	0.0	+13.9	+36.6	+43.9	+44.8
2.80	- 0.1	+28.0	+40.1	+45.4	+46.7
2.85	+ 0.1	+35.1	+42.1	+45.5	+47.5
2.90	+14.4	+39.6	+44.3	+46.8	+47.8
2.95	+25.2	+42.6	+44.3	+45.2	+48.2
3.00	+25.0	+42.8	+44.2	+45.0	+48.5

TABLE F6. (Continued)

Data:

Injectant	Air	Air	Air	Air	Air
P_{os} (psig)	50	100	150	200	250
T_{op} (^oR)	450	444	441	440	440
T_{os} (^oR)	490	482	474	467	463
X(in)	ΔP(inHg)	ΔP(inHg)	ΔP(inHg)	ΔP(inHg)	ΔP(inHg)
3.20	-20.6	-42.9	-42.4	-41.9	-42.3
3.25	- 5.3	-39.2	-41.3	-41.0	-41.0
3.30	- 2.6	-27.1	-40.1	-41.3	-42.0
3.35	- 1.3	-10.3	-32.6	-38.4	-41.1
3.40	- 1.1	- 4.9	-22.5	-33.9	-38.6
3.50	- 1.1	- 0.5	- 7.2	-19.2	-26.2
3.60	- 0.9	- 0.4	- 3.7	- 9.0	-16.1
3.65	---	---	---	---	---
3.70	- 0.3	+ 1.6	+ 1.5	- 1.0	- 5.3
3.80	- 1.5	- 0.7	- 0.5	- 1.7	- 4.8
3.85	- 1.0	- 0.8	- 0.4	- 1.3	- 3.6
3.90	- 0.7	- 0.7	- 0.4	- 0.4	- 1.5
4.05	- 0.3	+ 1.1	+ 1.9	+ 1.8	+ 0.9
4.20	- 0.3	+ 0.5	+ 0.8	+ 0.8	+ 0.1
4.35	- 0.3	+ 0.8	_ 1.5	+ 1.2	+ 0.6
4.55	- 0.6	+ 0.2	∓ 0.5	+ 0.4	- 0.1
4.80	- 0.2	_ 0.2	+ 0.4	+ 0.1	- 0.6
5.05	- 0.3	∓ 0.1	- 0.4	- 0.9	- 1.6
5.30	- 0.9	- 1.0	- 1.3	- 1.7	- 2.5
5.55	- 1.1	- 1.8	- 1.5	- 1.7	- 2.8
6.05	- 0.7	- 1.6	+ 0.9	- 0.2	- 4.2
6.55	- 0.6	- 0.6	- 0.5	- 1.2	- 2.9
7.05	- 0.8	- 1.6	- 0.9	- 0.7	- 3.3

TABLE F7

Date: 29 November 1967

Test Conditions:

Angle of Attack 10 degrees
Slot Width 0.024 inches
Barometric Pressure 14.46 psia
Local Static Pressure 27.64 psia

Data:

Injectant	Air	Air	Air	Air	Air
P_{os} (psig)	50	100	150	200	250
T_{op} (^oR)	453	445	443	443	443
T_{os} (^oR)	494	485	478	473	470
X(in)	ΔP(inHg)	ΔP(inHg)	ΔP(inHg)	ΔP(inHg)	ΔP(inHg)
0.85	- 0.2	- 0.2	- 0.2	- 0.2	- 0.1
0.95	+ 0.1	- 0.2	0.0	+ 0.1	+ 0.7
1.05	- 0.1	- 0.1	0.0	- 0.1	0.1
1.25	- 0.1	- 0.4	+ 0.1	- 0.1	- 0.3
1.35	+ 0.1	- 0.3	- 0.1	- 0.1	0.0
1.451	+ 0.2	- 0.3	- 0.1	- 0.3	- 0.2
1.55	+ 0.1	- 0.4	- 0.2	- 0.4	- 0.2
1.65	0.0	- 0.1	0.0	- 0.1	- 0.3
1.75	+ 0.1	- 0.1	- 0.1	- 0.2	- 0.2
1.85	± 0.2	- 0.2	+ 0.2	- 0.2	- 0.2
1.95	0.0	- 0.3	- 0.1	- 0.2	- 0.3
2.05	+ 0.2	0.0	+ 0.2	0.0	0.0
2.10	+ 0.1	- 0.3	0.0	- 0.2	- 0.2
2.15	0.0	- 0.4	- 0.2	- 0.4	- 0.3
2.20	- 0.1	- 0.4	- 0.3	- 0.3	- 0.5
2.25	+ 0.1	- 0.3	- 0.2	- 0.1	- 0.3
2.30	+ 0.1	- 0.3	0.0	- 0.3	- 0.2
2.35	+ 0.1	- 0.3	- 0.1	- 0.2	- 0.1
2.40	+ 0.3	- 0.2	- 0.1	- 0.3	- 0.4
2.45	- 0.1	- 0.4	- 0.2	- 0.2	+ 7.5
2.50	0.0	- 0.7	0.0	+ 0.9	+12.5
2.55	+ 0.1	+ 0.2	+ 0.6	+ 8.7	+27.0
2.60	+ 0.1	+ 0.2	+ 4.3	+22.1	+32.6
2.65	+ 0.1	+ 0.2	+13.9	+29.8	+36.1
2.70	+ 0.1	+ 0.4	+24.6	+34.0	+38.0
2.75	+ 0.2	+ 7.4	+30.6	+37.0	+39.7
2.80	+ 0.3	+24.5	+35.9	+39.2	+41.0
2.85	+ 4.1	+31.7	+37.4	+40.6	+41.6
2.90	+20.8	+35.9	+39.6	+42.0	+42.1
2.95	+27.6	+38.2	+40.2	+41.1	+41.3
3.00	+30.1	+40.1	+40.5	+42.1	+41.7

TABLE F7 (Continued)

Data:

Injectant	Air	Air	Air	Air	Air
P_{os} (psig)	50	100	150	200	250
T_{op} (^oR)	453	445	443	443	443
T_{os} (^oR)	494	485	478	473	470

X(in)	ΔP(inHg)	ΔP(inHg)	ΔP(inHg)	ΔP(inHg)	ΔP(inHg)
3.20	-27.9	-37.1	-35.8	-35.4	-35.4
3.25	-10.4	-33.6	-34.0	-34.8	-33.4
3.30	- 3.0	-26.1	-32.1	-34.7	-33.7
3.35	- 1.4	-12.6	-27.5	-31.3	-33.3
3.40	- 0.8	- 6.0	-20.9	-26.8	-31.5
3.50	- 0.7	- 1.3	-10.4	-17.1	-22.6
3.60	- 0.4	- 0.5	- 4.3	- 8.0	-12.3
3.65	---	---	---	---	---
3.70	- 2.5	+ 0.9	- 0.2	- 2.4	- 4.3
3.80	- 1.2	- 1.4	- 1.3	- 2.5	- 4.6
3.85	- 0.2	+ 0.5	+ 0.1	- 0.8	- 3.0
3.90	- 0.1	0.0	- 0.4	- 0.9	- 2.2
4.05	- 1.1	- 0.2	+ 1.7	+ 1.6	+ 0.1
4.20	+ 0.5	+ 0.4	+ 1.9	+ 2.3	+ 0.2
4.35	- 1.3	- 0.3	+ 0.4	+ 0.4	- 0.4
4.55	+ 0.2	+ 0.7	+ 0.7	+ 0.5	- 0.2
4.80	0.0	+ 1.2	- 0.2	- 0.5	- 1.0
5.05	- 0.7	- 0.4	- 0.8	- 1.3	- 1.5
5.30	- 0.7	- 0.9	- 1.2	- 1.3	- 1.3
5.55	- 0.6	- 0.9	- 1.3	- 1.1	- 0.9
6.05	+ 0.5	+ 0.2	- 0.1	0.0	+ 0.7
6.55	+ 0.7	+ 0.7	+ 3.8	+ 1.6	+ 2.6
7.05	+ 2.6	+ 2.4	+ 0.7	+ 2.1	- 0.1

TABLE F8

Date: 1 December 1967

Test Conditions:
Angle of Attack 5 degrees
Slot Width 0.024 inches
Barometric Pressure 14.48 psia
Local Static Pressure 21.97 psia

Data:

Injectant	Air	Air	Air	Air	Air
P_{os} (psig)	50	100	150	200	250
T_{op} (^oR)	454	449	444	444	443
T_{os} (^oR)	492	485	478	474	471
X(in)	ΔP(inHg)	ΔP(inHg)	ΔP(inHg)	ΔP(inHg)	ΔP(inHg)
0.75	---	+ 0.1	+ 0.3	- 0.4	0.0
0.85	+ 0.2	0.0	+ 0.1	+ 0.3	0.0
0.95	- 0.3	0.0	+ 0.1	+ 0.3	- 0.2
1.05	+ 0.1	- 0.1	0.0	- 0.2	+ 0.1
1.25	+ 0.1	0.0	+ 0.1	- 1.1	0.0
1.35	+ 0.2	0.0	0.0	- 1.2	- 0.1
1.45	+ 0.1	- 0.1	0.0	- 0.2	+ 0.4
1.55	+ 0.1	- 0.1	+ 0.3	0.0	- 0.1
1.65	+ 0.2	0.0	+ 0.1	- 0.1	---
1.75	---	---	---	---	---
1.85	+ 0.1	- 0.1	+ 0.3	- 0.3	- 0.2
1.95	+ 0.1	- 0.2	- 0.1	+ 0.6	- 0.1
2.05	+ 0.2	- 0.7	+ 0.6	- 0.1	- 0.1
2.10	+ 0.1	- 0.1	0.0	- 0.2	0.0
2.15	+ 0.2	0.0	0.0	- 0.1	- 0.1
2.20	+ 0.1	0.0	+ 0.1	- 0.1	+ 0.1
2.25	+ 0.4	+ 0.2	+ 0.2	+ 0.1	+ 0.1
2.30	+ 0.2	0.0	+ 0.2	0.0	+ 0.4
2.35	+ 0.3	0.0	0.0	- 0.1	- 0.3
2.40	+ 0.2	0.0	+ 0.1	0.0	0.0
2.45	+ 0.2	+ 0.1	+ 0.2	+ 0.1	+10.2
2.50	+ 0.6	+ 0.5	+ 0.6	+ 1.6	+15.5
2.55	+ 0.2	- 0.1	+ 0.4	+10.1	+25.7
2.60	+ 0.2	0.0	+ 5.8	+22.1	+30.4
2.65	0.0	+ 0.2	+17.7	+28.3	+33.0
2.70	+ 0.1	+ 3.0	+24.3	+31.3	+34.3
2.75	---	---	---	---	---
2.80	+ 0.8	+14.5	+32.2	+35.6	+36.2
2.85	+10.7	+29.7	+34.4	+37.4	+37.4
2.90	+21.2	+32.1	+35.1	+37.7	+36.7
2.95	+30.5	+39.0	+38.7	+41.5	+41.6
3.00	+35.0	+40.8	+38.8	+43.1	+43.6

TABLE F8.(Continued)

Data:

Injectant	Air	Air	Air	Air	Air
P_{os} (psig)	50	100	150	200	250
T_{op} (^oR)	454	449	444	444	443
T_{os} (^oR)	492	485	478	474	471
X(in)	ΔP(inHg)	ΔP(inHg)	ΔP(inHg)	ΔP(inHg)	ΔP(inHg)
3.20	-25.3	-30.2	-30.3	-31.2	-30.2
3.25	-14.8	-27.4	-29.1	-30.8	-29.5
3.30	- 4.7	-22.9	-26.8	-29.7	-29.1
3.35	- 1.6	-14.4	-23.3	-27.8	-28.5
3.40	- 0.8	- 5.4	-16.8	-23.0	-27.6
3.50	+ 0.2	- 2.0	- 7.3	-12.2	-17.9
3.60	+ 0.1	- 0.8	- 3.2	- 5.1	- 8.8
3.65	---	---	---	---	---
3.70	- 0.9	- 0.9	- 2.2	- 3.7	- 3.9
3.80	- 0.2	+ 0.8	0.0	- 1.1	- 1.8
3.85	- 0.1	+ 0.7	+ 0.6	- 0.2	- 0.8
3.90	- 2.0	- 1.9	- 2.1	- 2.8	- 3.0
4.05	- 0.2	+ 1.2	+ 1.5	+ 1.3	+ 0.5
4.20	- 0.3	+ 0.3	0.0	- 0.1	- 0.2
4.35	- 1.6	- 1.7	- 1.6	- 2.0	- 2.0
4.55	- 2.1	- 2.5	- 2.7	- 3.0	- 2.9
4.80	- 1.1	- 1.2	- 1.8	- 2.4	- 2.2
5.05	- 0.1	+ 0.1	- 0.2	- 0.9	- 1.0
5.30	+ 0.4	+ 0.7	+ 0.6	0.0	+ 0.3
5.55	+ 0.6	+ 0.1	+ 1.1	+ 0.7	+ 1.4
6.05	- 0.1	+ 0.5	+ 0.8	+ 0.8	+ 1.5
6.55	- 0.1	+ 0.2	+ 0.7	- 0.1	+ 0.5
7.05	+ 0.6	+ 0.8	+ 0.9	- 2.1	+ 0.2

TABLE F9

Date: 5 December 1967

Test Conditions:

Angle of Attack 0 degrees
Slot Width 0.024 inches
Barometric Pressure 14.50 psia
Local Static Pressure 17.39 psia

Data:

Injectant	Air	Air	Air	Air	Air
P_{os} (psig)	50	100	150	200	250
T_{op} (^oR)	458	451	450	449	449
T_{os} (^oR)	449	490	484	478	473

X(in)	ΔP(inHg)	ΔP(inHg)	ΔP(inHg)	ΔP(inHg)	ΔP(inHg)
0.75	---	---	---	- 0.1	---
0.85	- 0.1	+ 0.1	+ 0.1	+ 0.1	+ 0.1
0.95	+ 0.1	+ 0.3	+ 0.3	- 0.2	+ 0.3
1.05	- 0.1	+ 0.1	0.0	- 0.2	- 0.1
1.25	- 0.2	+ 0.2	- 0.1	- 0.3	- 0.1
1.35	- 0.2	+ 0.1	- 0.1	- 0.3	- 0.1
1.45	+ 0.1	+ 0.2	0.0	- 0.3	0.0
1.55	+ 0.1	+ 0.4	0.0	- 0.2	0.0
1.65	0.0	+ 0.1	- 0.1	+ 0.5	- 0.1
1.75	---	---	---	---	---
1.85	+ 0.1	+ 0.3	0.0	- 0.2	- 0.1
1.95	+ 1.0	+ 0.4	+ 1.3	+ 1.2	+ 0.5
2.05	- 0.1	+ 0.1	0.0	+ 0.7	0.0
2.10	- 0.3	+ 0.3	- 0.2	- 0.4	- 0.3
2.15	+ 0.2	+ 0.5	+ 0.7	+ 0.8	+ 0.9
2.20	+ 0.1	+ 0.3	0.0	- 0.2	- 0.2
2.25	- 0.1	+ 0.2	+ 0.3	0.0	+ 0.1
2.30	- 0.2	+ 1.0	- 0.1	0.0	+ 0.5
2.35	0.0	+ 1.3	0.0	- 0.2	+ 0.4
2.40	+ 0.1	+ 0.4	+ 0.2	+ 0.2	+ 0.4
2.45	+ 0.3	+ 0.3	- 0.1	+ 0.7	+ 1.1
2.50	+ 0.2	+ 0.4	+ 0.3	+ 7.6	+18.8
2.55	+ 0.3	+ 0.2	+ 4.6	+20.5	+20.6
2.60	+ 0.5	+ 0.4	+16.1	+25.0	+25.8
2.64	+ 0.6	+ 1.8	+20.8	+26.5	+28.6
2.70	+ 0.3	+ 4.3	+22.3	+27.6	+29.5
2.75	---	---	---	---	---
2.80	+ 2.3	+22.4	+27.2	+30.4	+27.9
2.85	+16.8	+27.2	+29.8	+31.1	+30.4
2.90	+21.3	+28.4	+30.2	+30.8	+30.7
2.95	+24.4	+29.7	+30.7	+31.0	+31.3
3.00	+28.4	+32.2	+32.1	+33.4	+35.0

TABLE F9. (Continued)

Data:

Injectant	Air	Air	Air	Air	Air
P_{os} (psig)	50	100	150	200	250
T_{op} (^oR)	458	451	450	449	449
T_{os} (^oR)	499	490	484	478	473
X(in)	ΔP(inHg)	ΔP(inHg)	ΔP(inHg)	ΔP(inHg)	ΔP(inHg)
3.20	-21.5	-22.9	-22.2	-21.9	-24.9
3.25	-16.8	-21.5	-20.9	-20.5	-21.4
3.30	- 8.3	-19.7	-20.8	-20.7	-21.2
3.35	- 2.5	-14.5	-20.0	-22.3	-23.5
3.40	- 1.5	- 7.2	-13.7	-18.7	-21.7
3.50	- 1.4	- 4.9	- 9.8	-14.4	-18.0
3.60	+ 0.1	- 2.3	- 3.6	- 6.2	- 8.7
3.65	---	---	---	---	---
3.70	+ 0.5	+ 0.4	- 1.2	- 2.4	- 3.7
3.80	0.0	+ 0.1	= 0.9	- 1.6	- 4.0
3.85	+ 0.4	+ 0.4	- 0.6	- 1.5	- 3.3
3.90	---	---	---	---	---
4.05	+ 0.8	_ 2.1	+ 2.1	+ 1.0	+ 1.0
4.20	- 0.5	- 0.3	0.0	- 0.1	+ 1.7
4.35	- 2.8	- 1.9	- 2.1	- 1.4	- 3.8
4.55	- 1.5	- 2.1	- 2.4	- 1.5	- 2.3
4.80	- 2.5	- 3.4	- 3.4	- 2.4	- 2.4
5.05	- 2.2	- 1.7	- 1.8	- 1.9	- 1.2
5.30	- 0.9	- 0.8	- 0.7	- 0.9	- 0.4
5.55	- 0.5	- 0.1	+ 0.1	0.0	+ 0.3
6.05	- 0.2	+ 0.1	+ 1.2	+ 1.6	+ 0.4
6.55	0.0	+ 0.4	+ 0.3	+ 2.2	+ 1.1
7.05	+ 0.2	+ 1.0	+ 1.5	+ 1.9	+ 1.1

TABLE F10

Date: 6 December 1967

Test Conditions:

Angle of Attack -5 degrees
Slot Width 0.024 inches
Barometric Pressure 14.41 psia
Local Static Pressure 13.48 psia

Data:

Injectant	Air	Air	Air	Air	Air
P_{os} (psig)	50	100	150	200	250
T_{op} (^oR)	469	461	459	458	457
T_{os} (^oR)	503	496	490	488	483

X(in)	ΔP(inHg)	ΔP(inHg)	ΔP(inHg)	ΔP(inHg)	ΔP(inHg)
0.75	+ 0.1	0.0	- 0.1	---	+ 0.1
0.85	+ 0.1	0.0	+ 0.1	+ 0.1	0.0
0.95	+ 0.1	+ 0.1	0.0	- 0.1	0.0
1.05	+ 0.1	+ 0.1	0.0	0.0	+ 0.1
1.251	+ 0.1	0.0	+ 0.1	+ 0.1	+ 0.2
1.35	+ 0.2	+ 0.1	0.0	0.0	+ 0.1
1.45	+ 0.1	+ 0.1	- 0.1	0.0	+ 0.1
1.55	0.0	0.0	+ 0.1	- 0.1	+ 0.2
1.65	+ 1.1	+ 0.2	- 1.1	- 0.3	+ 0.3
1.75	0.0	+ 0.1	+ 0.3	+ 0.1	---
1.85	- 0.1	0.0	- 0.1	- 0.2	- 0.2
1.95	+ 0.1	+ 0.2	+ 0.1	+ 0.3	+ 0.6
2.05	0.0	= 0.1	- 1.0	- 0.2	- 0.2
2.10	+ 0.2	+ 0.1	+ 0.2	+ 0.1	+ 0.4
2.15	+ 0.2	+ 0.3	+ 0.4	+ 0.4	+ 0.8
2.20	- 0.1	+ 0.1	0.0	+ 0.2	+ 0.5
2.25	- 0.2	- 0.2	- 0.2	- 0.2	+ 0.2
2.30	- 0.1	0.0	- 1.2	- 0.5	- 0.6
2.35	- 0.2	- 0.2	- 0.2	0.0	+ 0.1
2.40	- 0.3	- 0.3	0.0	+ 0.1	+ 0.1
2.45	- 0.5	- 0.4	0.0	+ 0.9	+13.9
2.50	+ 0.6	+ 0.5	+ 0.8	+11.9	+20.8
.255	0.0	0.0	+ 0.8	+13.8	+19.6
2.60	0.0	0.0	+ 3.0	+19.9	+22.7
2.65	- 0.3	+ 2.4	+18.2	+23.0	+26.2
2.70	+ 0.3	+ 6.3	+20.0	+23.5	+26.2
2.75	---	---	---	---	---
1.80	+ 1.0	+ 8.3	+10.8	+23.1	+24.2
2.85	+ 5.2	+21.9	+24.1	+25.0	+25.4
2.90	+ 8.7	+22.2	+24.6	+25.4	+25.8
2.95	+12.4	+25.0	+25.2	+25.6	+25.5
3.00	+13.9	+24.1	+24.3	+24.8	+24.6

TABLE F10. (Continued)

Data:

Injectant	Air	Air	Air	Air	Air
P_{os} (psig)	50	100	150	200	250
T_{op} (^oR)	469	461	459	458	457
T_{os} (^oR)	503	496	490	488	483
X(in)	ΔP(inHg)	ΔP(inHg)	ΔP(inHg)	ΔP(inHg)	ΔP(inHg)
3.20	-15.7	-17.9	-16.0	-18.0	-18.5
3.25	-12.5	-16.6	-16.4	-16.0	-16.4
3.30	- 9.1	-16.2	-16.7	-16.4	-16.6
3.35	- 2.8	-11.9	-15.5	-15.7	-16.2
3.40	- 1.0	- 7.9	-13.4	-15.6	-16.9
3.50	- 2.2	- 5.5	- 9.2	-12.6	-14.9
3.60	- 0.7	- 3.3	- 4.8	- 7.1	- 9.8
3.65	---	---	---	---	---
3.70	+ 0.3	- 1.6	- 2.2	- 2.2	- 3.0
3.80	- 0.3	- 2.5	- 24.	- 2.9	- 4.4
3.85	+ 1.0	- 0.3	- 1.3	- 2.1	- 2.8
3.90	+ 1.5	+ 0.1	- 1.1	- 1.9	- 2.6
4.05	+ 0.6	+ 0.1	+ 0.1	- 0.6	- 1.2
4.20	+ 1.5	+ 0.5	+ 0.6	+ 0.8	+ 0.8
4.35	= 0.2	- 1.8	- 2.2	- 2.5	- 3.1
4.55	+ 1.8	+ 0.8	- 0.1	- 0.5	0 1.0
4.80	+ 0.3	- 1.5	- 1.8	- 1.6	- 1.8
5.05	- 0.6	= 1.6	- 1.8	- 1.7	- 2.1
5.30	- 0.1	- 1.3	- 1.8	- 2.0	- 2.4
5.55	+ 0.4	- 0.8	- 1.1	- 1.2	- 1.6
6.05	+ 0.5	- 0.5	- 0.4	0.0	- 0.3
6.55	- 0.3	- 1.6	- 1.2	- 1.2	- 2.0
7.05	+ 0.3	- 0.8	+ 0.2	+ 0.5	- 0.9

TABLE F11

Date: 4 December 1967

Test Conditions:

Angle of Attack 5 degrees
Slot Width 0.024 inches
Barometric Pressure 14.53 psia
Local Static Pressure 22.08 psia

Data:

Injectant	Argon	Helium	Nitrogen	Argon
P_{os} (psig)	150	150	150	200
T_{op} (^oR)	451	456	453	451
T_{os} (^oR)	473	492	484	463
X(in)	ΔP(inHg)	ΔP(inHg)	ΔP(inHg)	ΔP(inHg)
0.75	---	---	---	---
0.85	- 0.1	- 0.4	- 0.1	0.0
0.95	+ 0.31	- 0.3	+ 0.1	+ 0.1
1.05	+ 0.11	- 0.4	0	+ 0.1
1.25	+ 0.3	- 0.2	+ 0.1	+ 0.2
1.35	+ 0.4	- 0.3	0	+ 0.2
1.45	+ 0.1	- 0.4	+ 0.1	0.0
1.55	- 0.1	- 0.4	0	- 0.2
1.65	+ 0.8	- 0.3	+ 0.2	- 0.2
1.75	0.0	- 0.5	0	- 0.1
1.85	- 0.1	- 0.4	+ 0.1	- 0.1
1.95	0.0	- 0.3	+ 0.1	- 0.1
2.05	0.0	- 0.4	- 0.2	- 0.2
2.10	+ 0.1	- 0.4	- 0.2	- 0.1
2.15	0.0	- 0.3	0.0	- 0.2
2.20	- 0.9	- 0.1	0.0	- 0.2
2.25	+ 0.1	- 0.2	- 0.2	- 0.1
2.30	- 0.2	- 0.4	- 0.1	- 0.2
2.351	0.0	0.0	0.0	0.0
2.40	+ 0.1	- 0.2	0.0	+ 0.1
2.45	- 0.1	- 0.2	+ 0.1	- 0.5
2.50	+ 0.4	+ 0.6	+ 0.4	+ 5.1
2.55	+ 1.2	+ 4.8	+ 0.6	+16.9
2.60	+10.1	+17.8	+ 6.7	+25.5
2.65	+20.3	+25.4	+18.6	+29.7
2.70	+25.6	+29.0	+25.0	+31.8
2.75	---	---	---	---
2.80	+30.3	+33.5	+32.0	+34.8
2.85	+33.8	+35.7	+34.1	+36.6
2.90	+34.6	+36.2	+34.6	+36.3
2.95	+33.8	+36.5	+33.2	+33.6
3.00	+33.4	+36.8	+32.8	+33.4

TABLE F11. (Continued)

Data:

Injectant	Argon	Helium	Nitrogen	Argon
P_{os} (psig)	150	150	150	200
T_{op} (^oR)	451	456	453	451
T_{os} (^oR)	473	492	484	463
X(in)	ΔP(inHg)	ΔP(inHg)	ΔP(inHg)	ΔP(inHg)
3.20	-29.9	-25.9	-31.2	-29.7
3.25	-29.3	-25.6	-30.2	-29.1
3.30	-29.2	-25.6	-28.4	=29.2
3.35	-26.7	-23.7	-23.4	-29.2
3.40	-20.8	-15.4	-16.7	-26.4
3.50	- 9.6	- 4.1	- 8.3	-17.6
3.60	- 3.5	+ 0.5	- 3.7	- 8.0'
3.65	---	---	---	---
3.70	- 1.9	+ 1.3	= 2.5	- 3.6
3.80	- 0.3	+ 2.0	- 0.3	- 1.2
3.85	+ 0.1	+ 1.4	+ 0.1	- 0.3
3.90	---	---	---	---
4.05	+ 1.2	+ 1.0	+ 1.3	+ 0.9
4.20	- 0.3	+ 0.7	- 0.1	- 0.2
4.35	- 1.4	- 0.4	- 1.7	- 1.4
4.55	- 2.4	- 1.1	- 2.8	- 3.3
4.80	- 1.5	- 0.9	- 1.8	- 2.1
5.05	- 0.3	- 0.7	- 0.3	- 0.7
5.30	+ 0.2	- 0.2	+ 0.3	+ 0.1
5.55	+ 0.9	+ 0.7	+ 0.9	+ 1.0
6.05	+ 0.9	- 0.1	+ 1.8	+ 1.2
6.55	+ 0.7	- 0.5	+ 0.5	+ 0.8
7.05	0.0	- 1.1	+ 0.1	+ 0.3

TABLE F12

Date: 7 December 1967

Test Conditions:

Angle of Attack 5 degrees
Slot Width 0.024 inches
Barometric Pressure 14.36 psia
Local Static Pressure 21.57 psia

Data:

Injectant	Argon	Argon	Helium	Helium	Nitrogen	Nitrogen
P_{os} (psig)	50	100	50	100	50	100
T_{op} (^oR)	458	453	453	453	456	453
T_{os} (^oR)	500	488	497	498	497	496
X(in),	ΔP(inHg)	ΔP(inHg)	ΔP(inHg)	ΔP(inHg)	ΔP(inHg)	ΔP(inHg)
0.75	---	---	---	---	---	---
0.85	- 0.1	- 0.2	- 0.1	- 0.1	---	- 0.2
0.95	- 0.2	- 0.2	- 0.1	- 0.1	---	- 0.2
1.05	- 0.2	- 0.2	- 0.1	0.0	+ 0.8	- 0.2
1.25	- 0.1	- 0.1	- 0.1	0.0	= 0.2	=-0.1
1.35	- 0.1	- 0.3	- 0.1	0.0	- 0.3	- 0.2
1.45	- 0.2	- 0.4	- 0.3	- 0.1	- 0.1	- 0.4
1.55	- 0.2	- 0.4	- 0.3	- 0.1	- 0.2	- 0.3
1.65	- 0.3	- 0.3	+ 0.2	= 0.2	- 0.3	- 0.3
1.75	- 0.1	- 0.3	- 0.1	- 0.1	- 0.2	- 0.3
1.85	- 0.1	- 0.3	- 0.2	+ 0.2	- 0.4	- 0.4
1.95	- 0.1	- 0.2	- 0.2	- 0.1	- 0.2	= 0.2
2.05	- 0.3	- 0.4	- 0.1	- 0.1	- 0.4	- 0.3
2.10	- 0.1	- 0.3	- 0.1	- 0.1	- 0.2	- 0.3
2.15	- 0.1	- 0.3	0.0	+ 0.1	- 0.2	- 0.3
2.20	0.0	= 0.3	- 0.1	- 0.1	- 0.1	- 0.2
2.25	- 0.2	- 0.1	- 0.1	- 0.1	- 0.2	- 0.3
2.30	- 0.2	- 0.2	- 0.1	- 0.1	- 0.1	- 0.3
2.35	0.0	- 0.2	+ 0.1	0.0	- 0.1	- 0.1
2.40	0.0	- 0.1	0.0	+ 0.1	- 0.1	= 0.1
2.45	- 0.1	- 0.3	0.0	+ 0.1	0.0	= 0.2
2.50	- 0.1	- 0.2	0.0	+ 0.2	- 0.2	- 0.2
2.55	0.0	- 0.2	0.0	- 0.1	- 0.1	0.0
2.60	- 0.3	- 0.3	- 0.1	0.0	- 0.4	- 0.2
2.65	- 0.2	- 0.1	- 0.1	+ 2.1	- 0.2	+ 0.2
2.70	- 0.2	+ 3.5	0.0	+13.2	_ 0.1	+ 3.7
2.75	---	---	---	---	---	---
2.80	+ 0.4	+22.9	+ 0.5	+24.8	+ 0.3	+20.8
2.85	+10.7	+29.7	+13.8	+30.2	+11.4	+30.2
2.90	+21.4	+32.2	+22.4	+32.0	+21.7	+31.9
2.95	+27.1	+32.7	+27.2	+33.4	+26.7	+32.8
3.00	+30.9	+32.2	+30.7	+32.9	+30.3	+32.3

TABLE F12 (Continued)

Data:

Injectant	Argon	Argon	Helium	Helium	Nitrogen	Nitrogen
P_{os} (psig)	50	100	50	100	50	100
T_{op} (^oR)	458	453	453	453	456	453
T_{os} (^oR)	500	488	497	498	497	496
X(in)	ΔP(inHg)	ΔP(inHg)	ΔP(inHg)	ΔP(inHg)	ΔP(inHg)	ΔP(inHg)
3.20	-23.1	-28.3	- 7.1	-24.5	-25.9	-26.9
3.25	-16.1	-25.5	- 3.2	-19.6	-17.7	-23.1
3.30	- 4.5	-23.8	+ 0.3	-19.5	- 6.3	-21.8
3.35	- 1.4	-18.0	+ 1.8	-14.0	- 3.3	-16.7
3.40	- 0.8	- 9.7	+ 1.6	- 4.9	- 2.3	- 9.2
3.50	- 1.2	- 3.7	- 0.5	- 0.6	- 2.5	- 4.5
3.60	- 0.2	- 1.7	+ 0.1	± 0.8	- 1.3	- 2.1
3.65	---	---	---	---	---	---
3.70	- 0.6	- 1.2	- 0.8	- 0.4	- 1.6	- 1.2
3.80	- 1.1	- 1.0	- 1.4	- 0.6	- 2.3	- 1.1
3.85	- 0.9	- 0.3	- 1.3	- 0.7	- 1.9	- 0.2
3.90	---	---	---	- 1.0	---	---
4.05	- 1.0	- 0.2	- 1.4	- 1.0	- 2.1	- 0.1
4.20	- 0.2	- 0.6	- 0.7	0.0	- 1.3	+ 0.7
4.35	- 2.2	- 2.5	- 2.0	- 1.6	- 3.3	- 2.9
4.55	- 1.6	- 1.7	- 1.4	- 1.2	- 2.7	- 1.5
4.80	- 0.7	- 0.7	- 0.9	- 0.7	- 1.8	- 0.3
5.05	+ 0.1	+ 0.3	- 0.5	- 0.6	- 0.9	+ 0.7
5.30	+ 0.5	+ 0.7	- 0.2	- 0.3	- 0.7	+ 0.8
5.55	± 0.5	+ 0.7	0.0	+ 0.2	- 0.6	+ 0.9
6.05	∓ 0.1	0.0	- 0.5	- 0.6	- 1.1	+ 0.2
6.55	- 0.7	- 0.8	- 0.9	- 1.1	- 1.7	- 0.2
7.05	+ 1.5	---	+ 2.9	+ 2.0	+ 0.4	+ 1.8

TABLE F13

Date: 8 December 1967

Test Conditions:
Angle of Attack 5^{o}
Slot Width 0.024 inches
Barometric Pressure 14.46 psia
Local Static Pressure 21.86 psia

Data:

Injectant	Nitrogen	Nitrogen	Ethane	Ethane
P_{os} (psig)	50	100	50	100
T_{op} (^{o}R)	453	457	454	454
T_{os} (^{o}R)	489	497	481	480
X(in)	ΔP(inHg)	ΔP(inHg)	ΔP(inHg)	ΔP(inHg)
0.75	---	---	---	---
0.85	- 0.2	0.0	- 0.2	- 0.2
0.95	- 0.2	- 0.1	- 0.1	- 0.1
1.05	- 0.1	+ 0.1	- 0.1	- 0.1
1.25	+ 0.1	- 0.2	- 0.2	0.0
1.35	0.0	- 0.1	- 0.1	- 0.1
1.45	- 0.3	- 0.1	- 0.2	- 0.1
1.55	- 0.3	- 0.1	- 0.2	- 0.1
1.65	+ 0.3	- 0.1	- 0.2	+ 0.3
1.75	- 0.3	- 0.2	- 0.2	- 0.2
1.85	- 0.2	- 0.1	- 0.2	- 0.1
1.95	- 0.4	- 0.1	- 0.3	+ 0.3
2.05	- 0.3	0.0	- 0.3	- 0.1
2.10	- 0.3	- 0.1	- 0.2	- 0.1
2.15	- 0.2	0.0	- 0.1	0.1
2.20	- 0.3	+ 0.1	- 0.1	0.0
2.25	- 0.2	+ 0.1	- 0.2	0.0
2.30	- 0.2	+ 0.1	- 0.2	- 0.1
2.35	- 0.1	+ 0.3	0.0	+ 0.1
2.40	= 0.1	+ 0.2	0.0	+ 0.3
2.45	- 0.1	+ 0.1	- 0.2	0.0
2.50	- 0.1	+ 0.11	0.0	+ 0.3
2.55	- 0.1	- 0.1	- 0.3	0.0
2.60	- 0.3	- 0.2	- 0.4	- 0.2
2.65	- 0.4	+ 0.3	- 0.3	+ 0.2
2.70	- 0.2	+ 4.1	- 0.3	+ 3.5
2.75	---	---	---	---
2.80	- 0.1	+22.6	- 0.2	+21.9
2.85	+11.0	+29.7	+ 9.4	+29.2
2.90	+21.2	+32.7	+20.9	+32.0
2.95	+26.6	+23.0	+26.9	+33.0
3.00	+30.2	+32.6	+30.9	+32.5

TABLE F13. (Continued)

Data:

Injectant	Nitrogen	Nitrogen	Ethane	Ethane
P_{os} (psig)	50	100	50	100
T_{op} (^oR)	453	457	454	454
T_{os} (^oR)	469	497	481	480
X(in)	ΔP(inHg)	ΔP(inHg)	ΔP(inHg)	ΔP(inHg)
3.20	-25.1	-27.8	-26.2	-29.3
3.25	-15.5	-24.9	-14.0	-26.1
3.30	- 4.9	-21.8	- 6.0	-21.2
3.35	- 23.	-17.3	- 1.9	-12.4
3.40	- 1.4	- 9.0	- 1.0	- 6.3
3.50	- 1.6	- 4.7	- 1.4	- 5.1
3.60	- 0.4	- 1.6	0.0	- 1.9
3.65	---	---	---	---
.370	- 0.8	- 1.0	- 1.5	- 1.2
3.80	- 1.3	- 0.8	- 1.0	- 1.1
3.85	- 0.9	- 0.2	- 0.6	- 0.4
3.90	---	---	---	--
4.05	- 1.1	0.0	- 0.9	- 0.2
4.20	- 0.3	+ 1.2	0.0	+ 1.0
4.35	- 2.5	- 2.9	- 2.4	- 3.1
4.55	- 1.9	- 1.8	- 1.9	- 2.1
4.80	- 0.9	- 0.5	- 0.8	- 0.8
5.05	0.0	+ 0.6	0.0	+ 0.5
5.30	+ 0.3	+ 0.8	+ 0.5	+ 0.8
5.55	+ 0.5	+ 0.8	+ 0.5	+ 0.8
6.05	0.0	+ 0.2	0.0	+ 0.1
6.55	+ 0.3	+ 0.4	- 0.5	- 0.5
7.05	+ 3.2	+ 2.7	= 0.4	+ 1.7

APPENDIX G

SAMPLE CALCULATIONS

The sample calculations are carried out for air as the secondary gas, an angle of attack of 15°, a slot width of 0.024 inches, and a secondary stagnation pressure of 150 psig. The relations between the total and static conditions were obtained from the one dimensional compressible flow functions of real air for an isentropic process contained in the Air Tables(103).

1. Test Conditions

Angle of Attack	15 degrees
Slot width	.024 inches
Slot area	.0451 square inches
Secondary gas	Air
Barometric pressure	14.58 psi

2. Data

Primary total pressure P_{op}	114.58 psia
Secondary total pressure P_{os}	164.58 psia
Primary total temperature T_{op}	441 °R
Secondary total temperature T_{os}	474 °R
Local static pressure without injection	34.23 psia
Separation distance, upstream (camera)	0.50 inches

Separation distance, downstream (camera) 0.45 inches

Separation distance, upstream (pressure data) 0.55 inches

Separation distance, downstream (Pressure data) 0.60 inches

3. Calculated Results

Speed of sound, secondary $a_s^* = V_s$

$$(a^*)^2 = gkRT_s = ghR(0.8300T_{os}) \qquad (1)$$

$$(a^*)^2 = 32.2\ (1.4)\ (53.35)\ (0.8300)\ (474)$$

$$a^* = V_s = 974 \text{ fps}$$

Secondary Weight Flow

$$\dot{W} = \rho_s V_s A = \frac{P_s V_s A}{RT_s} = \frac{(0.5270) P_{os} V_s A}{R(0.8300)T_{os}} \qquad (2)$$

$$\dot{W} = \frac{(0.5270)\ (164.58)\ (53.35)\ (974)\ (.0451)}{53.35\ (0.8300)\ (474)}$$

$$\dot{W} = 0.1809 \text{ lb/sec}$$

Integrated pressure, upstream of slot* 7.350 lb/inch

Integrated pressure, downstream of slot* -4.465 lb/inch

Net aerodynamic force* 2.885 lb/inch

---

*Obtained from IBM 7094 Computer, FORTRAN IV program for Simpson's rule, manometer data from TABLE F

Normal Jet Force

$$F_j = \frac{\dot{W}V_s}{g} + (P_s - P_a)\ A = \frac{\dot{W}V_s}{g} + (0.5270\ P_{os} - P_a)A \qquad (3)$$

$$F_j = \frac{(0.1809)(974)}{32.2} + ((0.5270)(164.58)-(34.23))(.0451)$$

$$F_j = 7.820 \text{ lbs}$$

Free Stream Normal Force

$$F_a = (P_a \text{in psig})(\text{Model width})(\text{Integration length}) \quad (4)$$

$$F_a = (19.65)(1.981)(1.30)$$

$$F_a = 50.09 \text{ lbs}$$

Interation Force

$$F_i = \underline{(\text{Net Aerodynamic Force})(\text{Model width})} \qquad (5)$$

$$F_i = (2.885)(1.981) = 5.715 \text{ lbs}$$